Astronomy 503
Observational Astronomy

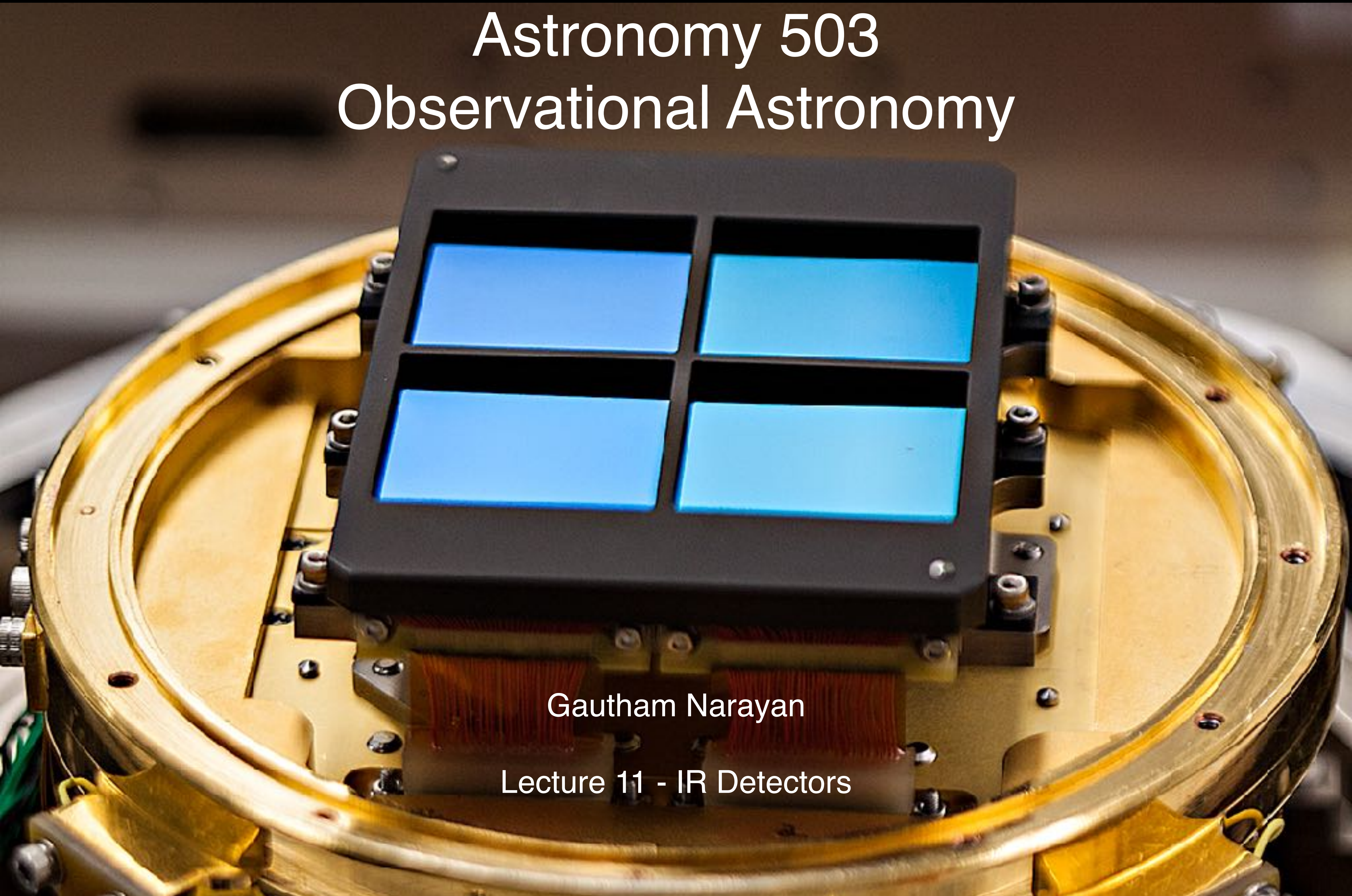

Gautham Narayan

Lecture 11 - IR Detectors

If you are planning to write a HST/WFC3/IR or JWST proposal, or anything using IR detectors, you should read G. Rieke (2006)

https://www.annualreviews.org/content/journals/10.1146/annurev.astro.44.051905.092436

Among other contributions, Rieke and his group discovered ultraluminous infrared galaxies, the starburst phenomenon, studies of the Galactic Center as a prototypical active galactic nucleus, the physical origin of the infrared emission of active galactic nuclei, planetary debris disks, as well as Solar System astronomy at infrared wavelengths.[3]

Rieke helped develop the first infrared-optimized telescope and constructed a series of state-of-the-art focal plane instruments. Rieke was involved with the Spacelab 2 infrared telescope, a pioneering infrared space mission. He led the MIPS instrument team for Spitzer. The highly sensitive MIPS camera was built at Ball Aerospace under Rieke's leadership. Also, Rieke is the lead scientist on a team to produce a Mid-Infrared Instrument (MIRI) for the James Webb Space Telescope.

Importance of infrared astronomy

- Science applications of IR astronomy:
  - High redshift galaxies
  - Dust- and gas-enshrouded star-forming regions.
  - Sgr A* and galactic center
  - Cold interstellar matter emits in the FIR
  - Rotational and vibrational molecular transitions:
    - ISM
    - Late-type, evolved stars

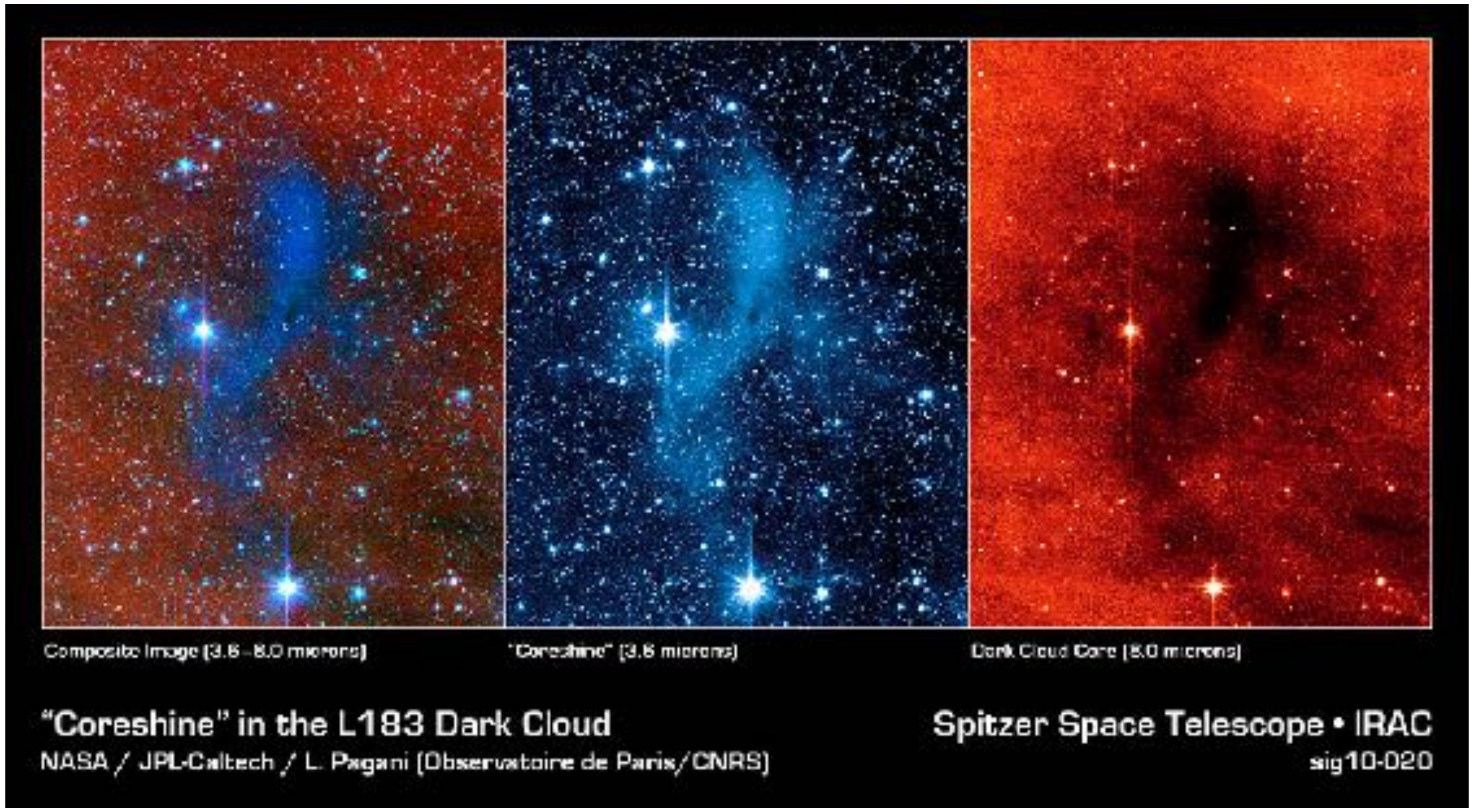

Beginnings

- **1979:** 3-4 meter class telescopes dedicated to infrared astronomy, the 3.8-m United Kingdom Infrared Telescope (UKIRT) and the NASA's 3-m Infrared Telescope Facility (IRTF).
- Located on 4.2 km (14,000 ft) summit of Mauna Kea, Hawaii, an exceptional site for IR work.
- **1983:** The Anglo-American-Dutch Infrared Astronomical Satellite (IRAS) mission gave astronomers the first deep all-sky survey in IR at wavelengths of 12, 25, 60 and 100 µm, produced a point source catalog of over 245,000 sources (>100 times the number known previously).
- European project, called ISO (Infrared Space Observatory), was launched successfully in late 1995 and operated until 1998
- American project, called SIRTF (Space Infrared Telescope Facility) was delayed and then finally launched in 2003, at which time it was renamed the **Spitzer Space Telescope**.
- In the interim an infrared instrument (NICMOS) was placed into service on Hubble.





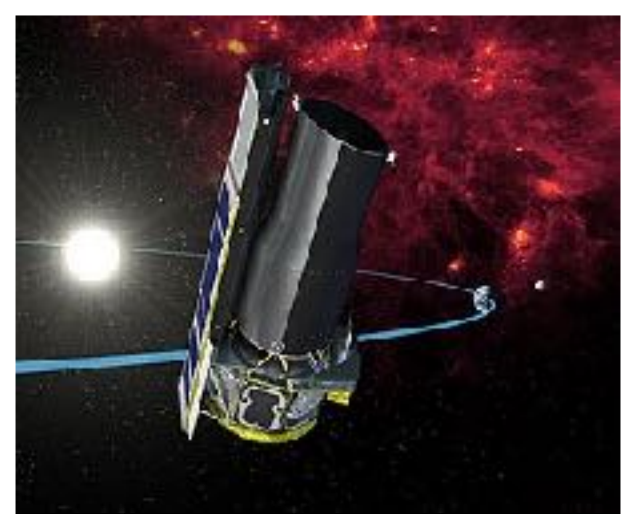


The Array Revolution in Infrared Astronomy

1968, 5-m telescope, 3 nights, single detector

~ 2000, 1.3-m telescope, 8 seconds, 256 X 256

~ 2006, 6.5-m telescope, 1 hour, 1024 X 1024 (would be 4 minutes with the 2x2 2048 X 2048 NIRCam mosaic)

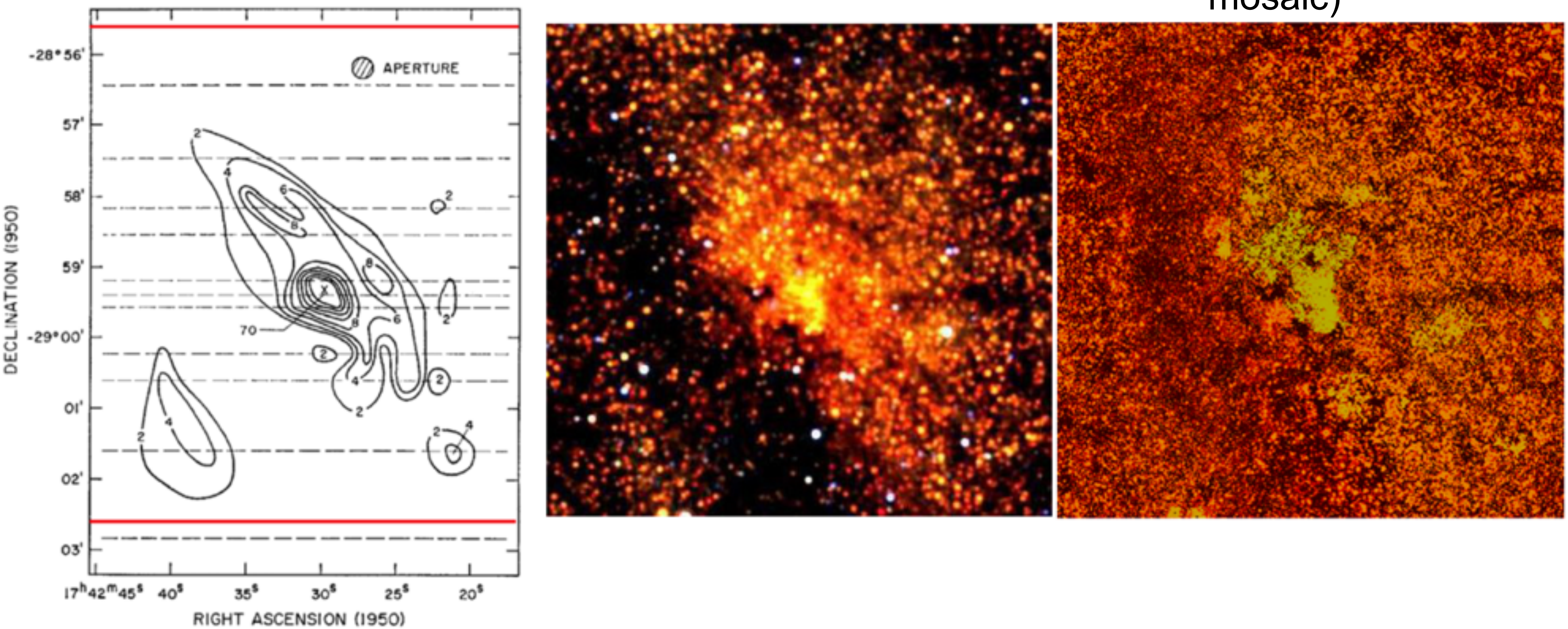

Images of the Galactic Center region at 2 μm. (*a*) The original map by Becklin & Neugebauer (1968), using a single detector with an aperture of 15 arcsec (reproduced by permission of the American Astronomical Society). The dashed lines show the actual scans across the region; the data were taken over three nights with the Palomar 200-in (5-m) telescope. The red lines delineate the roughly 7 × 7 arcmin field shown in panels *b* and *c*. (*b*) The 2MASS image of the same region, using a 256 × 256 detector array on a 1.3-m telescope and with integrations of 8 s per point. The image includes data at 1.25 μm, which identifies foreground stars as blue in the false color image (courtesy of 2MASS/UMass/IPAC-Caltech/NASA/NSF). (*c*) A mosaic obtained by Laycock et al. (private communication) on the 6.5-m Magellan Telescope with a 1 K × 1 K array. The typical resolution is 0.5 arcsec and the total time for the area shown was about an hour. At the depth of this image, Olber's Paradox comes to mind—nearly every line of sight seems to intersect a star.

Infrared regime

- The red limit of sensitivity of the human eye is ~720 nm (or 0.72 µm).
- With the advent of CCDs, "optical" astronomy extended its territorial claims to about 1.1 µm, the cut-off wavelength for detection of light imposed by the fundamental band-gap of silicon ($\lambda_c = 1.24/E_G$; for E_G = 1.13 eV, λ_c = 1.1 µm).
- Where is the "real" optical-IR boundary for ground-based astronomy?
- A reasonable response is "2.2-2.4 µm" because at these wavelengths there is a marked and fundamental change in the nature of the "background" light entering the telescope/detector.
- There is a practical change in observing methods and instrument too.
- For wavelengths shorter than ~2.2 µm, the background comes mainly from OH emission in Earth's upper atmosphere, whereas at longer wavelengths the dominant source of background radiation is thermal (heat) emission from the atmosphere and telescope components.

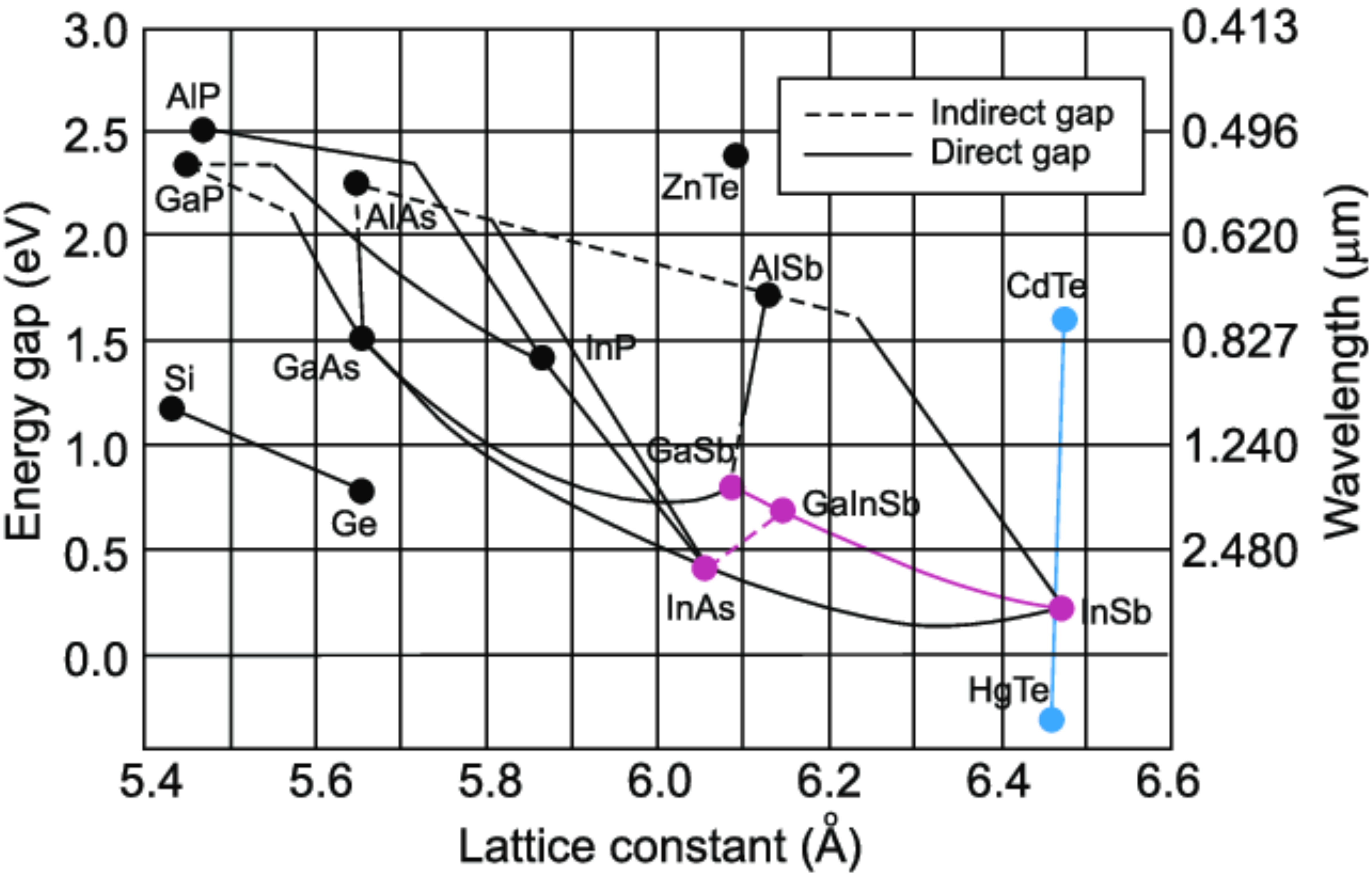
3.0
2.5
2.0
1.5
1.0
0.5
0.0
Energy gap (eV)
0.413
0.496
0.620
0.827
1.240
2.480
Wavelength (μm)
5.4
5.6
5.8
6.0
6.2
6.4
6.6
Lattice constant (Å)
Indirect gap
Direct gap
AlP
GaP
AlAs
GaAs
Si
Ge
InP
ZnTe
AlSb
GaSb
GaInSb
InAs
InSb
CdTe
HgTe

The “hybrid” structure for IR arrays

An IR array must meet same requirements on CCD: convert radiation to electrical charge by the internal photoelectric effect (or bolometer) and:

- store the charge at the site (pixel) of generation
- transfer the charge on each pixel to a single (or a small number of) outlets (the multiplexing task)
- enable the charges to be removed sequentially as a voltage which can be digitized

Initially tried to make CCD from non-silicon semiconductor – manufacturing challenges too steep. Instead adopted “hybrid” design:

IR detector + Silicon ROIC

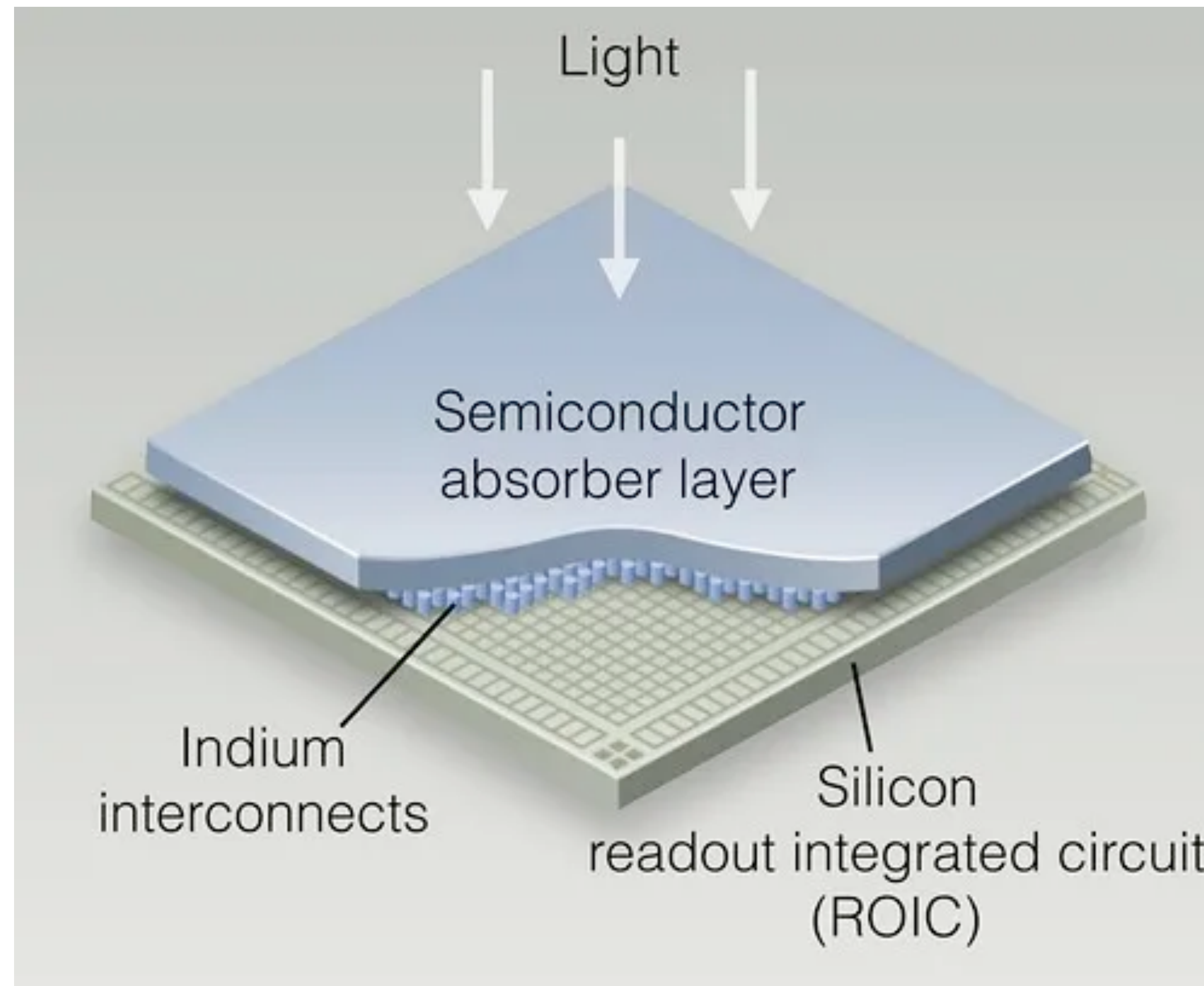

ROIC: readout-integrated circuit (silicon)

- Best performance with silicon integrated circuit readout
  - Cannot manufacture high quality electronics in other semiconductors
  - CCD-type readout has charge transfer problems at cold temperatures
- … but silicon has a large band gap - and IR photons don't have much energy

- Direct hybrid construction
  - Fields of indium bumps evaporated on detector array, readout amplifiers
  - Aligned and squeezed together - very carefully

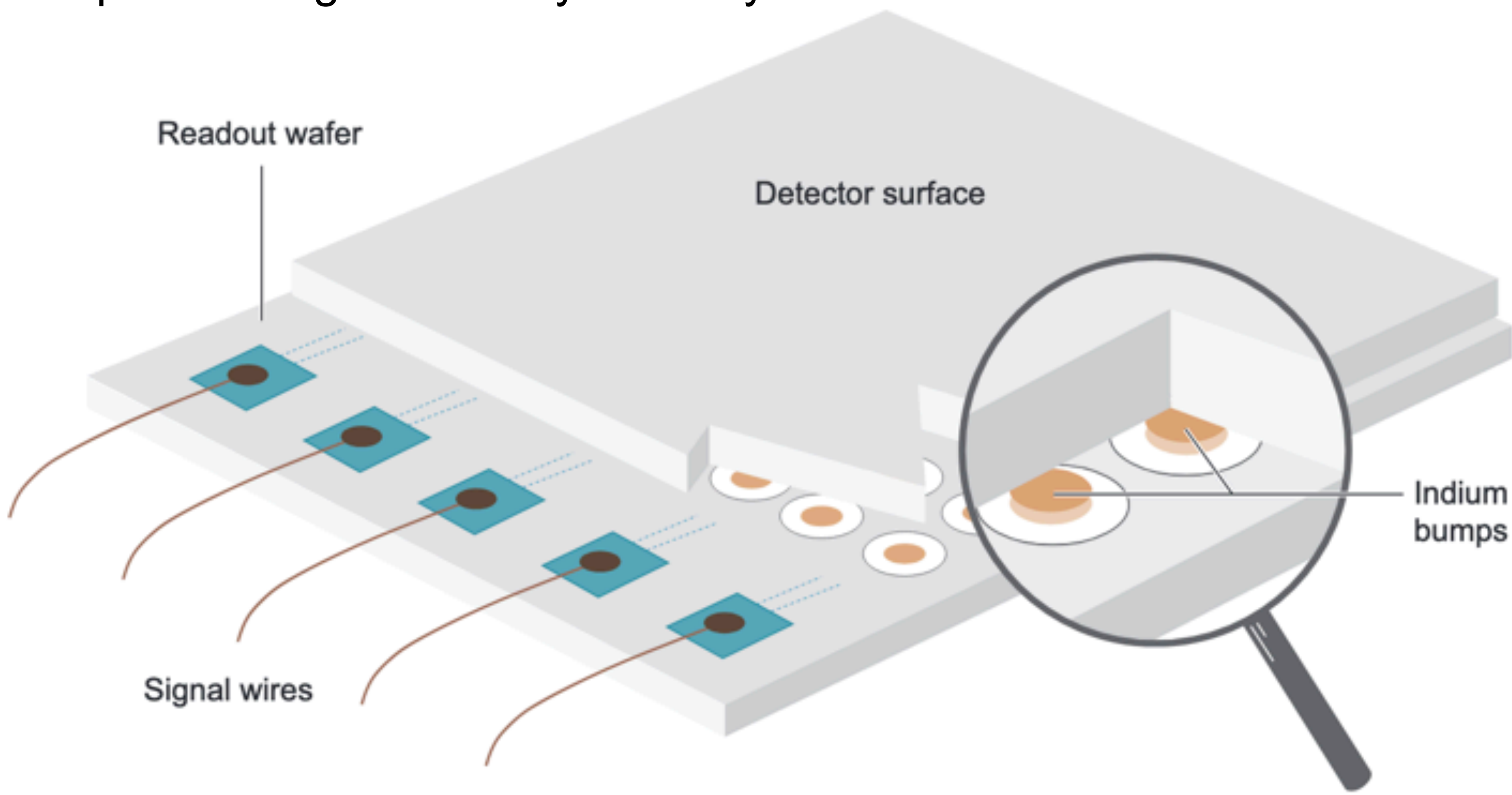

Figure 4

In direct hybrid construction, a wafer of detectors is attached to a silicon wafer (carrying the readout amplifiers and associated circuitry) through matching grids of indium bumps. When the wafers are aligned and pressed together, the bumps distort, their indium oxide skins crack, and the exposed indium metal welds the detector outputs to their individual amplifier inputs to complete the array. Figure from Rieke (2006), reprinted by permission of the University of Arizona Press.

Reminder: CMOS (complementary metal oxide semiconductor) detectors

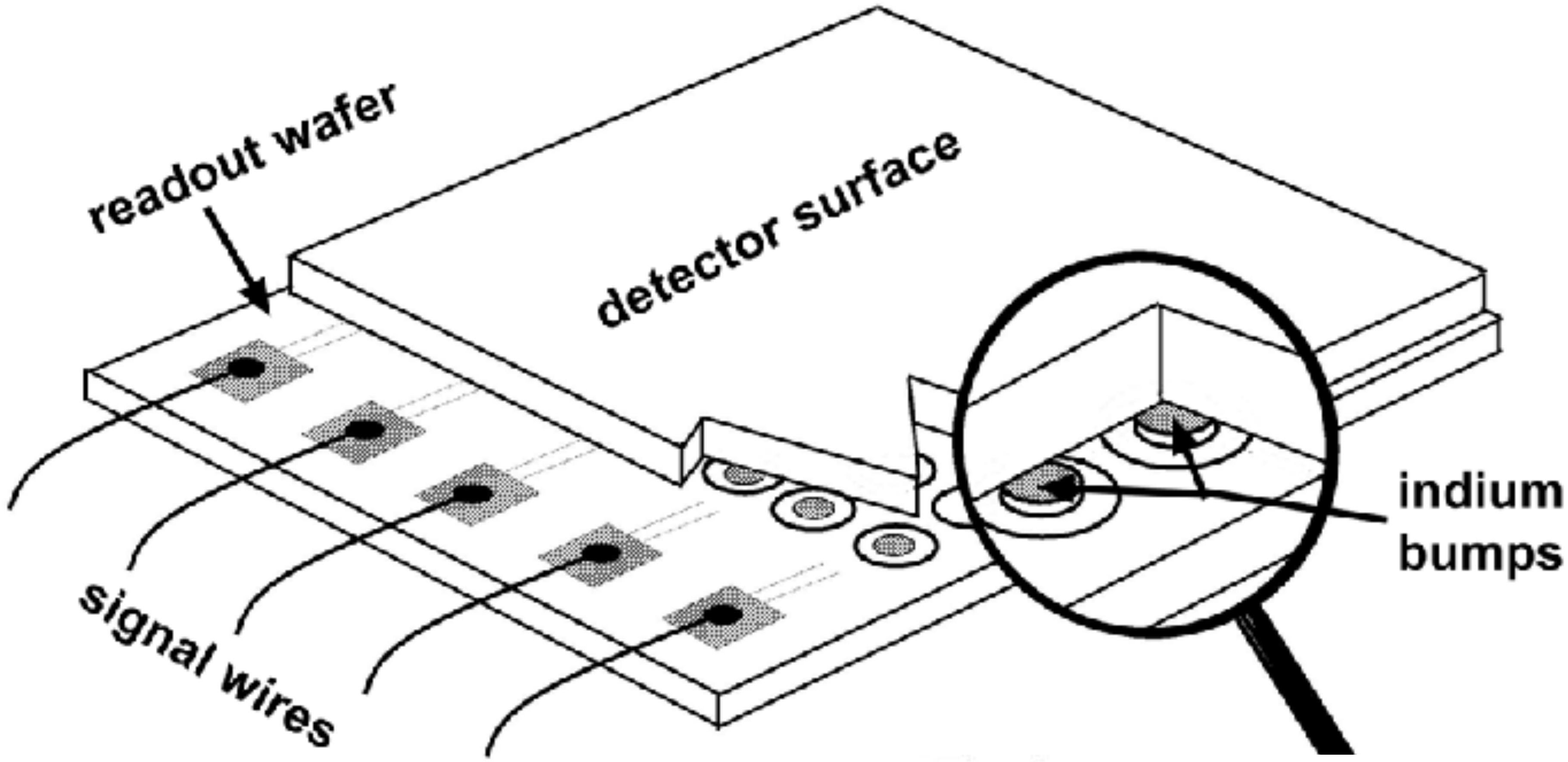

CMOS detectors are like taking just the readout for an infrared array and placing photodiodes on the inputs of the amplifiers.

Because they can be made in standard integrated circuit foundries, they are relatively cheap. They can also be made with a lot of the support electronics on the same silicon chip. To the right is Sony's diagram of how one works.

Fig. 1

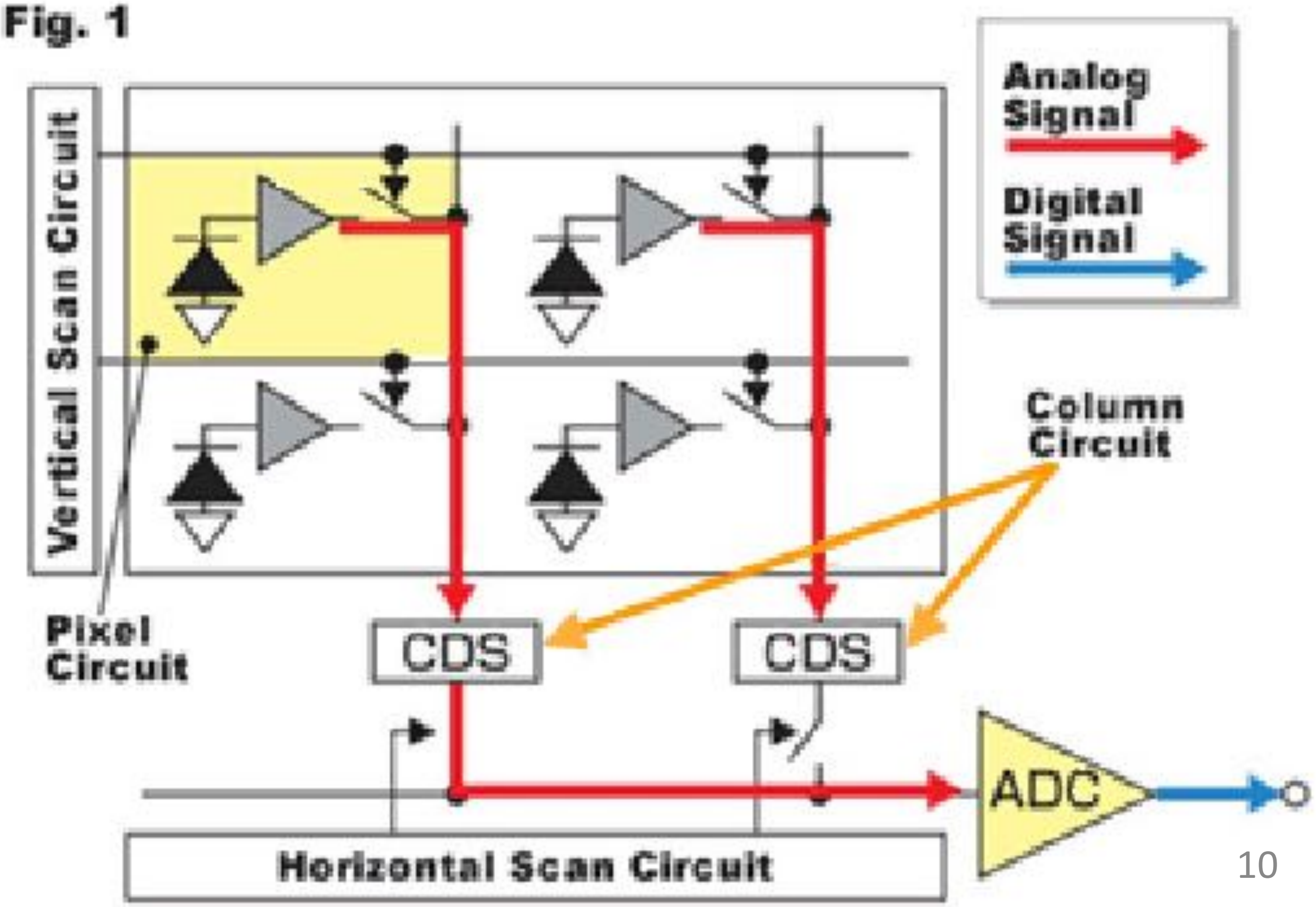

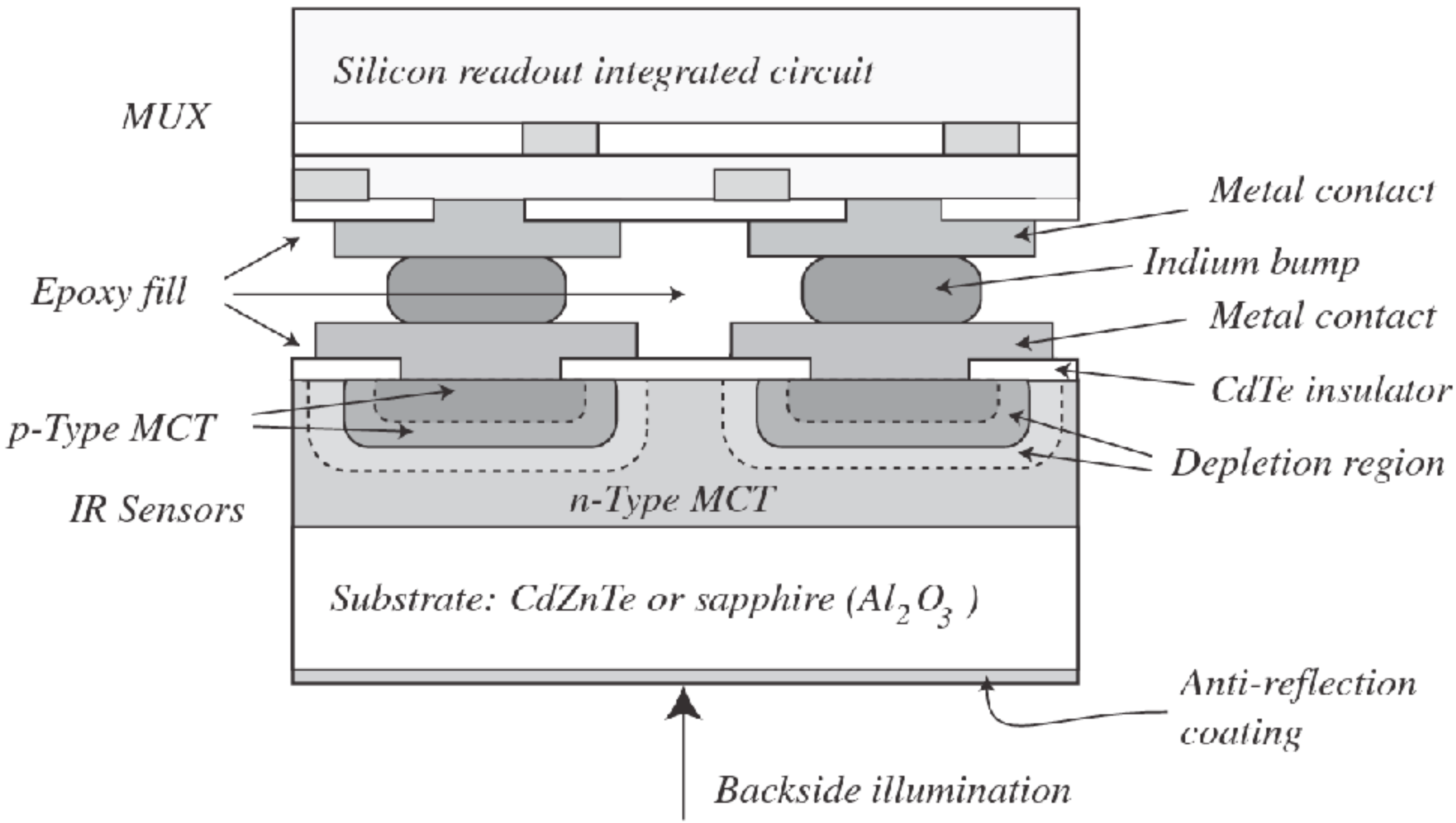
Silicon readout integrated circuit
MUX
Metal contact
Indium bump
Epoxy fill
Metal contact
CdTe insulator
p-Type MCT
Depletion region
IR Sensors
n-Type MCT
Substrate: CdZnTe or sapphire (Al_2O_3)
Anti-reflection
coating
Backside illumination

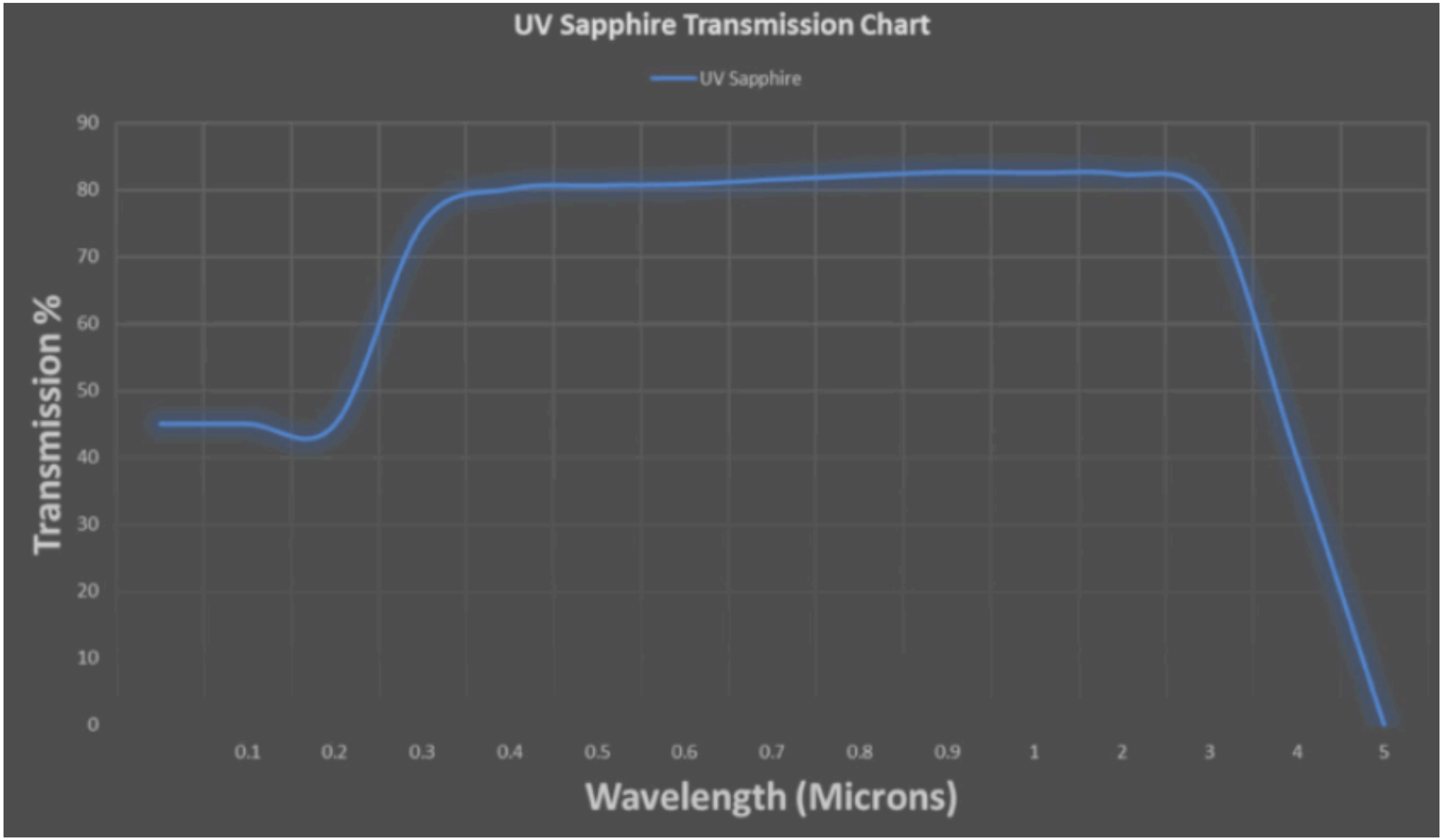
UV Sapphire Transmission Chart
UV Sapphire
Transmission %
90
80
70
60
50
40
30
20
10
0
0.1
0.2
0.3
0.4
0.5
0.6
0.7
0.8
0.9
1
2
3
4
5
Wavelength (Microns)

Reminder: CMOS detectors can be really big!

To the left, an X-ray detector; to the right a garden variety 18 Mpix camera detector.

An example: Fairchild CIS2521F

- 2560 X 2160 pixels
- 6.5 μm X 6.5 μm pixel pitch
- Readout speed maximum: 100 frames per second
- Read noise < 1.5 electrons rms
- Peak quantum efficiency > 52%

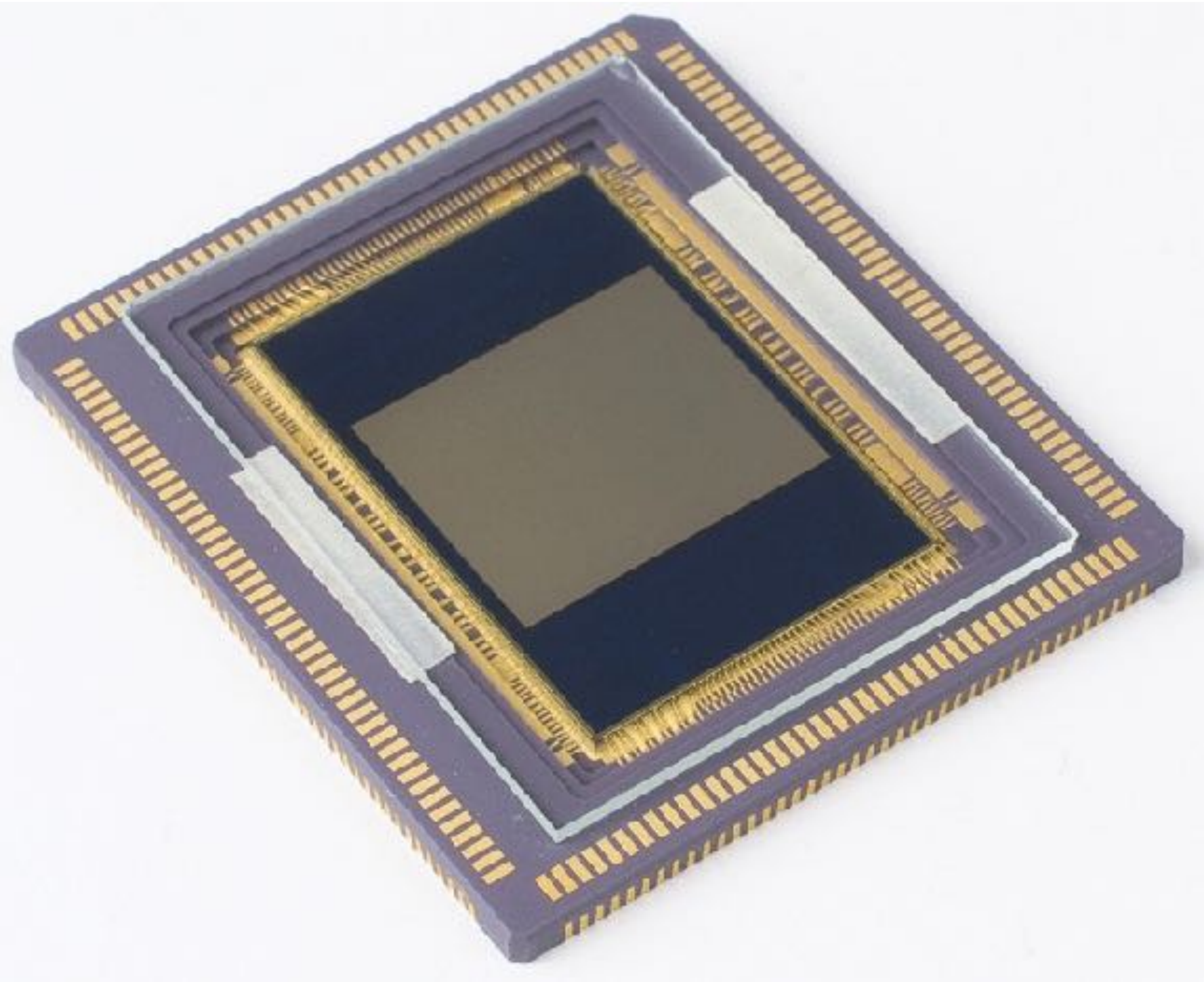

Differences with CCDs

- No charge-coupling:
  - pixels accessed directly and their voltage fed to the output bus.
- A single voltage pulse is required to reset the charge collection node at each pixel.
- Can perform a “**non-destructive**” readout.
- Even at the shortest infrared wavelengths the pixels can fill up in a few tens of seconds in broad band imaging applications and the maximum integration time drops to milli-seconds in the thermal IR.
- In fact, it is customary to sum many short on-chip exposures in a “co-adder” before writing a data frame to disk. **Thus the integration time is the product of the on-chip exposure time and the number of “coadds” used**.
- Readout times for a full frame are much faster than with CCDs.

Types of IR arrays

- **Mecury-Cadmium-Telluride (HgCdTe) arrays:**
  - Light enters from back through sapphire substrate; transmits to 6.5 µm.
  - Percentage of Hg to Cd determines cut-off wavelength. For example, with $Hg_{1-x}Cd_x Te$ then for $x = 0.196$ $E_G = 0.09$ eV and $\lambda_c = 14$ µm. Similarly, $x = 0.295$ yields $E_G = 0.25$ eV and $\lambda_c = 5$ µm, and $x = 0.55$ gives $E_G = 0.73$ eV and $\lambda c = 1.7$ µm.
  - Newer devices are “substrate removed” somewhat like thinned, back-illuminated CCDs, and it is this process that not only provides response down to visible wavelengths but also improves resistance to particle damage for space applications.
- **Indium-antimonide (InSb) arrays:**
  - Indium antimonide photodiode arrays.
  - The pn junctions are diffused into the InSb substrate.

Teledyne Hawaii Chips

- hybrid CMOS arrays
- HgCdTe (“mircad”)
- Hawaii 2k (2048x2048) 18 um pixel pitch
- 80-90% QE

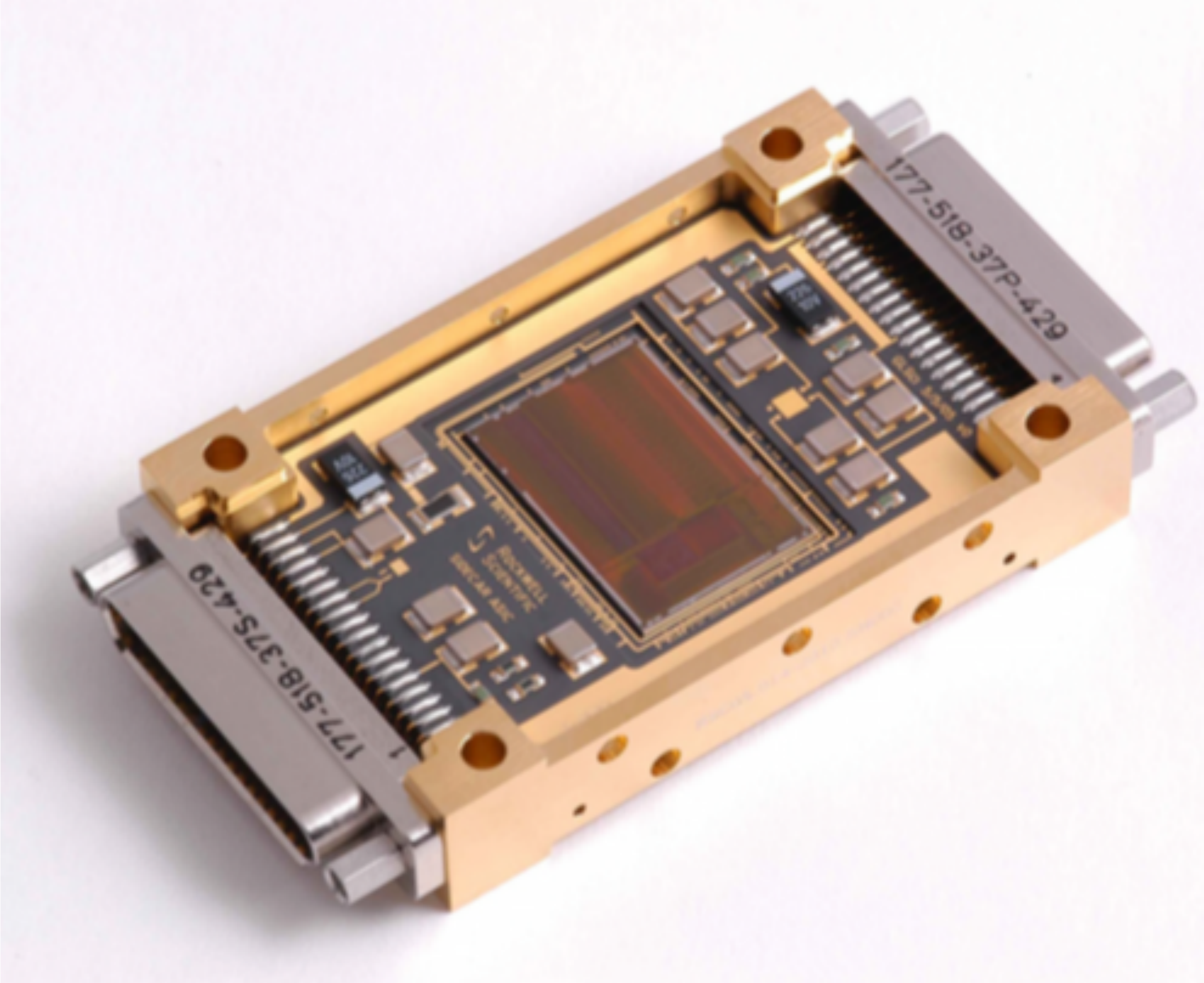

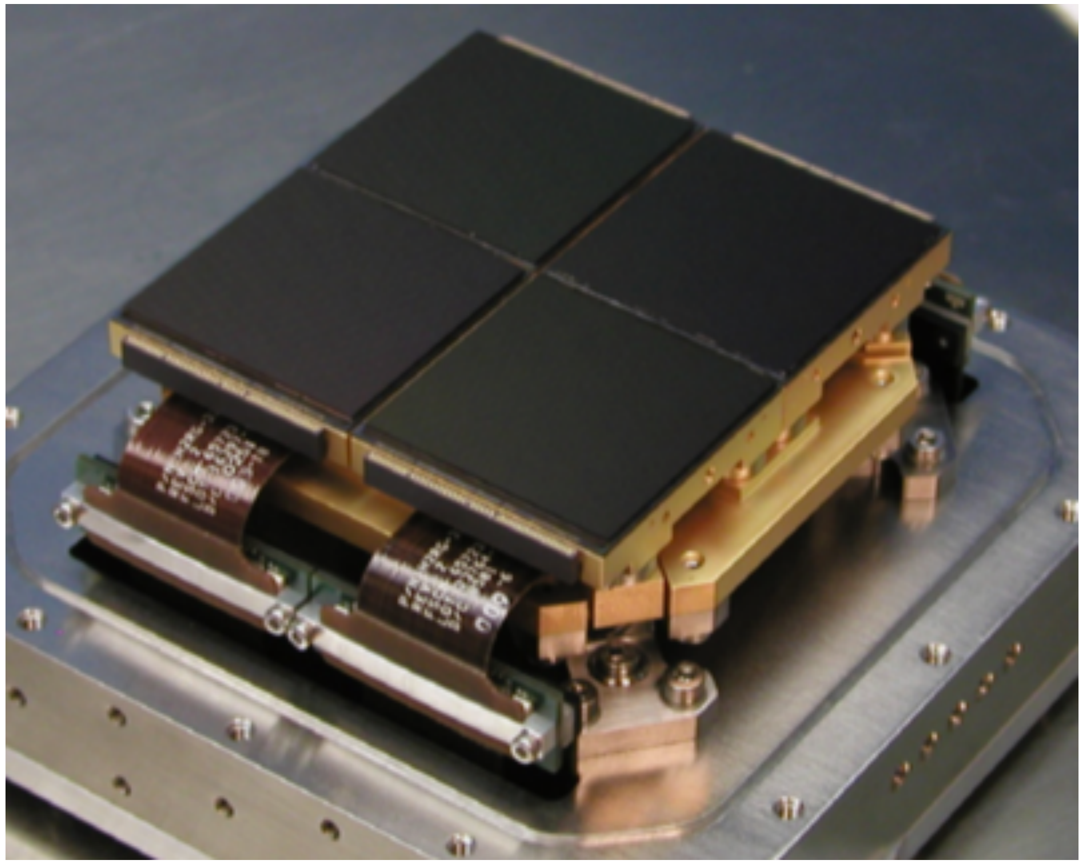

- WISE — Hawaii 1K
- HST/WFC3 — Hawaii 1k
- JWST/NIRCam — Hawaii 2k
- Roman — Hawaii 4k

Raytheon Detectors

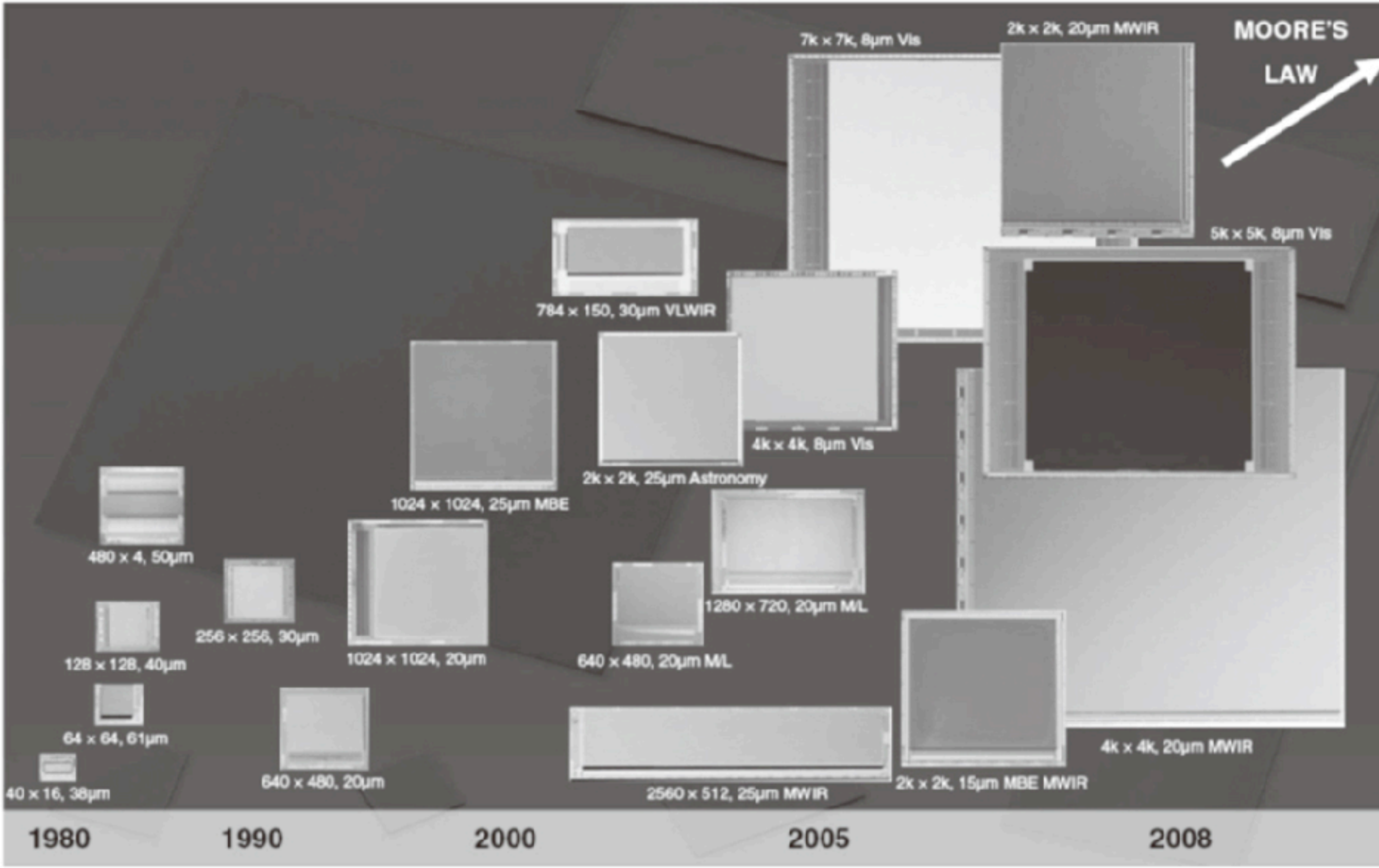

Lots of Other Applications

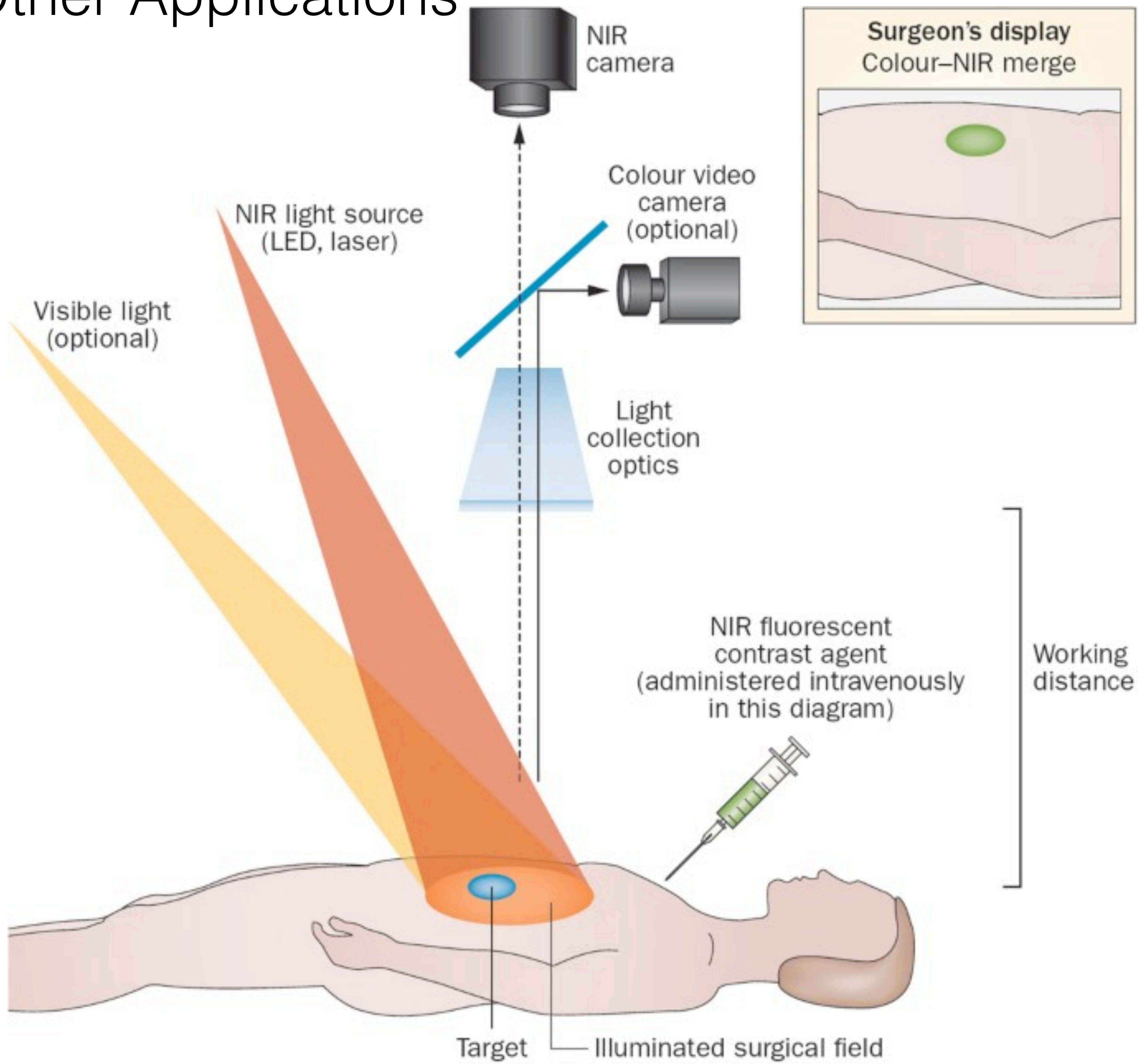

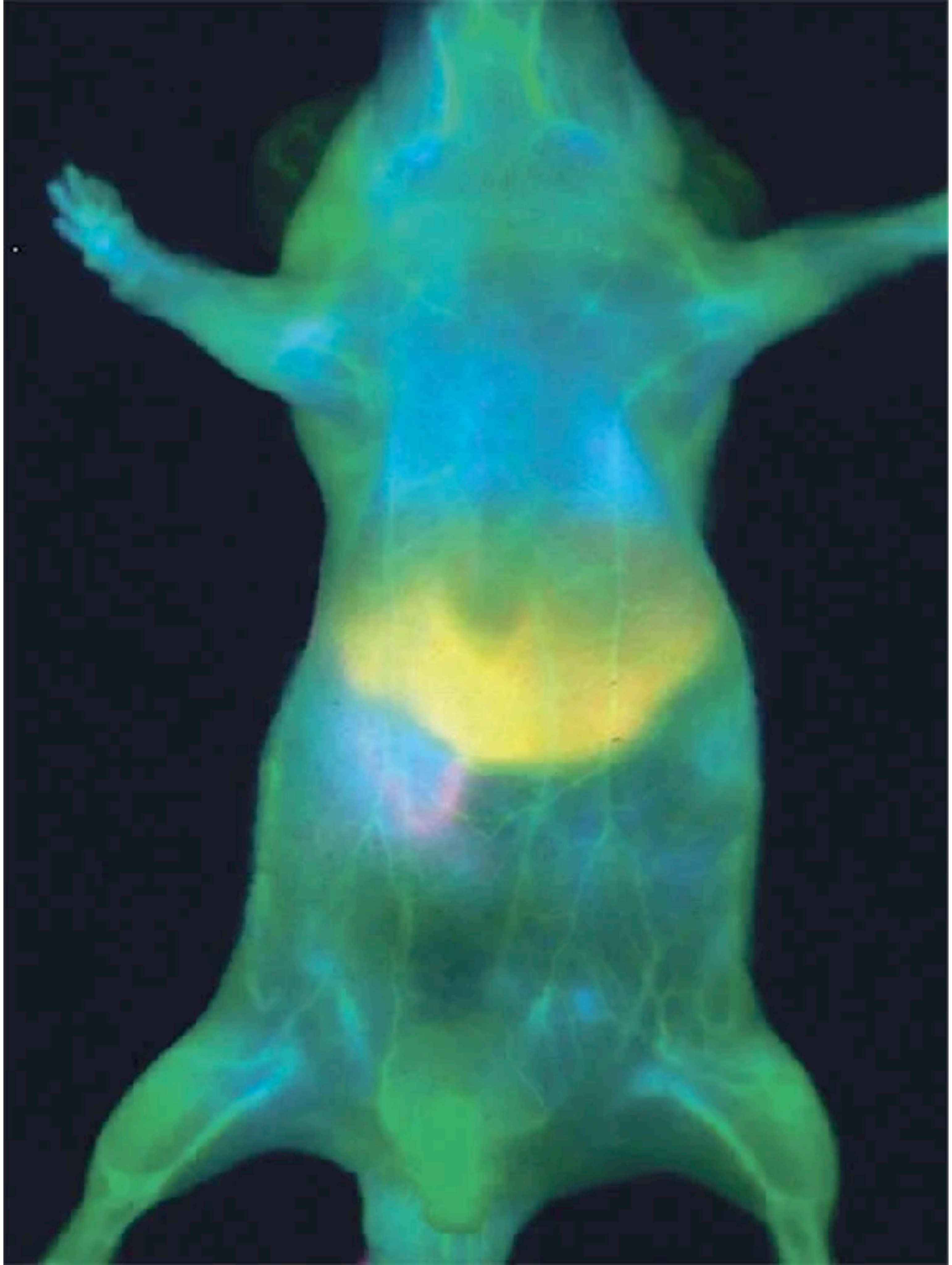

Fluorescence in vivo imaging of an anesthetized mouse injected with ICG. The real-time signal is acquired in the NIR-II (~900-1700 nm) window.

The enhanced depth and contrast allow for clear vasculature imaging, organs delineation, and metabolism.

Backgrounds

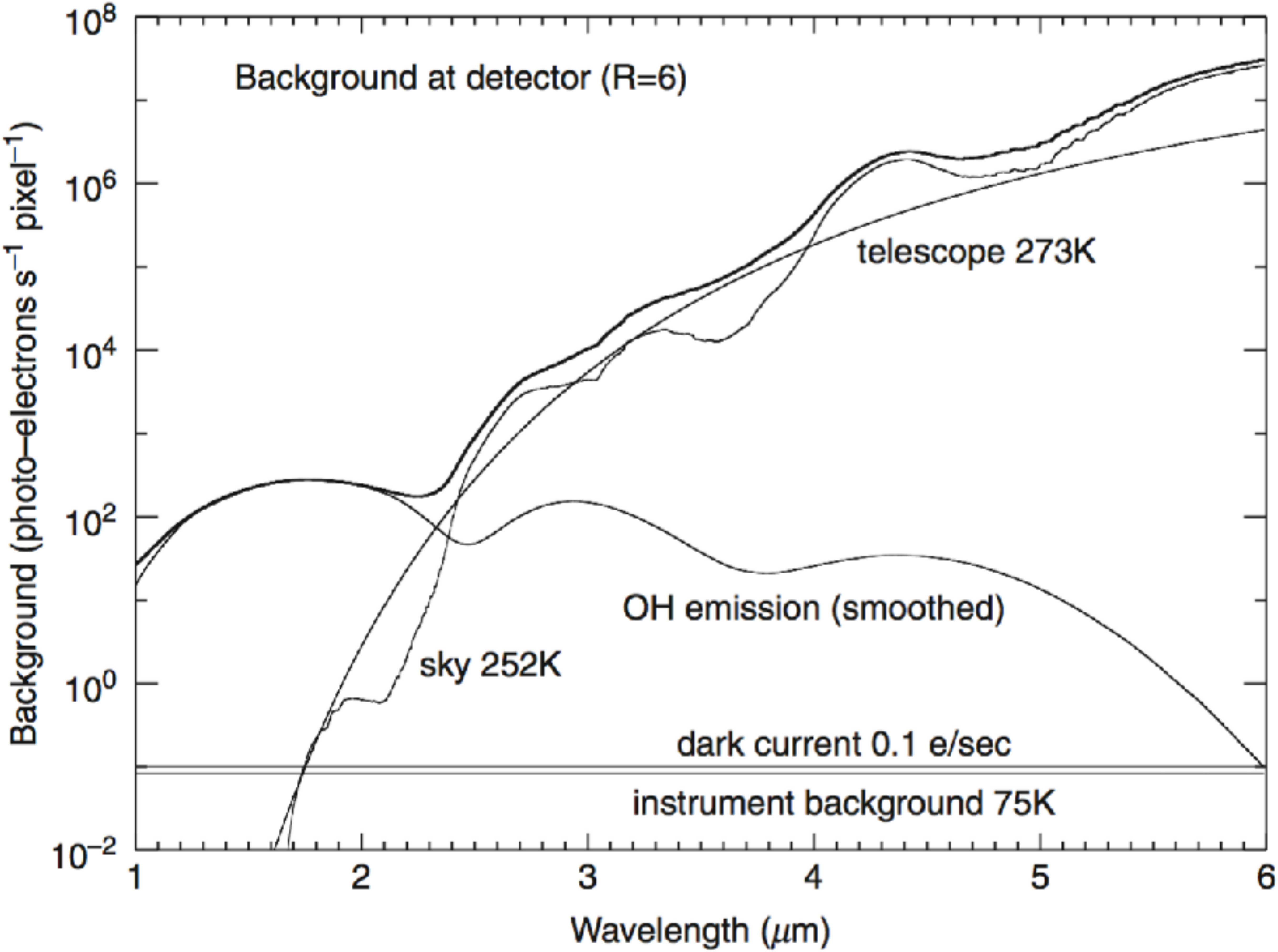

Background at detector (R=6)
Background (photo–electrons s^{-1} pixel^{-1})
10^8
10^6
10^4
10^2
10^0
10^{-2}
telescope 273K
OH emission (smoothed)
sky 252K
dark current 0.1 e/sec
instrument background 75K
1
2
3
4
5
6
Wavelength (μm)

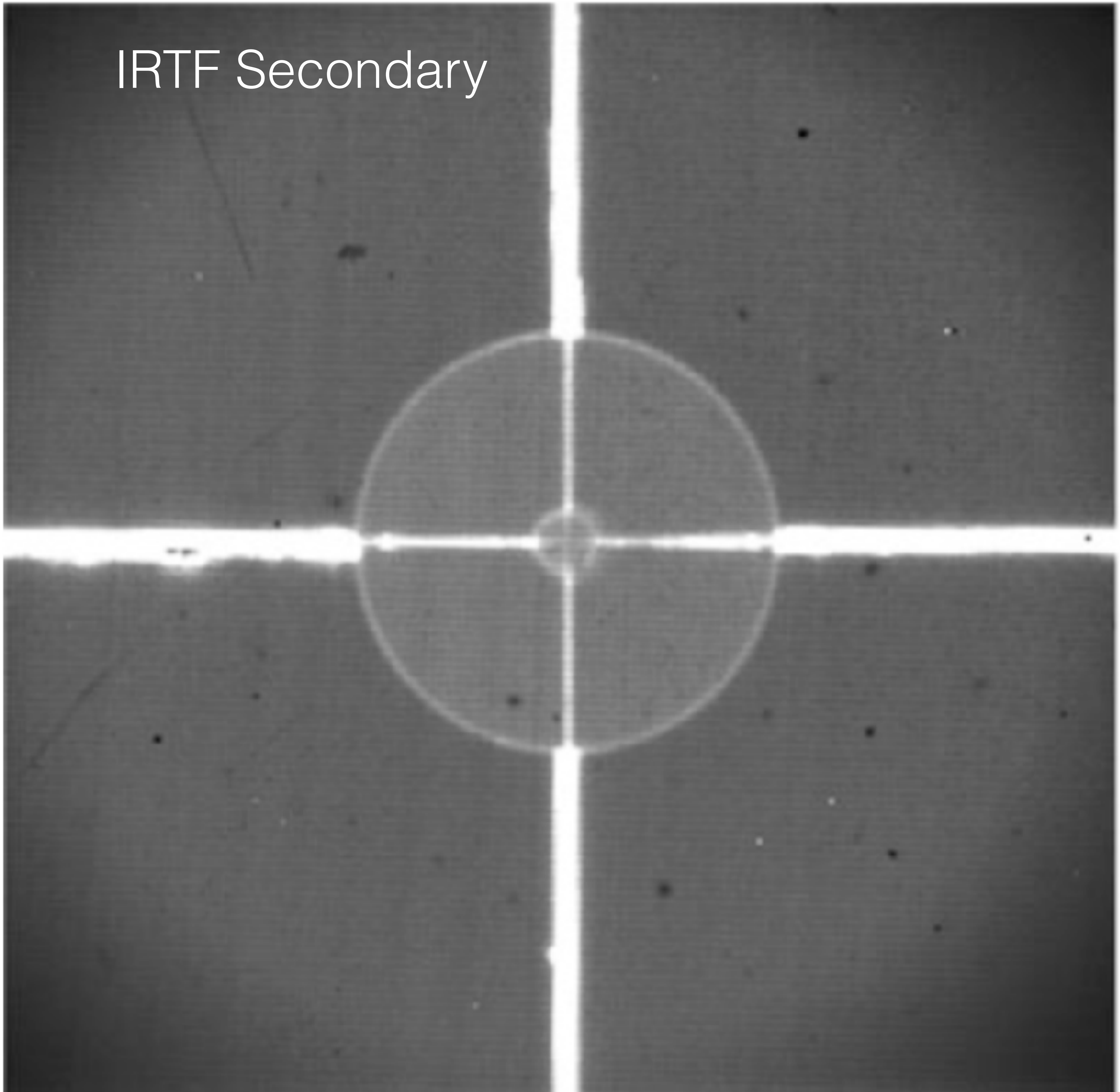
IRTF Secondary

Infrared band sub-divisions

- **Near-infrared (NIR)** is the interval from 0.9-5.5 µm.
  - Short Wave Infra-Red (SWIR) is used specifically for 0.9-2.5 µm
  - *thermal* near-infrared refers to the part from 2.5-5.5 µm.
  - NIR detectors overlap with CCDs for wavelengths less than 1.1 µm and some of the newest IR devices will perform down to ~0.5 µm.
  - Because large format IR arrays are readily available, the NIR regime merges smoothly with the classical optical regime.
- **Mid-infrared (MIR)** extends from ~5-30 µm
- **Far-infrared (FIR)** stretches from ~30 to ~200 µm.
  - Observations at these longer wavelengths are more challenging from the ground hence the interest in observations from the stratosphere.
- **Wavelengths longer than about 200 µm (or 0.2 mm) are now referred to as the sub-millimeter**, and although sub-millimeter astronomy is closely allied with infrared wavelengths in terms of the objects and regions of space which are studied, its techniques are more akin to those of radio astronomy.

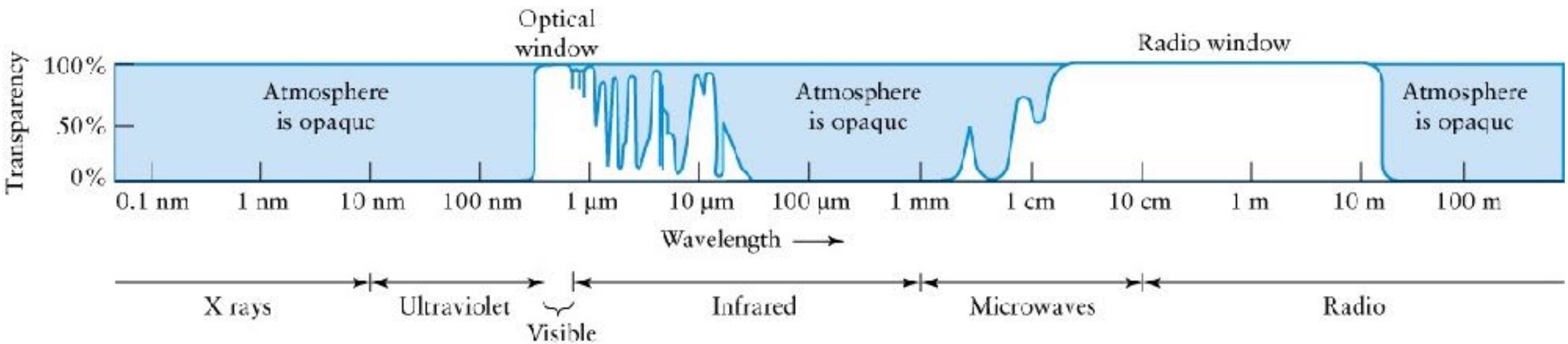

Optical
window
Radio window
Transparency
100%
50%
0%
Atmosphere
is opaque
Atmosphere
is opaque
Atmosphere
is opaque
0.1 nm
1 nm
10 nm
100 nm
1 µm
10 µm
100 µm
1 mm
1 cm
10 cm
1 m
10 m
100 m
Wavelength
X rays
Ultraviolet
Visible
Infrared
Microwaves
Radio

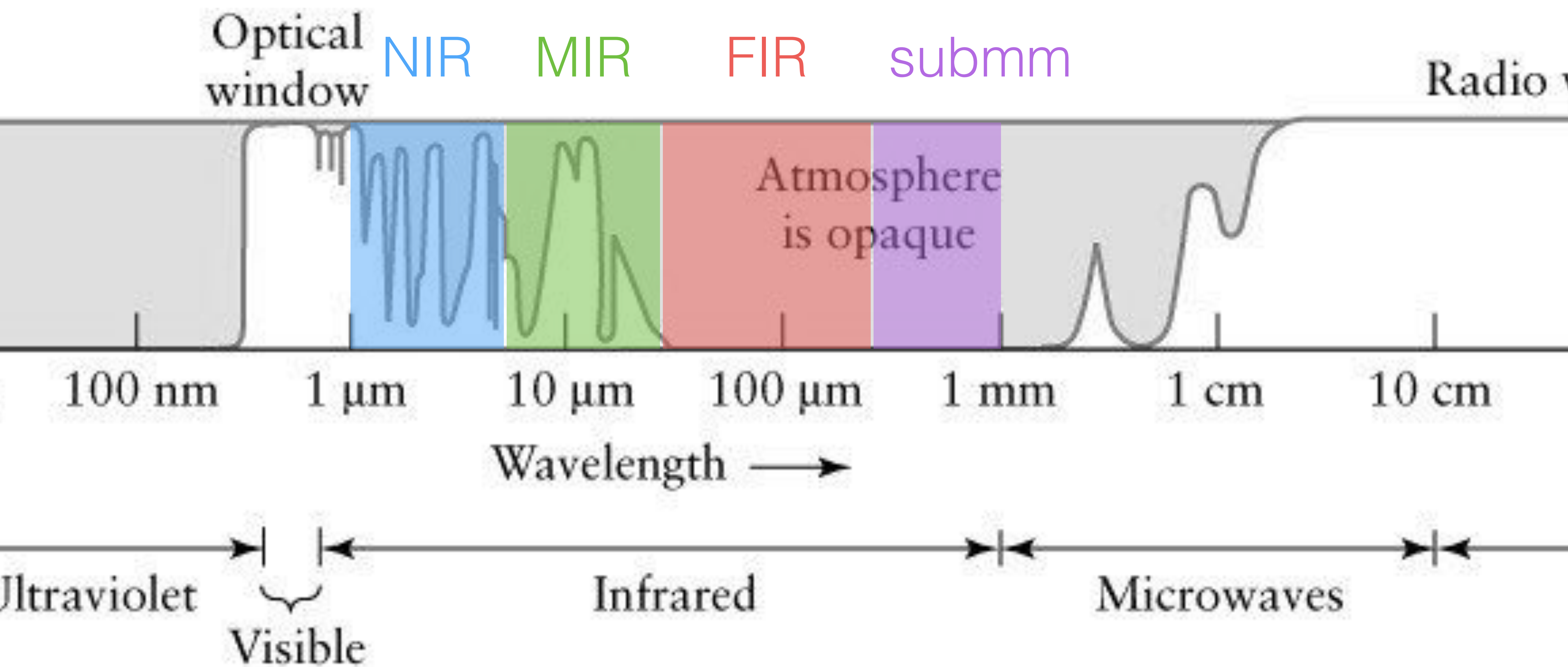

Optical window
NIR
MIR
FIR
submm
Radio
Atmosphere is opaque
100 nm
1 μm
10 μm
100 μm
1 mm
1 cm
10 cm
Wavelength
Ultraviolet
Visible
Infrared
Microwaves

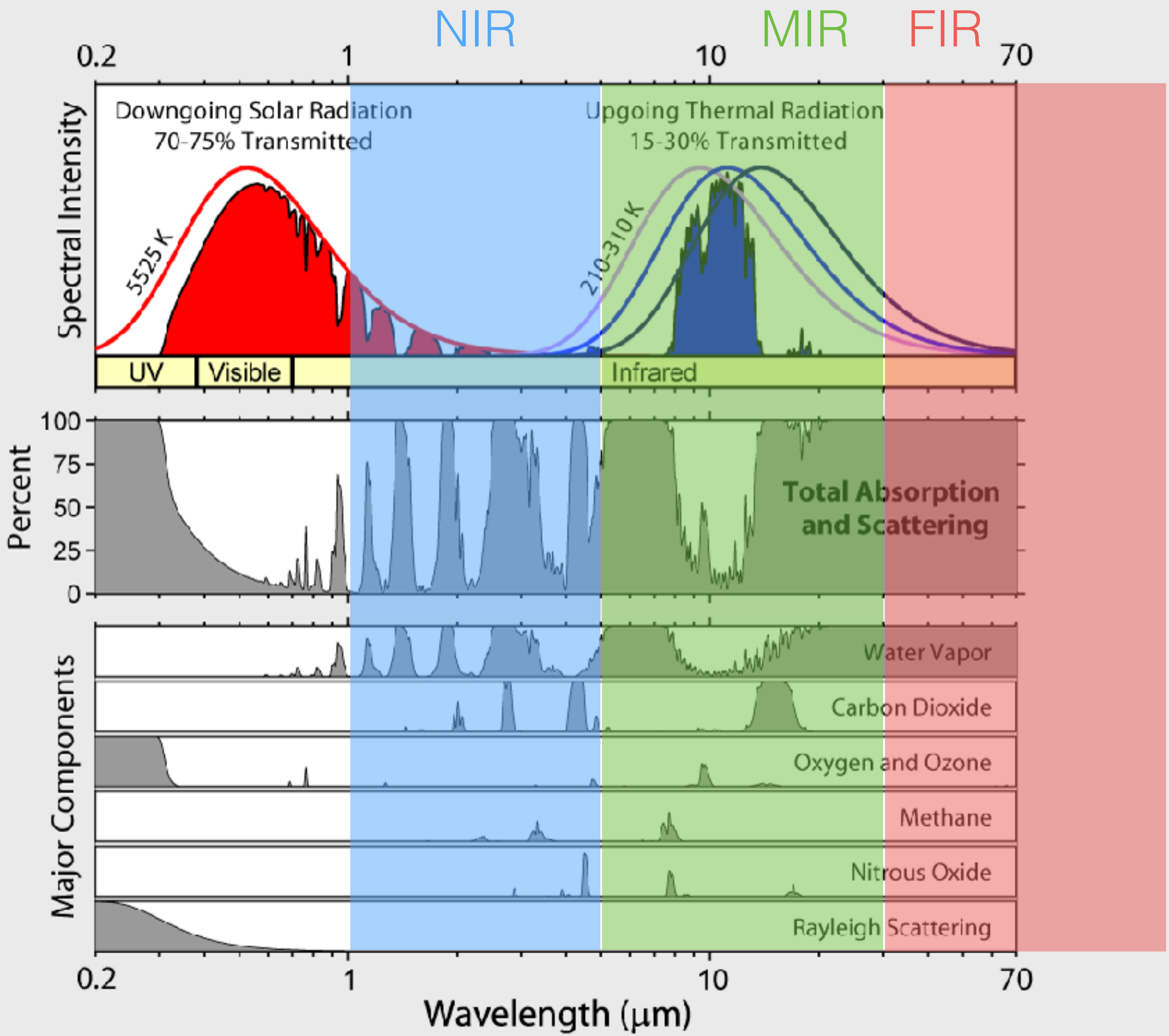

NIR
MIR
FIR
0.2
1
10
70
Spectral Intensity
Downgoing Solar Radiation
70-75% Transmitted
Upgoing Thermal Radiation
15-30% Transmitted
5525 K
210-310 K
UV
Visible
Infrared
Percent
100
75
50
25
0
Total Absorption
and Scattering
Major Components
Water Vapor
Carbon Dioxide
Oxygen and Ozone
Methane
Nitrous Oxide
Rayleigh Scattering
0.2
1
10
70
Wavelength (μm)

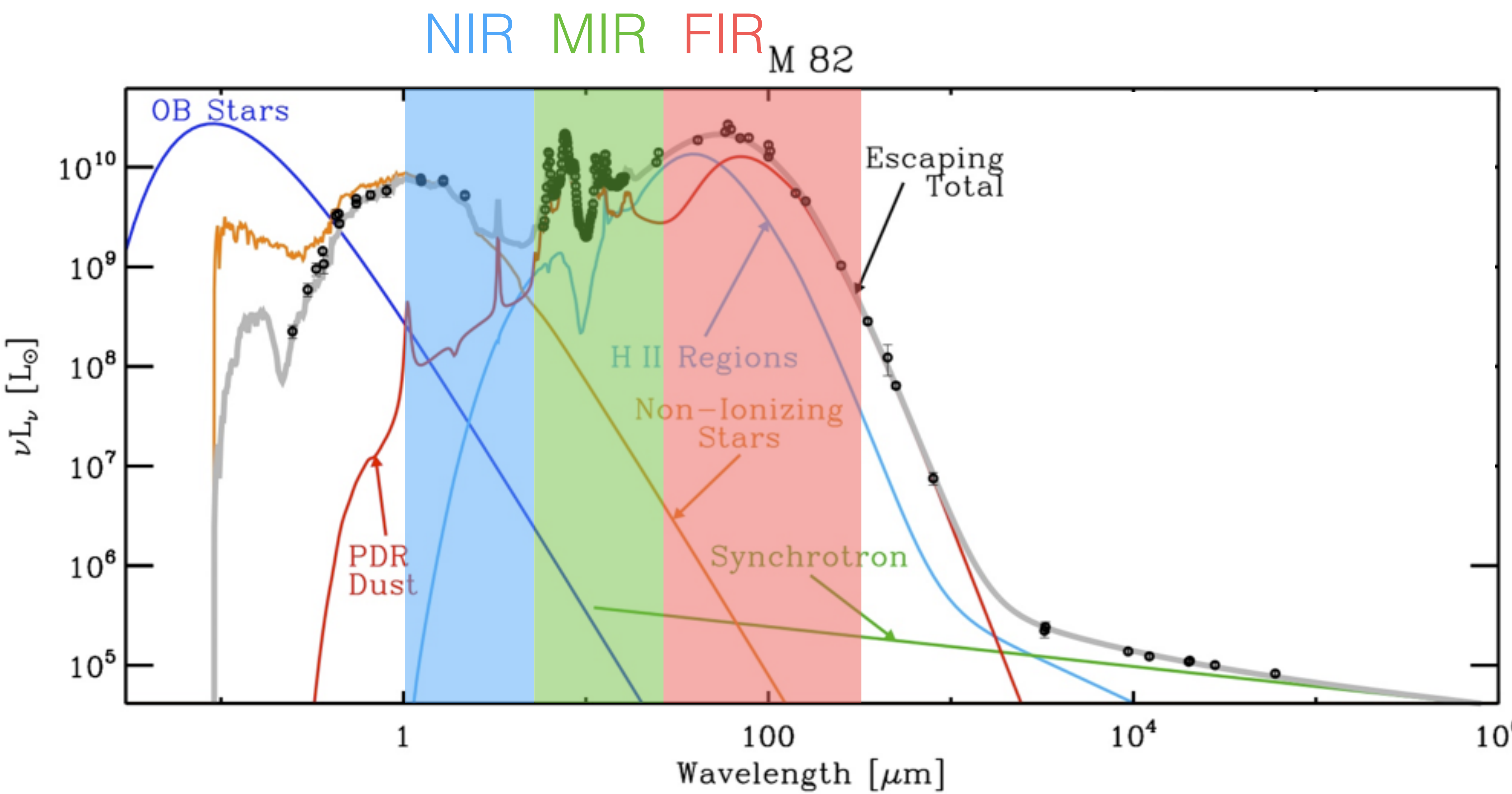

Galliano, Dwek & Chanial 2008

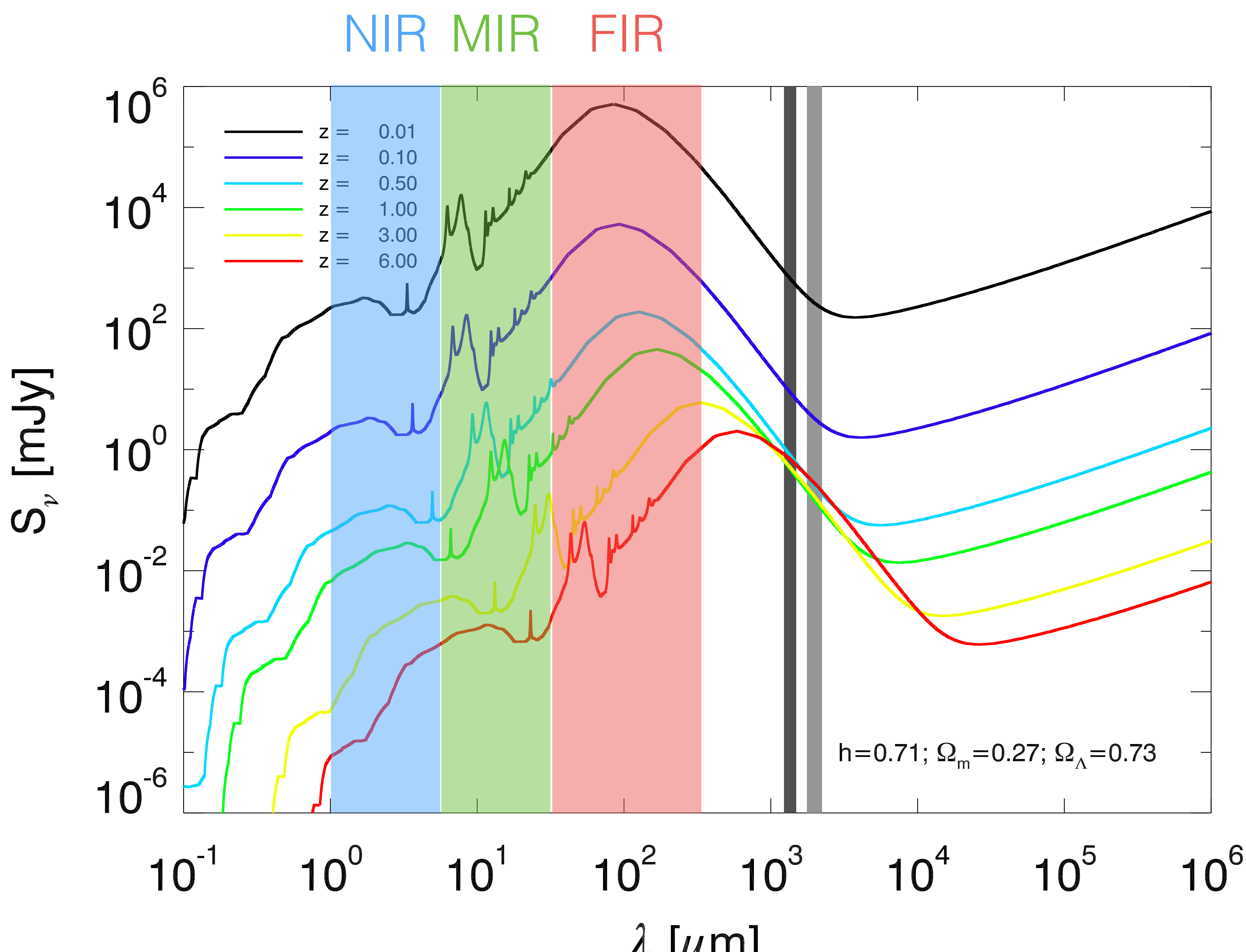

NIR MIR FIR
z = 0.01
z = 0.10
z = 0.50
z = 1.00
z = 3.00
z = 6.00
h=0.71; Ω_m=0.27; Ω_Λ=0.73
S_ν [mJy]
λ [μm]
10^{-1} 10^{0} 10^{1} 10^{2} 10^{3} 10^{4} 10^{5} 10^{6}
10^{6} 10^{4} 10^{2} 10^{0} 10^{-2} 10^{-4} 10^{-6}

NIR Windows Bands

- Water vapor (H_2O) and carbon dioxide (CO_2) block lots of IR radiation from space.
- Water vapor absorption is sensitive to altitude and wavelength.
- These windows of transparency allow us to define photometric bands.
- The standard windows are listed by central wavelength.

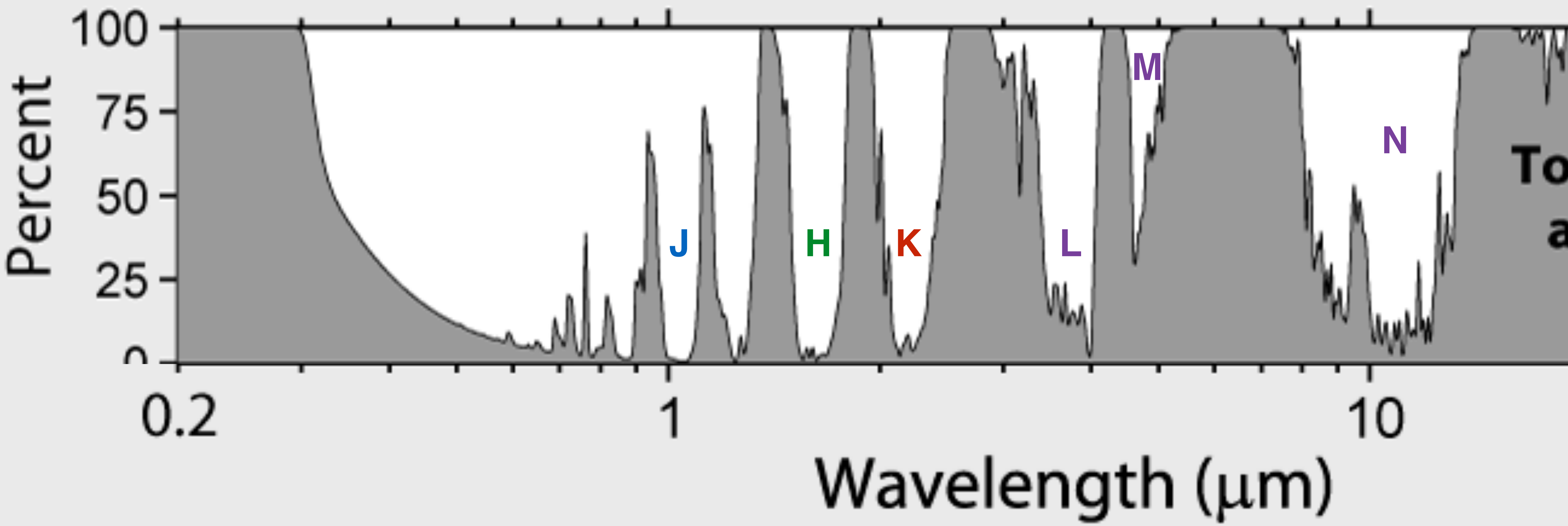

Chopping

• The beam is switched rapidly from the source position and a nearby reference position, by an oscillating or "wobbling" secondary mirror in the telescope itself.

• **Chopping** takes place at a frequency of ~10-20 Hz.

• By forming the difference, the sky signal is eliminated provided it has remained constant.

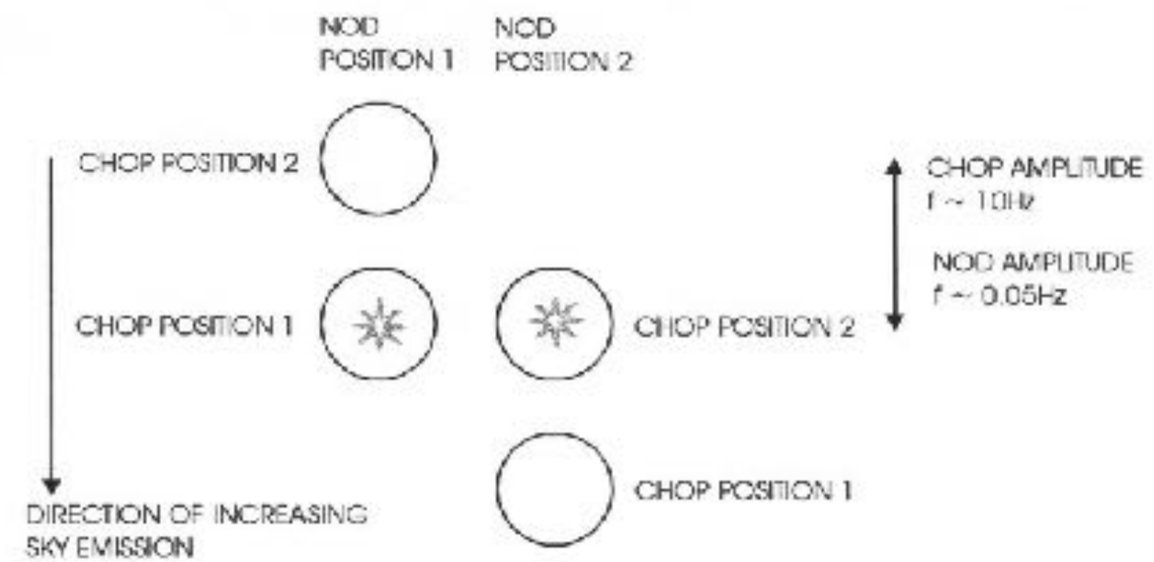

In addition, it is usually necessary to move the entire telescope every minute or so to enable the sky on the "other side" of the object to be measured and thereby eliminate any systematic trend or gradient; this step is called "**nodding**" and the amount of the nod is usually the same as the "throw" of the chop for symmetry (Fig. 11.2).

Chopping

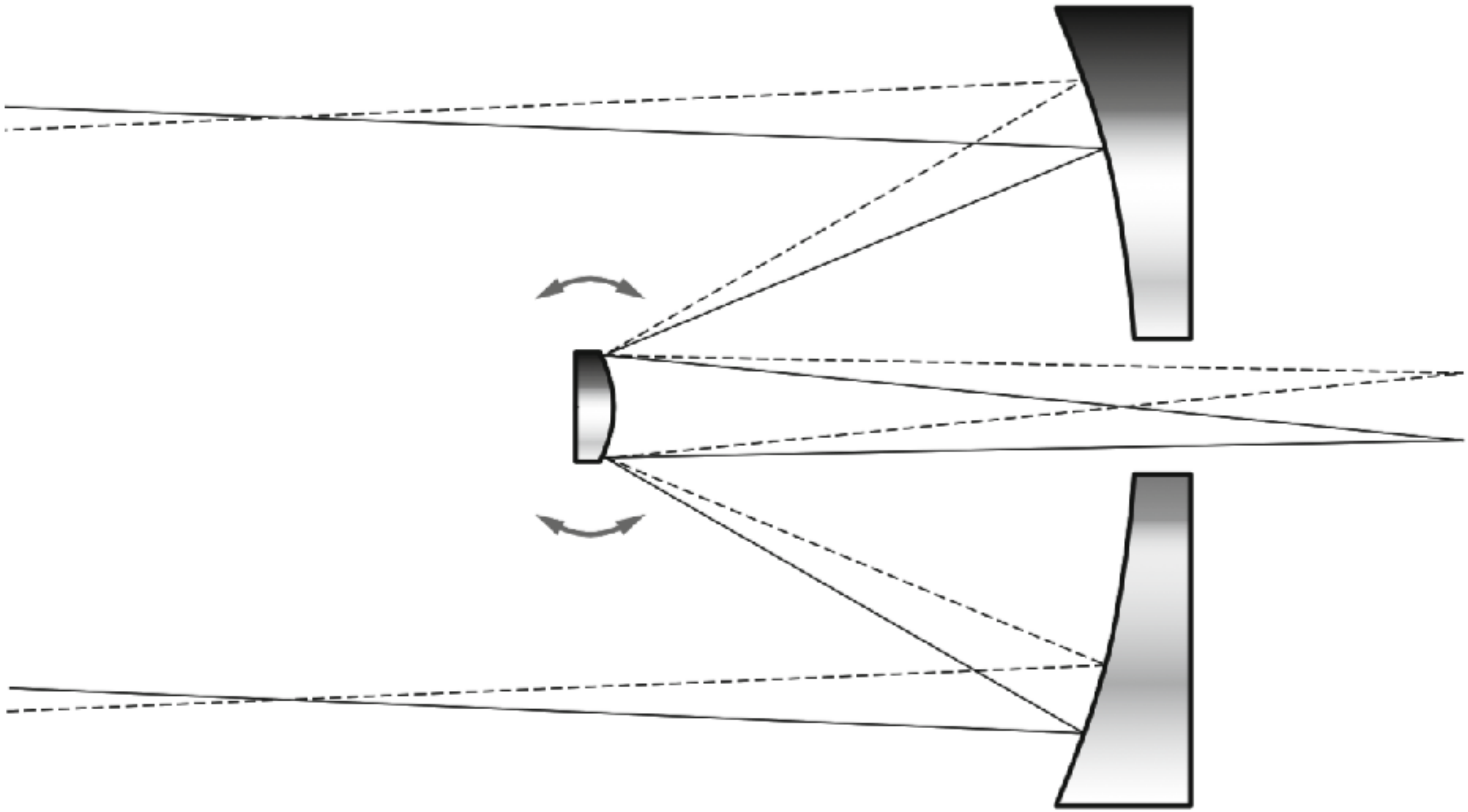

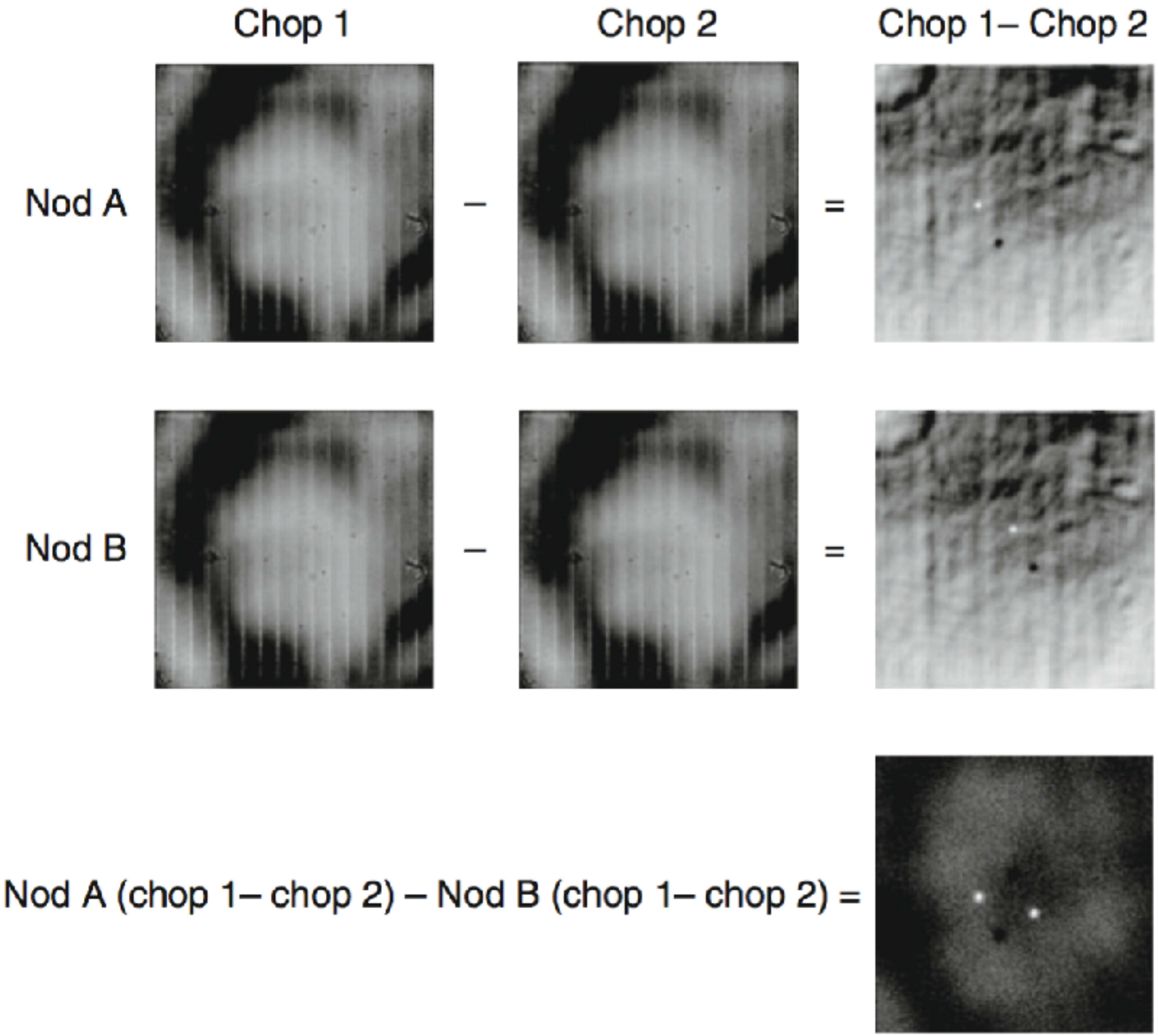

Chop 1
Chop 2
Chop 1– Chop 2
Nod A
–
=
Nod B
–
=
Nod A (chop 1– chop 2) – Nod B (chop 1– chop 2) =

Mid-IR

- The mid-IR is home to fundamental vibrational resonances of a wide range of molecules
  - Breath Analysis
  - Industrial Process Monitoring
  - Environmental Monitoring
- Absorption/Transmission Spectroscopy
    - Broadband spectroscopic data on liquids/powders/solids
  - Biomedical Imaging
    - In-vivo imaging
    - Micro-biology
  - Pharmaceutical Industry
    - Drug Development
    - Process/Quality Control
    - Counterfeit Analysis
  - Food Industry
    - Meat processing
    - Beverage quality screening
  - Material Science

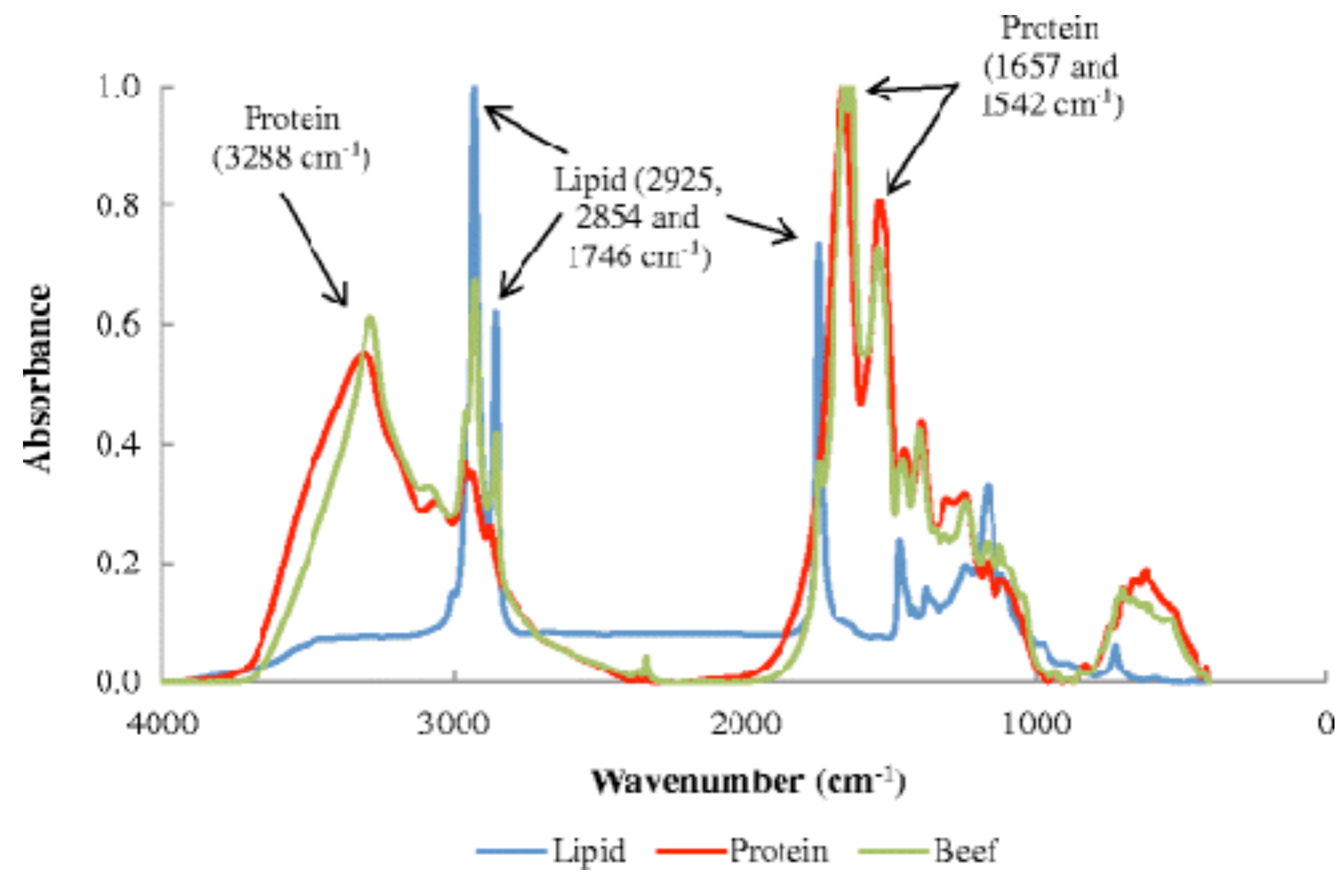

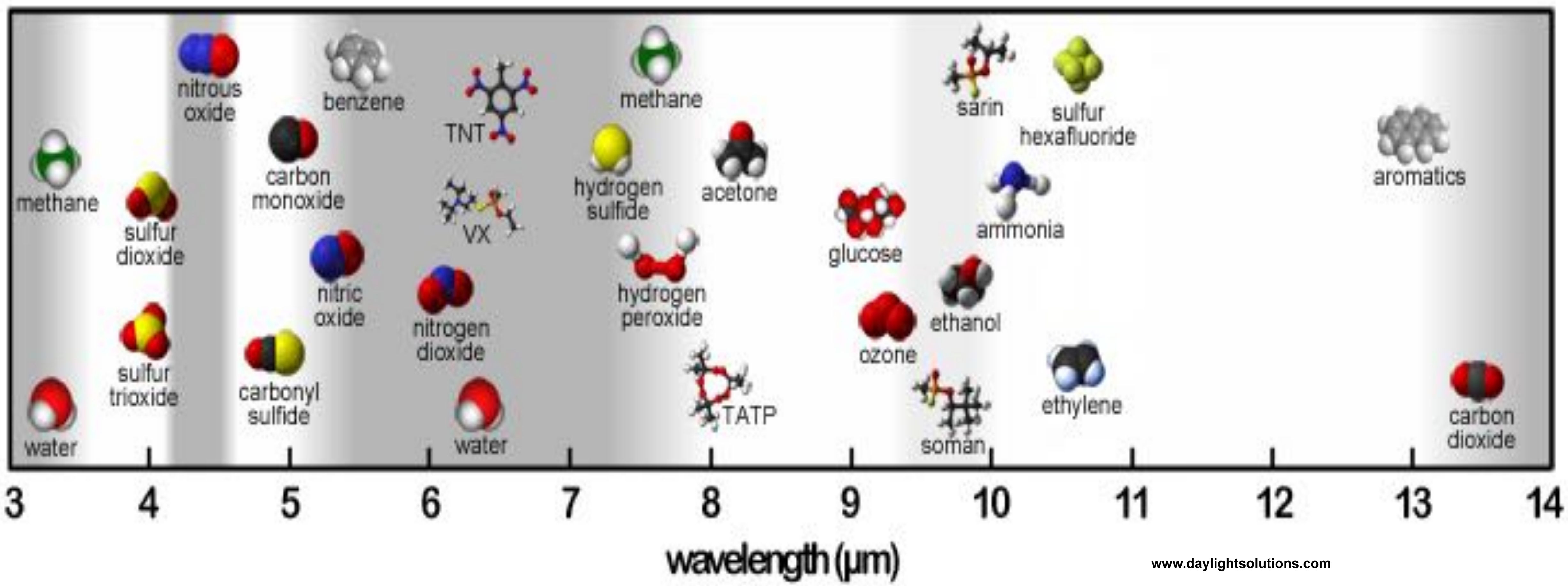

www.daylightsolutions.com

Mid-IR

- Everything emits in the mid-IR…..
- Important frequency range for defense applications
  – Thermal imaging
  – Countermeasures

- www.imaging1.com
(Sierra Pacific Innovations)

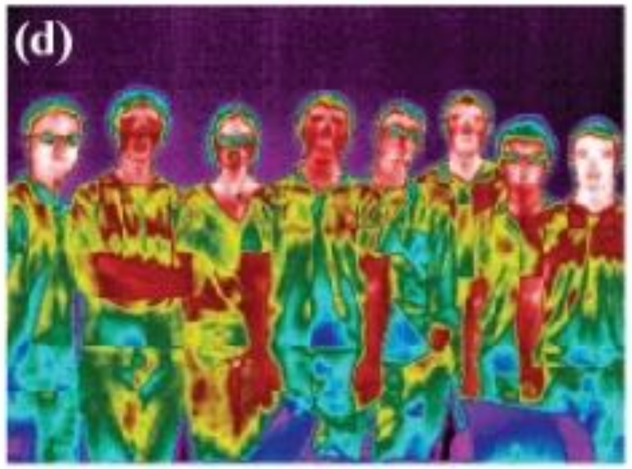

Ultrasensitive NH_3 sensor for urban air quality

(Tao *et al.*, *Opt. Lett*., 2012; Sun *et al.*, *Appl. Phys. B*, 2012; Miller *et al.*, *AMTD*, 2013)

- Mobile mapping, > 4500 km in CA/NJ
- Quantify emissions by tracer-tracer plots where one tracer's emissions known
  dairies: 0.8% NH_3 per CH_4 emitted
  vehicles: 2% NH_3 per CO emitted
- NASA TES NH_3 satellite validation
- fast response: >10X change in conc. in 1 s

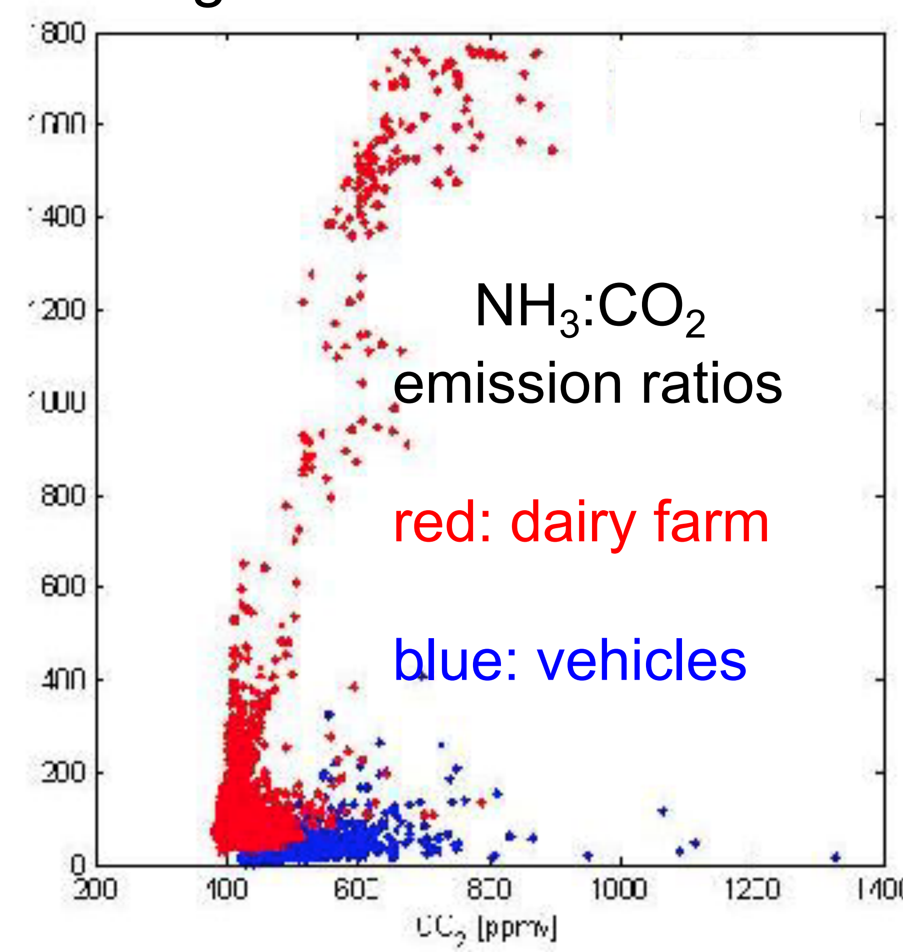

Infrared instruments

- **<u>Challenges of IR instrument design and construction:</u>**
  - Everything, not just the chip, must be at cryogenic temperatures.
  - Many of the more robust IR optical materials (e.g. zinc sulfide, zinc selenide) don't transmit well in the visible, which hampers alignment and set up.
  - On the other hand, crystalline materials like calcium fluoride and barium fluoride which do transmit both optical and IR light are fragile and harder to work optically.
  - Cryogenic refractive indexes are also needed.
  - Elimination of diffusely scattered light using blackened baffles requires care because anything truly black has almost 100% emissivity and will therefore be a strong infrared emitter unless very cold.
  - All dimensions will change during cool-down of the instrument and worse, parts not made from the same materials will shrink by different amounts due to dissimilar coefficients of expansion.
  - Lens holders could crush their optical components, optical separations will change and materials may experience stress.
  - All these things must be calculated beforehand and each component must be constructed in such a way as to achieve the correct dimensions after it is cold.

Materials

- Most optically transparent materials in the mid-IR are semiconductors
- High index of refraction (high Ref.)
- Phonon resonances in 20-60um range

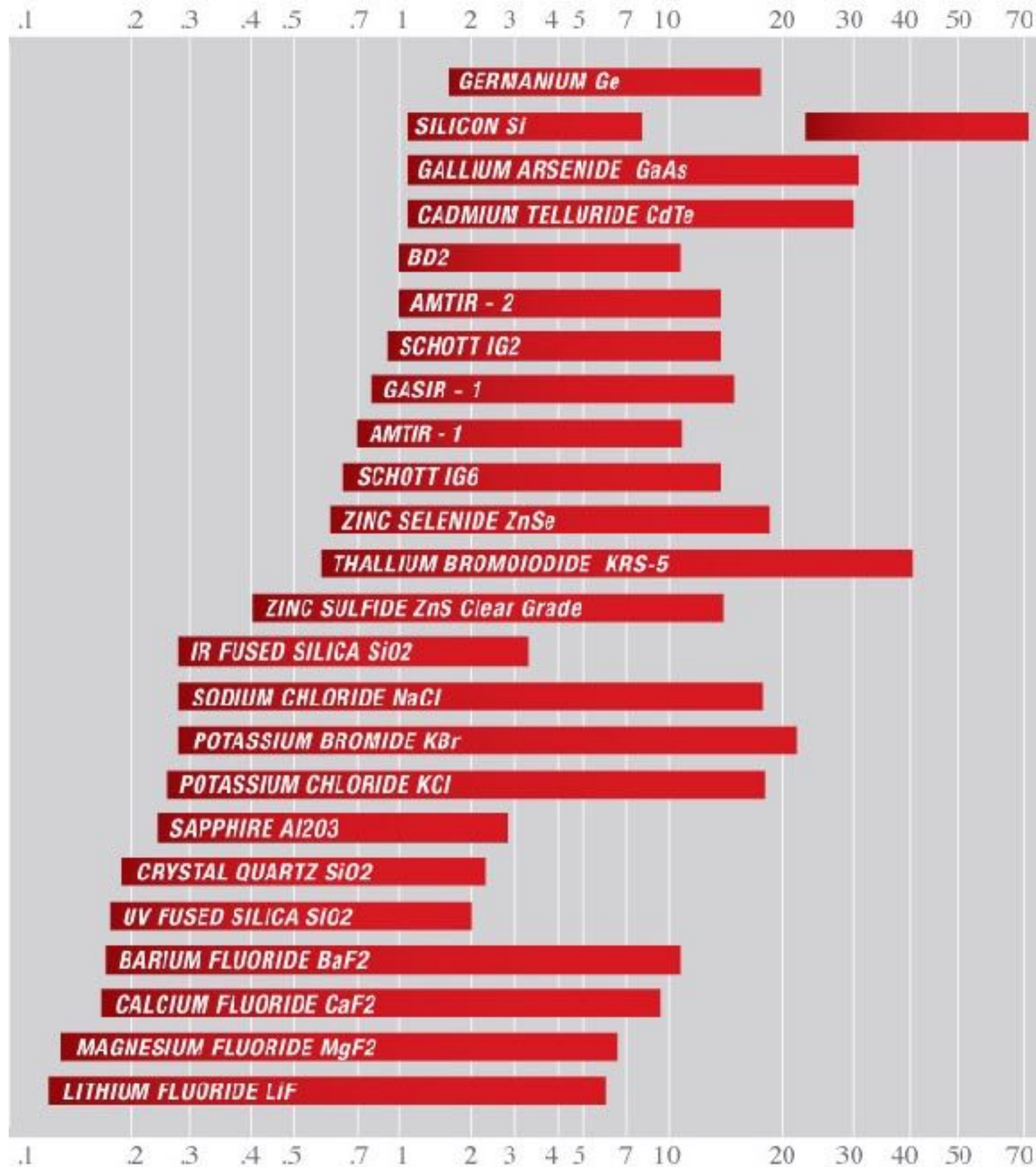

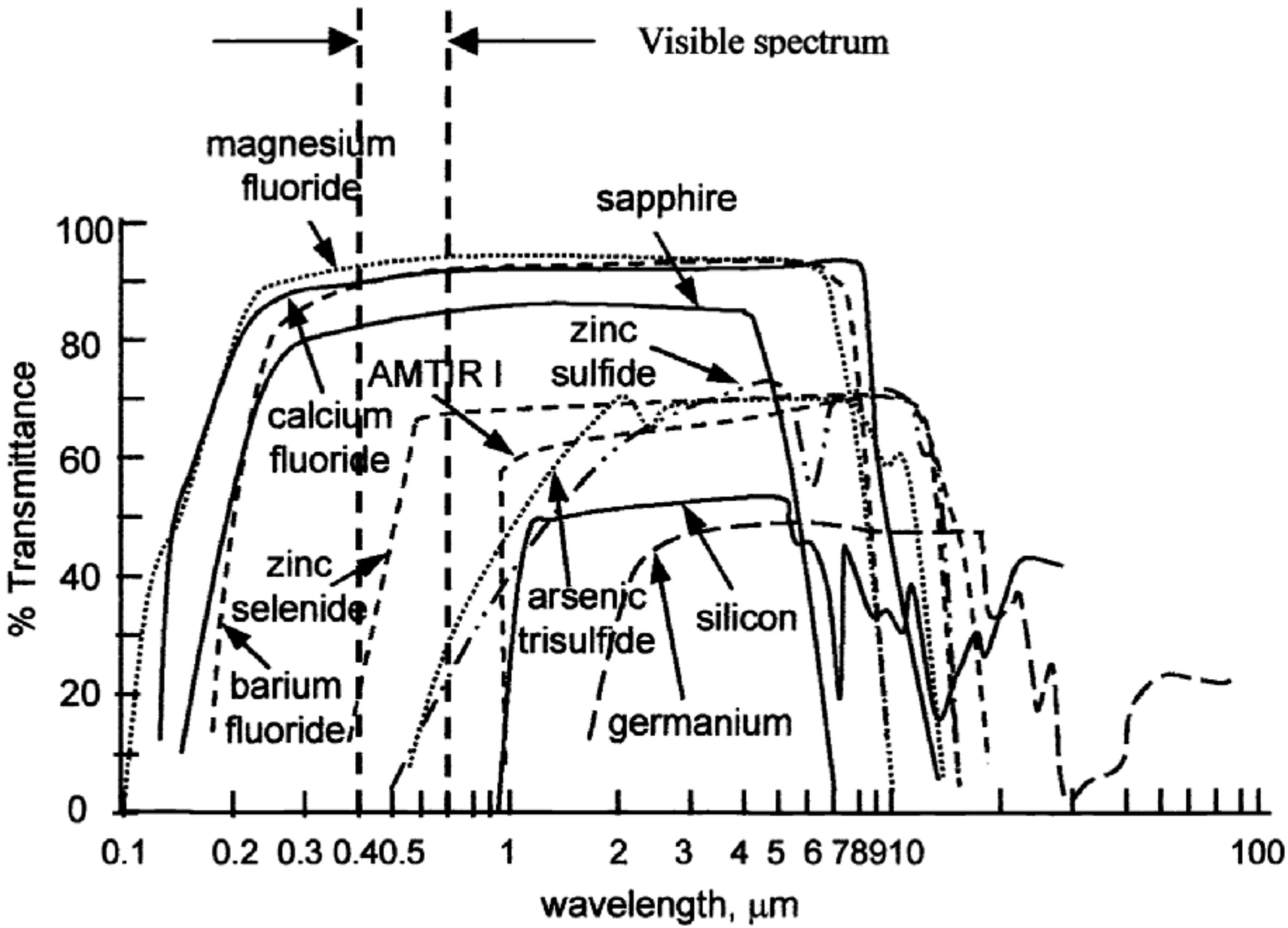

Visible spectrum
magnesium fluoride
sapphire
100
80
60
40
20
0
% Transmittance
zinc sulfide
AMTIR I
calcium fluoride
zinc selenide
barium fluoride
arsenic trisulfide
silicon
germanium
0.1
0.2
0.3
0.4
0.5
1
2
3
4
5
6
7
8
9
10
100
wavelength, µm

Far-infrared Ge arrays

- **Longer than 40 μm there are no appropriate shallow dopants for silicon and therefore extrinsic germanium (Ge) must be used.**
- There are a number of problems with the use of germanium.
  - To control dark current, Ge must be relatively lightly doped; then absorption lengths are 3-5 mm.
  - Because diffusion lengths are also large (250-300 μm), pixel dimensions of 500-700 μm are required to minimize crosstalk.
  - Large pixels imply higher hit rates for cosmic rays, especially in space, and this in turn implies that the readout device must have very low noise so that the background limit is reached in the shortest possible exposure time.
  - But a large detector pixel means a large capacitance and more noise.
  - Also, the photoconductive gain is inversely proportional to the inter-electrode spacing resulting in poor QE unless side-illuminated detectors with transverse contacts are used.
  - Finally, because of the very small energy band gaps, these detectors must operate at liquid helium temperatures well below the silicon "freeze-out" range.

The net absorption is characterized by the absorption coefficient, *a*. Note the difference between direct and indirect absorption (e.g., silicon vs. GaAs). Quantum mechanical selection rules do not permit transfers at the band gap energy for indirect absorbers.

The **quantum efficiency** is:

$$\eta_{ab} = \frac{S_0 - S_0\, e^{-a(\lambda)\, d_1}}{S_0} = 1 - e^{-a(\lambda)\, d_1}, \qquad (3)$$

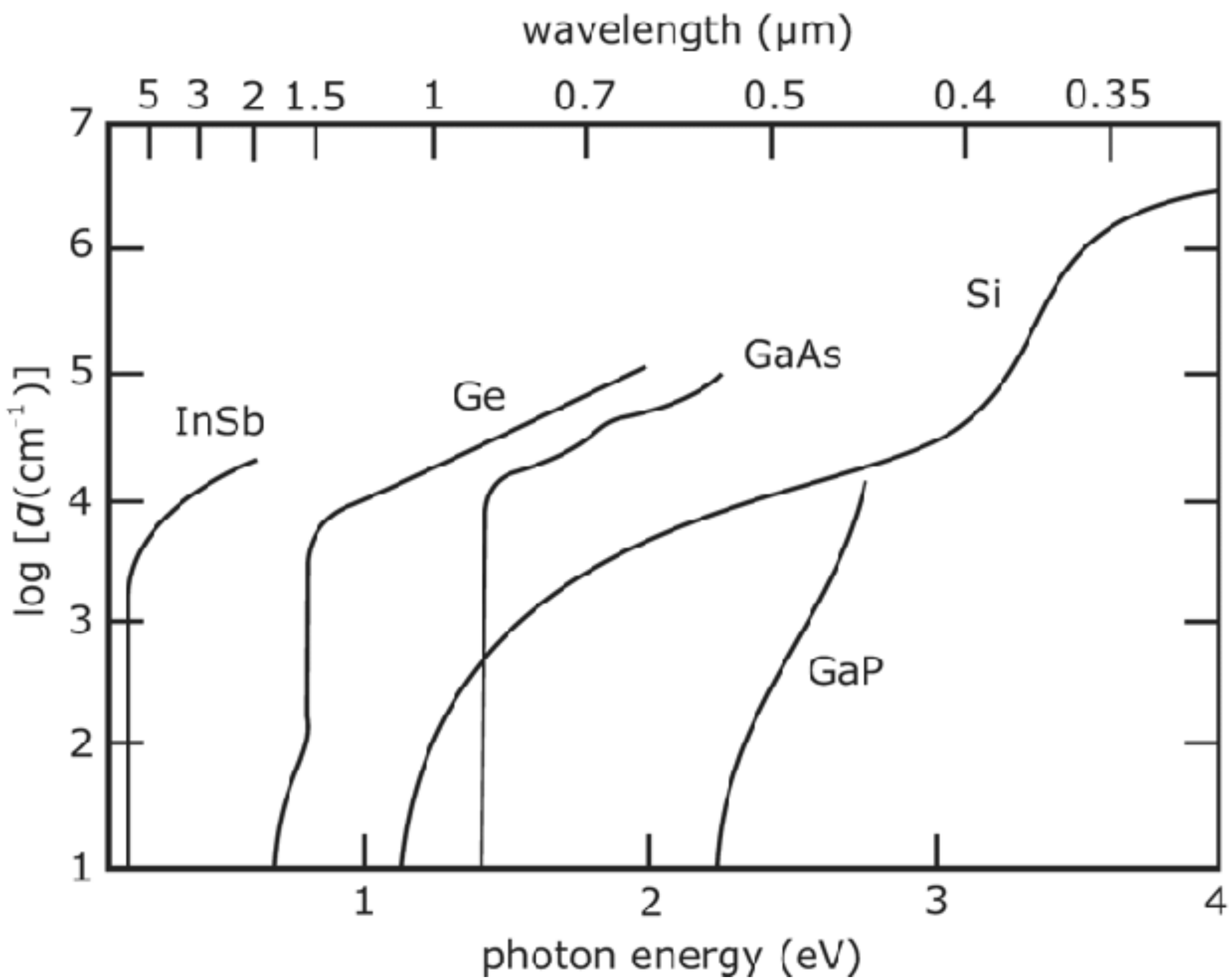

- Here are some photodiode materials and their cutoff wavelengths.

HgCdTe has a variable bandgap set by the relative amounts of Hg and Te in the crystal. AlGaAsSb behaves similarly.

- Indirect absorbers will have poor QE just short of the cutoff

Material	Cutoff wavelength (μm)
Si	1.1 (indirect)
Ge	1.8 (indirect)
InAs	3.4 (direct)
InSb	6.8 (direct)
HgCdTe	~1.2 - ~ 15 (direct)
GaInAs	1.65 (direct)
AlGaAsSb	0.75 – 1.7 (direct)

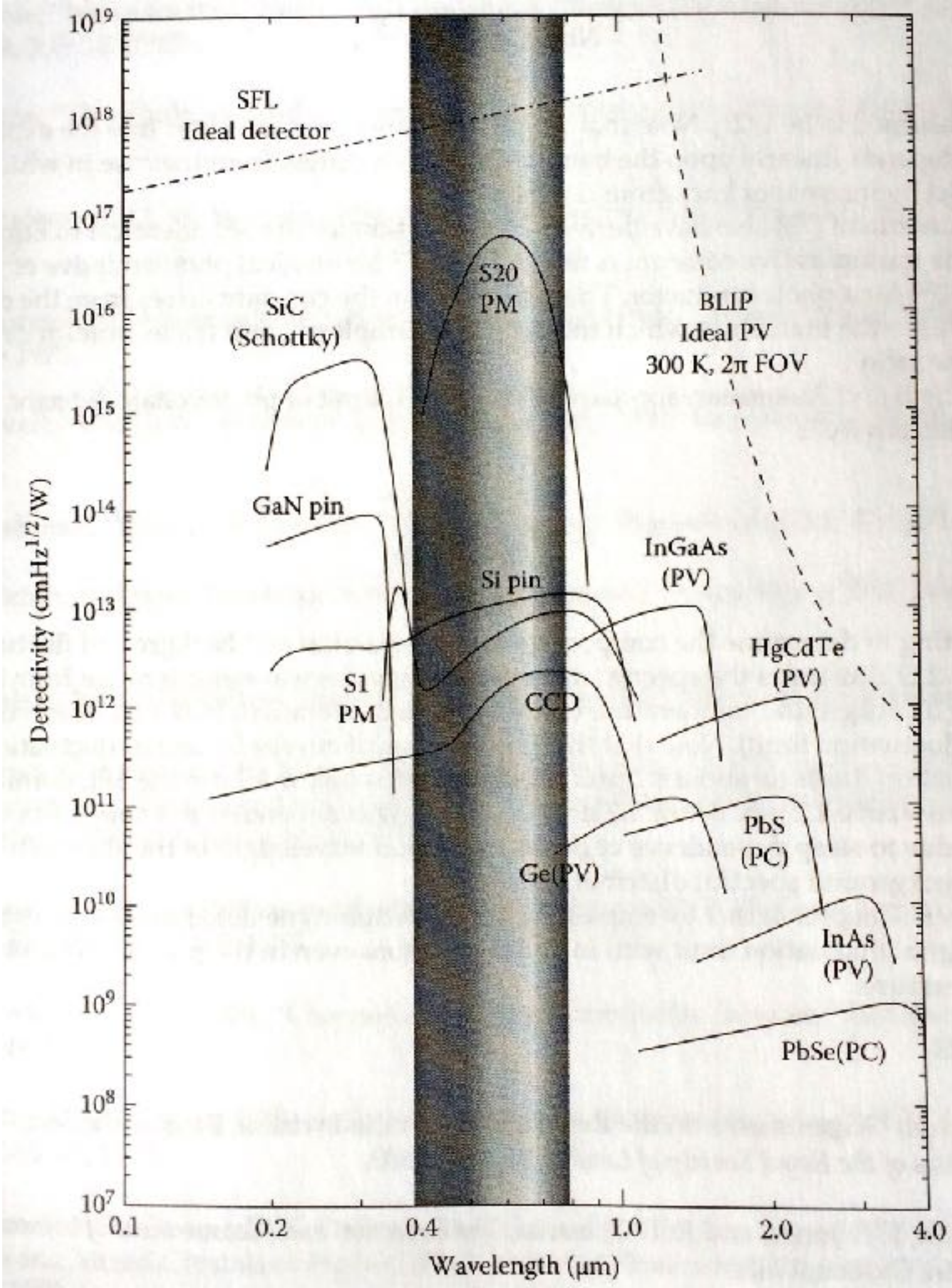

SFL
Ideal detector
SiC
(Schottky)
S20
PM
BLIP
Ideal PV
300 K, 2π FOV
GaN pin
InGaAs
(PV)
Si pin
HgCdTe
(PV)
S1
PM
CCD
PbS
(PC)
Ge(PV)
InAs
(PV)
PbSe(PC)
Detectivity (cmHz^1/2/W)
Wavelength (μm)
10^19
10^18
10^17
10^16
10^15
10^14
10^13
10^12
10^11
10^10
10^9
10^8
10^7
0.1
0.2
0.4
1.0
2.0
4.0

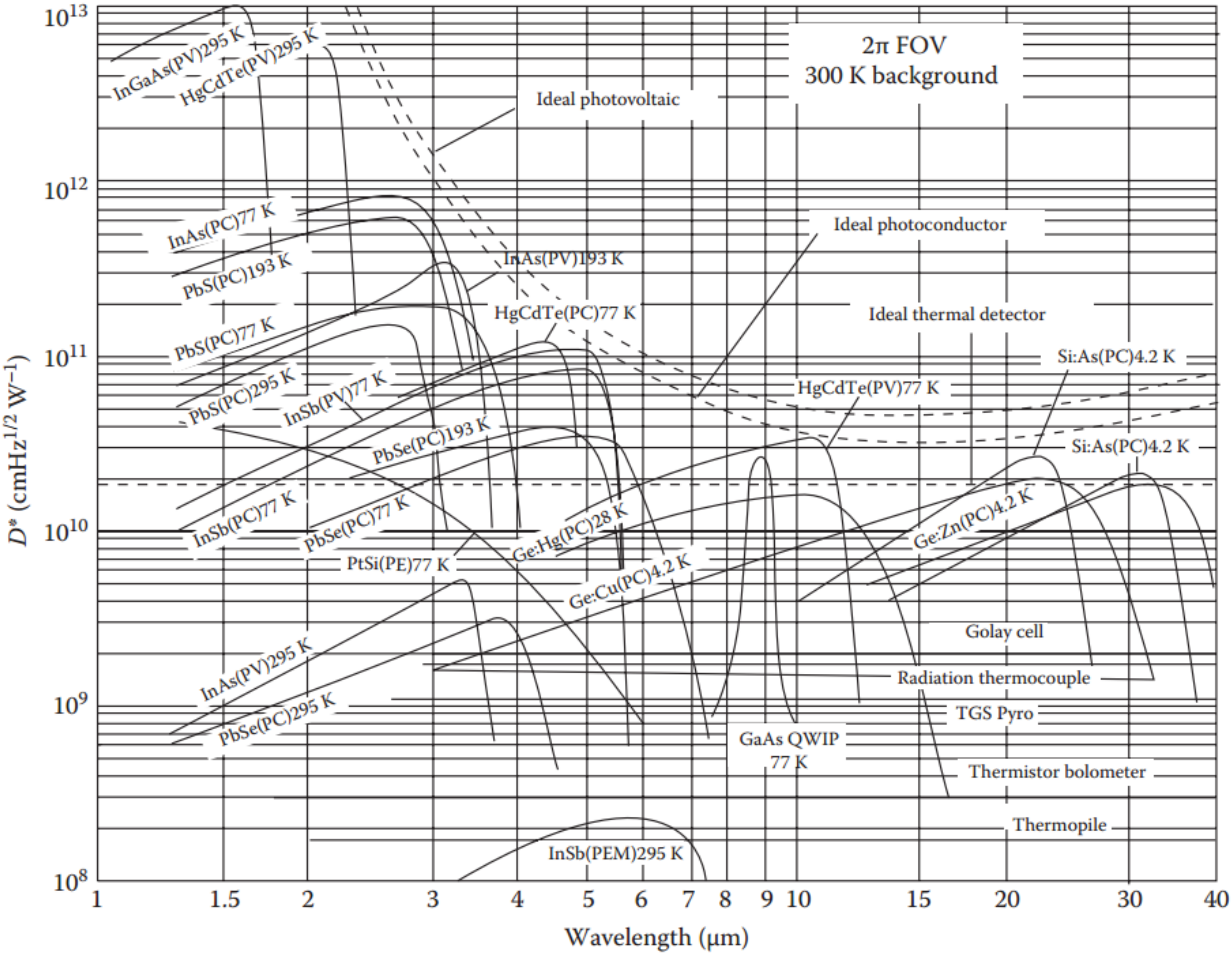

2π FOV
300 K background
Ideal photovoltaic
Ideal photoconductor
Ideal thermal detector
InGaAs(PV)295 K
HgCdTe(PV)295 K
InAs(PC)77 K
PbS(PC)193 K
InAs(PV)193 K
HgCdTe(PC)77 K
PbS(PC)77 K
PbS(PC)295 K
InSb(PV)77 K
PbSe(PC)193 K
InSb(PC)77 K
PbSe(PC)77 K
PtSi(PE)77 K
Ge:Hg(PC)28 K
Ge:Cu(PC)4.2 K
HgCdTe(PV)77 K
Si:As(PC)4.2 K
Si:As(PC)4.2 K
Ge:Zn(PC)4.2 K
InAs(PV)295 K
PbSe(PC)295 K
Golay cell
Radiation thermocouple
TGS Pyro
GaAs QWIP
77 K
Thermistor bolometer
Thermopile
InSb(PEM)295 K
D^* (cmHz$^{1/2}$ W^{-1})
Wavelength (μm)

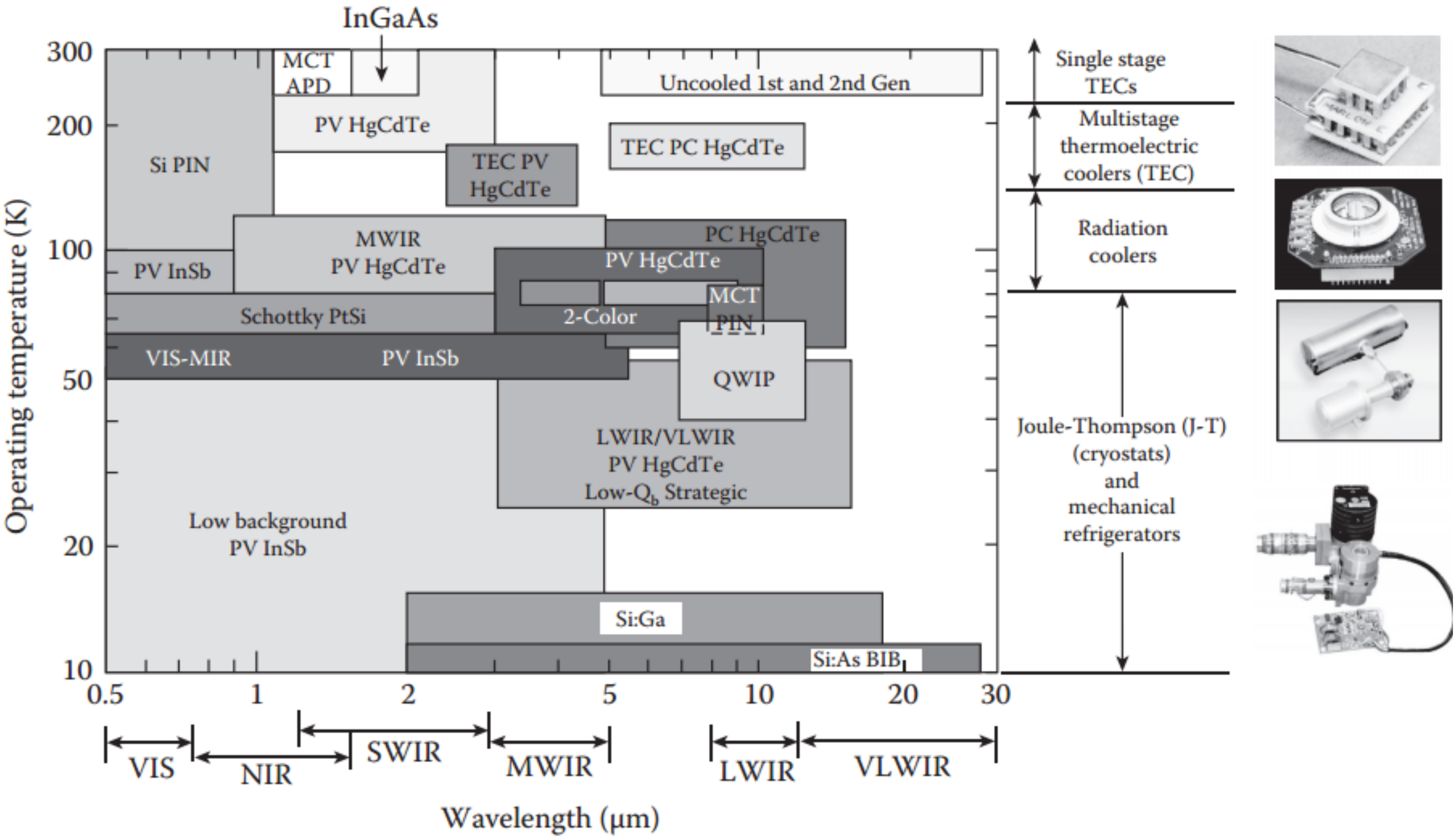

InGaAs
MCT APD
PV HgCdTe
Si PIN
TEC PV HgCdTe
Uncooled 1st and 2nd Gen
TEC PC HgCdTe
MWIR PV HgCdTe
PC HgCdTe
PV HgCdTe
PV InSb
2-Color
MCT PIN
Schottky PtSi
VIS-MIR
PV InSb
QWIP
LWIR/VLWIR PV HgCdTe Low-Q_b Strategic
Low background PV InSb
Si:Ga
Si:As BIB
Operating temperature (K)
300
200
100
50
20
10
0.5
1
2
5
10
20
30
VIS
NIR
SWIR
MWIR
LWIR
VLWIR
Wavelength (μm)
Single stage TECs
Multistage thermoelectric coolers (TEC)
Radiation coolers
Joule-Thompson (J-T) (cryostats) and mechanical refrigerators

Detector Type			Advantages	Disadvantages
Thermal (thermopile, bolometers, pyroelectric)			Light, rugged, reliable, & low cost Room temperature operation	Low detectivity at high frequency Slow response (ms order)
Photon	Intrinsic	IV–VI (PbS, PbSe, PbSnTe)	Easier to prepare More stable materials	Very high thermal expansion coefficient Large permittivity
		II–VI (HgCdTe)	Easy bandgap tailoring Well-developed theory & experience Multicolor detectors	Nonuniformity over large area High cost in growth and processing Surface instability
		III–V (InGaAs, InAs, InSb, InAsSb)	Good material & dopants Advanced technology Possible monolithic integration	Heteroepitaxy with large lattice mismatch Long wavelength cutoff limited to 7 μm (at 77 K)
	Extrinsic (Si:Ga, Si:As, Ge:Cu, Ge:Hg)		Very long wavelength operation Relatively simple technology	High thermal generation Extremely low temperature operation
	Free carriers (PtSi, Pt_2Si, IrSi)		Low-cost, high yields Large & close packed 2-D arrays	Low quantum efficiency Low temperature operation
	Quantum wells	Type I (GaAs/AlGaAs, InGaAs/AlGaAs)	Matured material growth Good uniformity over large area Multicolor detectors	High thermal generation Complicated design and growth
		Type II (InAs/InGaSb, InAs/InAsSb)	Low Auger recombination rate Easy wavelength control Multicolor detectors	Complicated design and growth Sensitive to the interfaces
	Quantum dots	InAs/GaAs, InGaAs/InGaP, Ge/Si	Normal incidence of light Low thermal generation	Complicated design and growth

IR Experiments

Infrared Astronomical Satellite (IRAS)

- First telescope to survey entire IR sky
- cooled to 2K with liquid Helium
- 1983 —>1983 (10 months)
- Mapped 96% of sky 4 times
- 12, 25, 60, 100 um
- 30”-2’ resolution
- discovered 350,000 sources
- 75,00 infrared starburst galaxies
- debris disks —> planetary systems in formation
- Huge impact on astronomy
- People STILL writing PhD theses with data !

IRAS 25, 60, 100 um

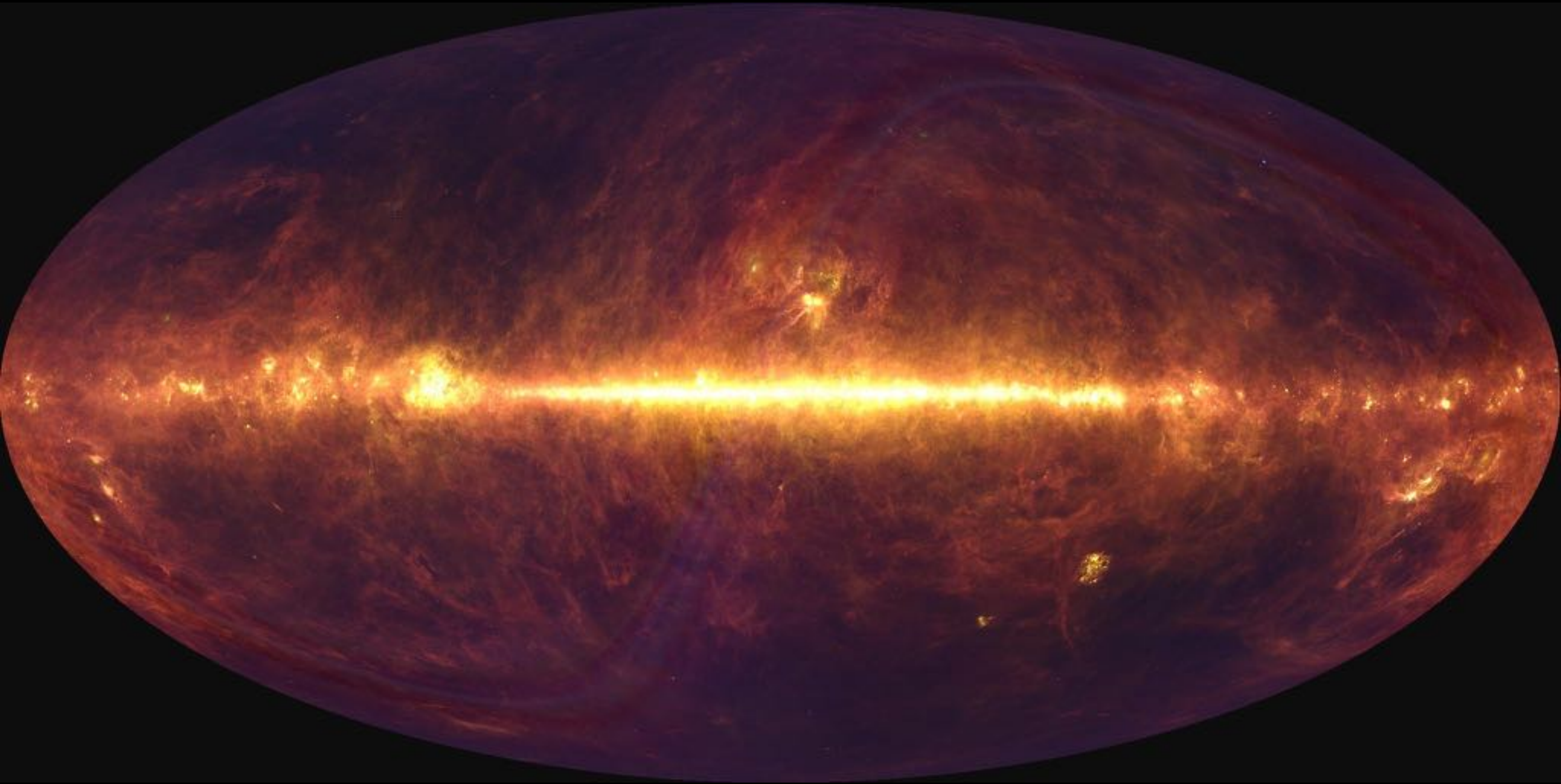

IRAS Point Source Catalog

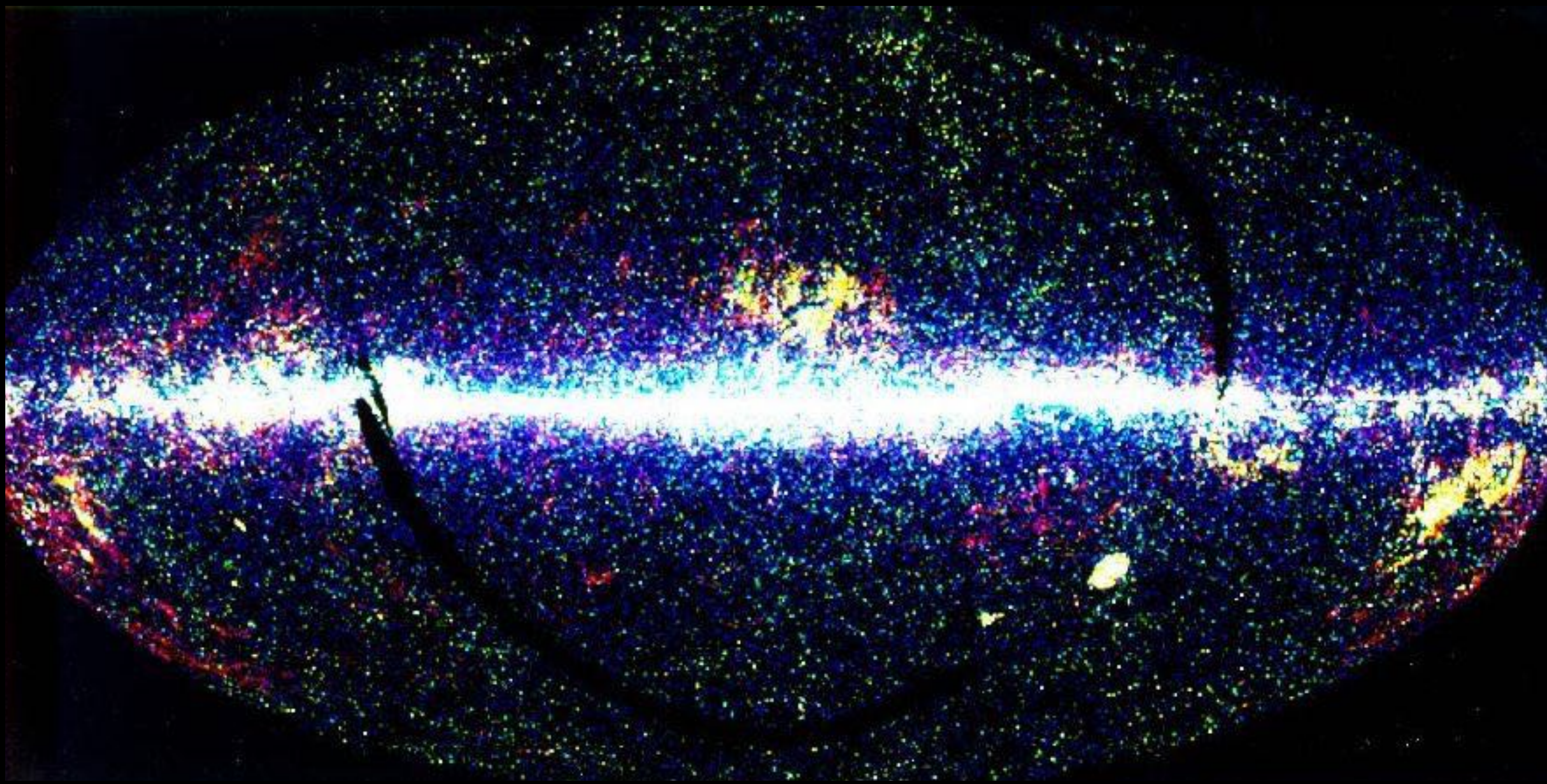

2 Micron All Sky Survey (2MASS)

- 1997-2001
- U.Mass, Caltech, IPAC
- Two 1.3m telescopes in Mt Hopkins, AZ, and CTIO, Chile
- J (1.25 μm), H (1.65 μm), and K_s (2.17 μm) to limiting magnitude ~14
- 300 million point sources and 1 million extended sources cataloged
- found many brown dwarfs
- cataloged many new star clusters
- catalogued many nearby galaxies and stars
- Is the standard reference catalog for astrometry.

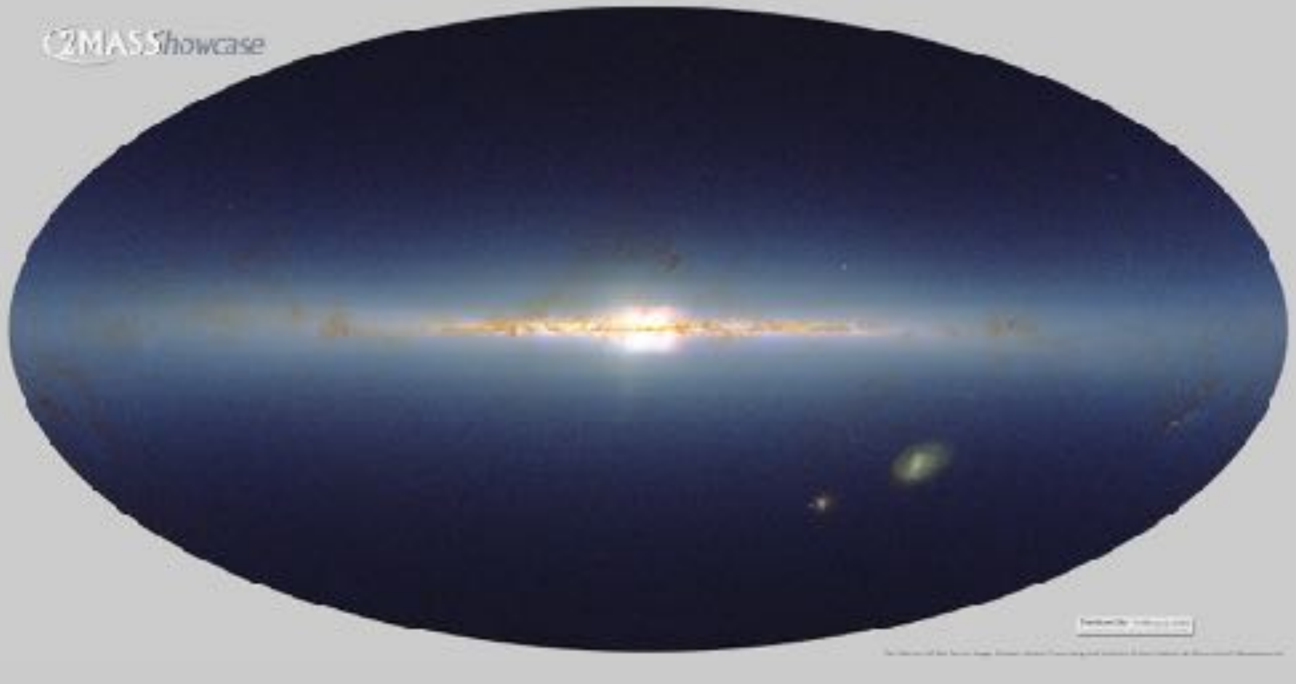

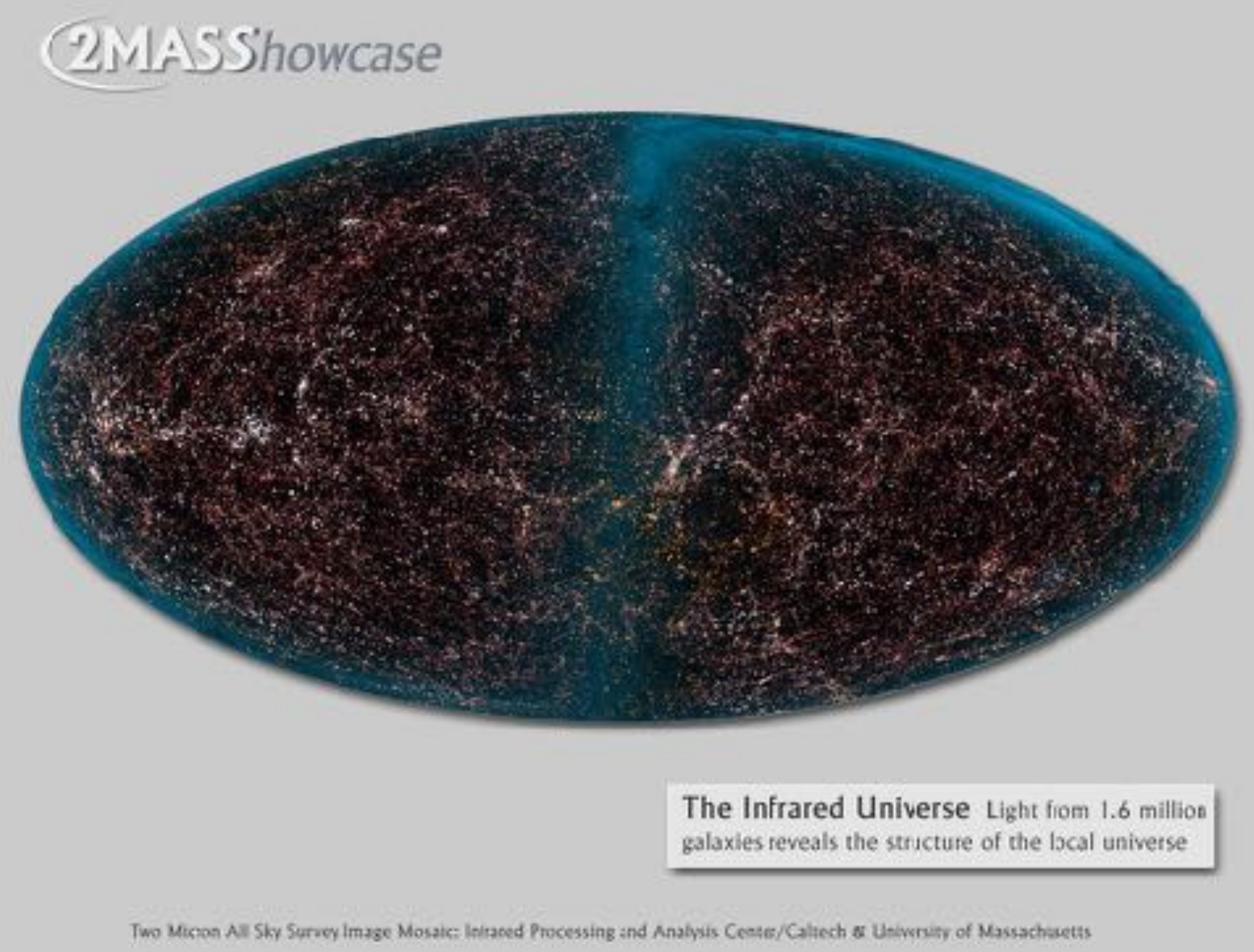

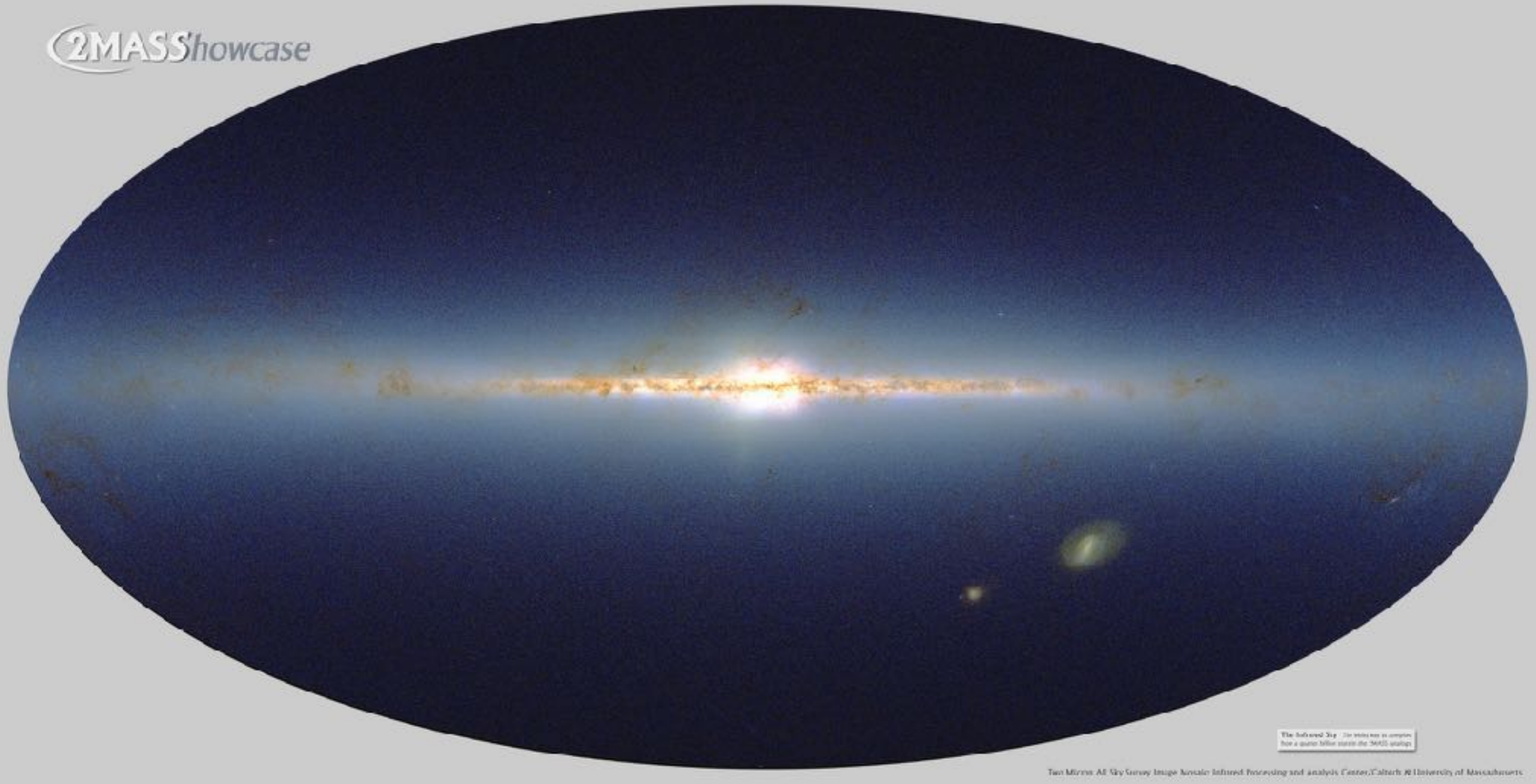
2MASSShowcase
The Infrared Sky
Two Micron All Sky Survey Image Mosaic Infrared Processing and analysis Center/Caltech & University of Massachusetts

2MASS*Showcase*

The Infrared Universe Light from 1.6 million galaxies reveals the structure of the local universe

Two Micron All Sky Survey Image Mosaic: Infrared Processing and Analysis Center/Caltech & University of Massachusetts

The VISTA Camera Array

VISTA is a 4-m wide-field survey telescope, equipped with a near infrared camera (1.65 degree diameter field of view) containing 67 million pixels of mean size 0.34 arcsec and broad band filters at Z,Y,J,H,Ks and a narrow band filter at 1.18 micron.

The VISTA camera contains 16 HgCdTe VIRGO detectors and is the largest IR mosaic thus far.

Previous IR Mission

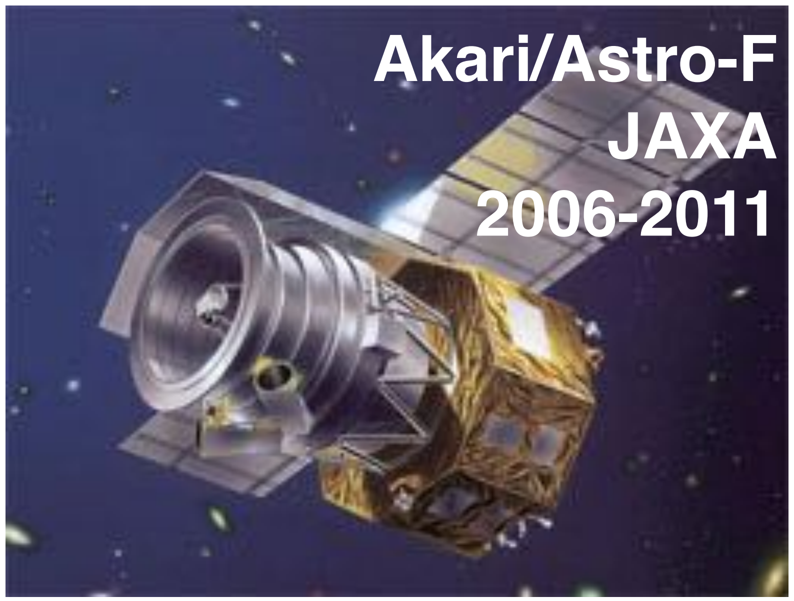

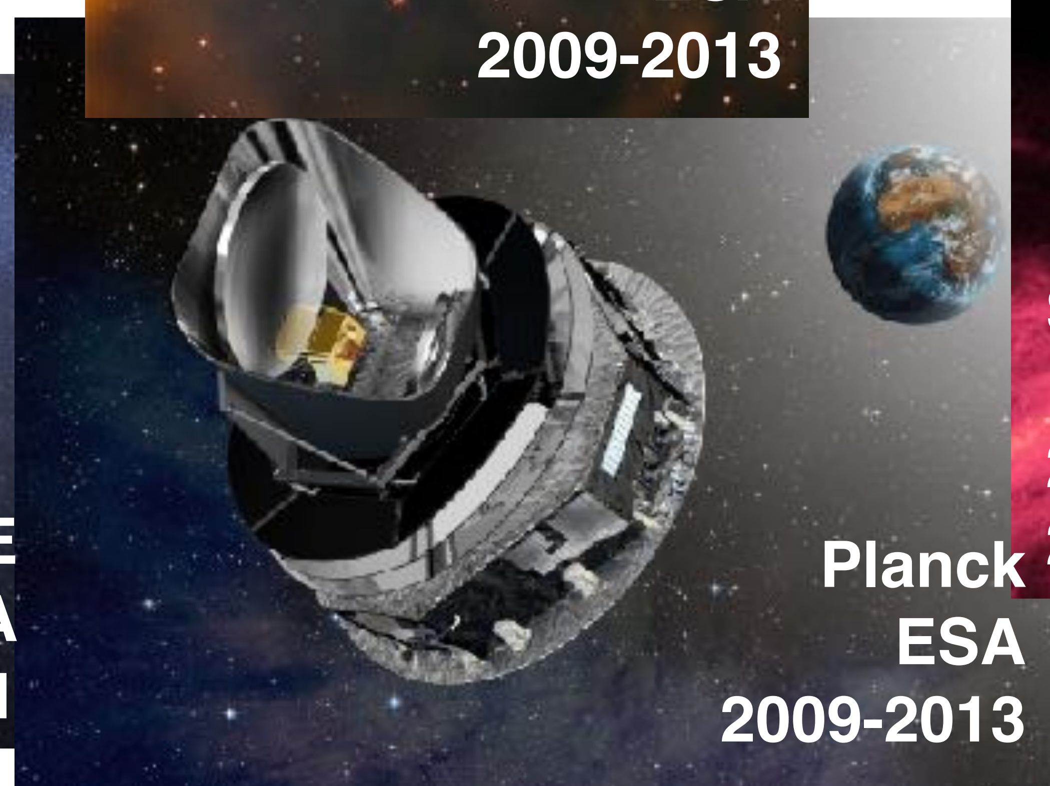

Wide Field Infrared Survey Explorer (WISE)

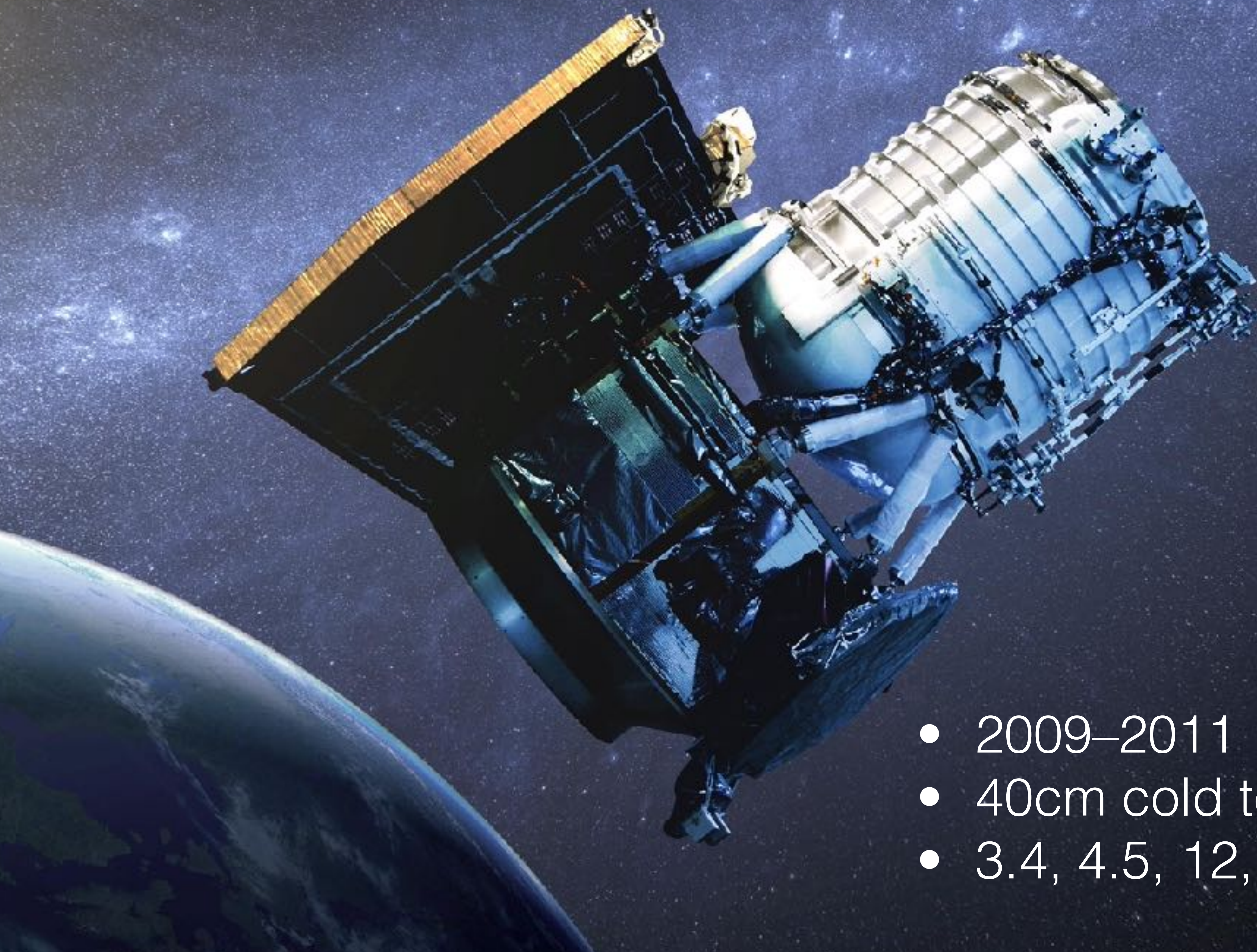

- 2009–2011
- 40cm cold telescope
- 3.4, 4.5, 12, 22 um

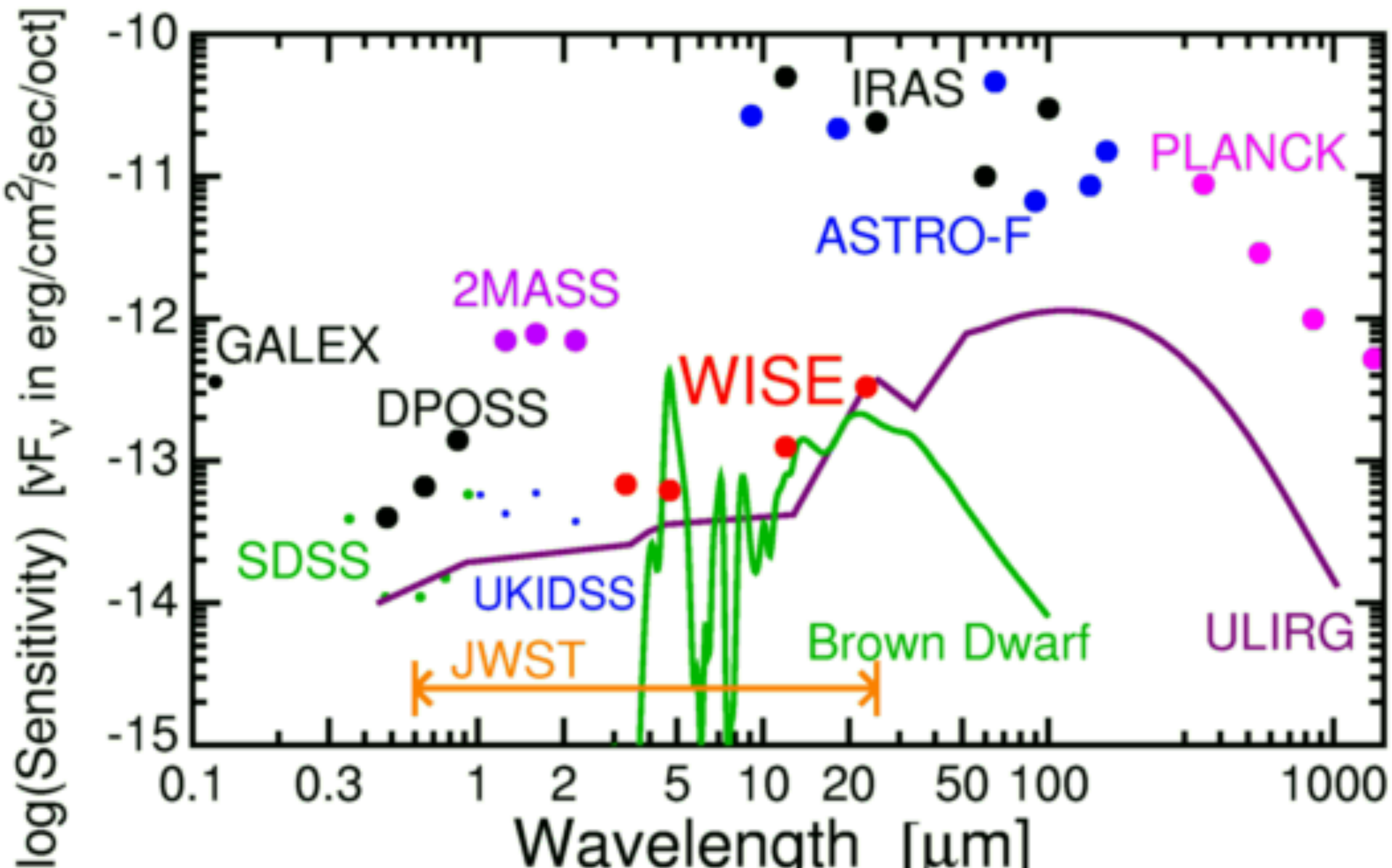

log(Sensitivity) [νFν in erg/cm²/sec/oct]
-10
-11
-12
-13
-14
-15
IRAS
PLANCK
ASTRO-F
2MASS
GALEX
WISE
DPOSS
SDSS
UKIDSS
ULIRG
Brown Dwarf
JWST
0.1
0.3
1
2
5
10
20
50
100
1000
Wavelength [μm]

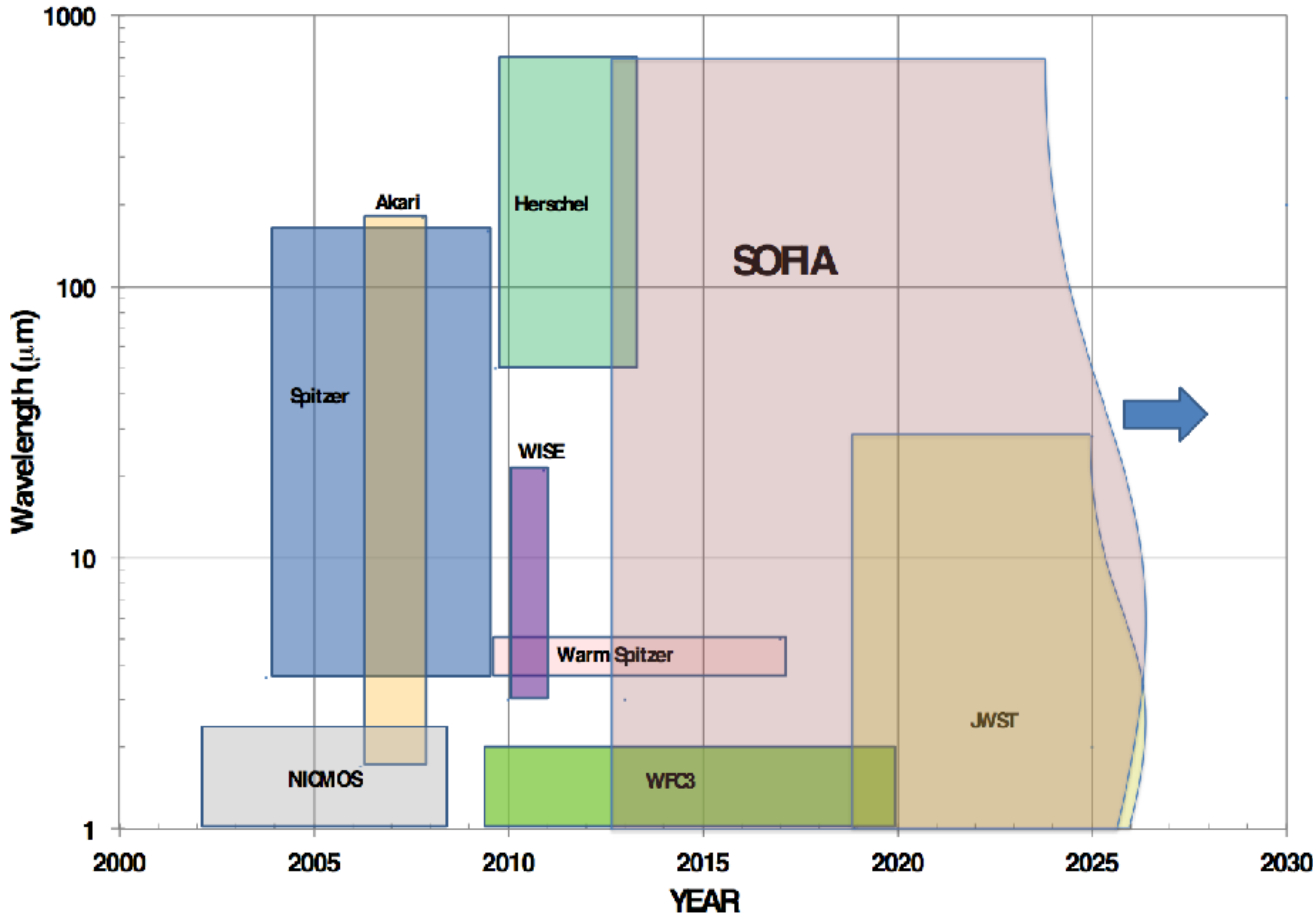
1000
100
10
1
Wavelength (μm)
2000
2005
2010
2015
2020
2025
2030
YEAR
Akari
Herschel
SOFIA
Spitzer
WISE
Warm Spitzer
JWST
NICMOS
WFC3

JWST
NASA
2021 —
10 years (probably more)

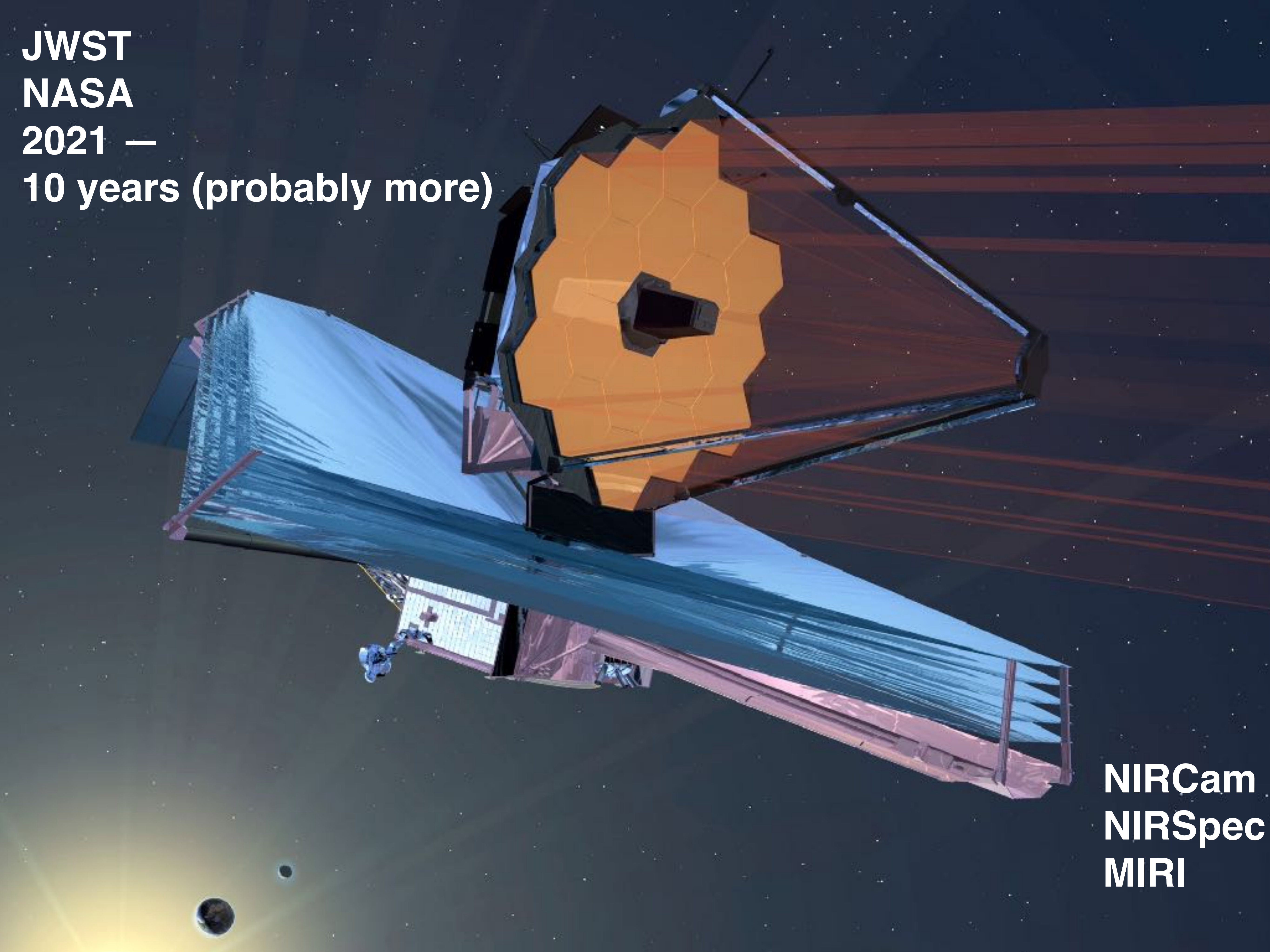

NIRCam
NIRSpec
MIRI

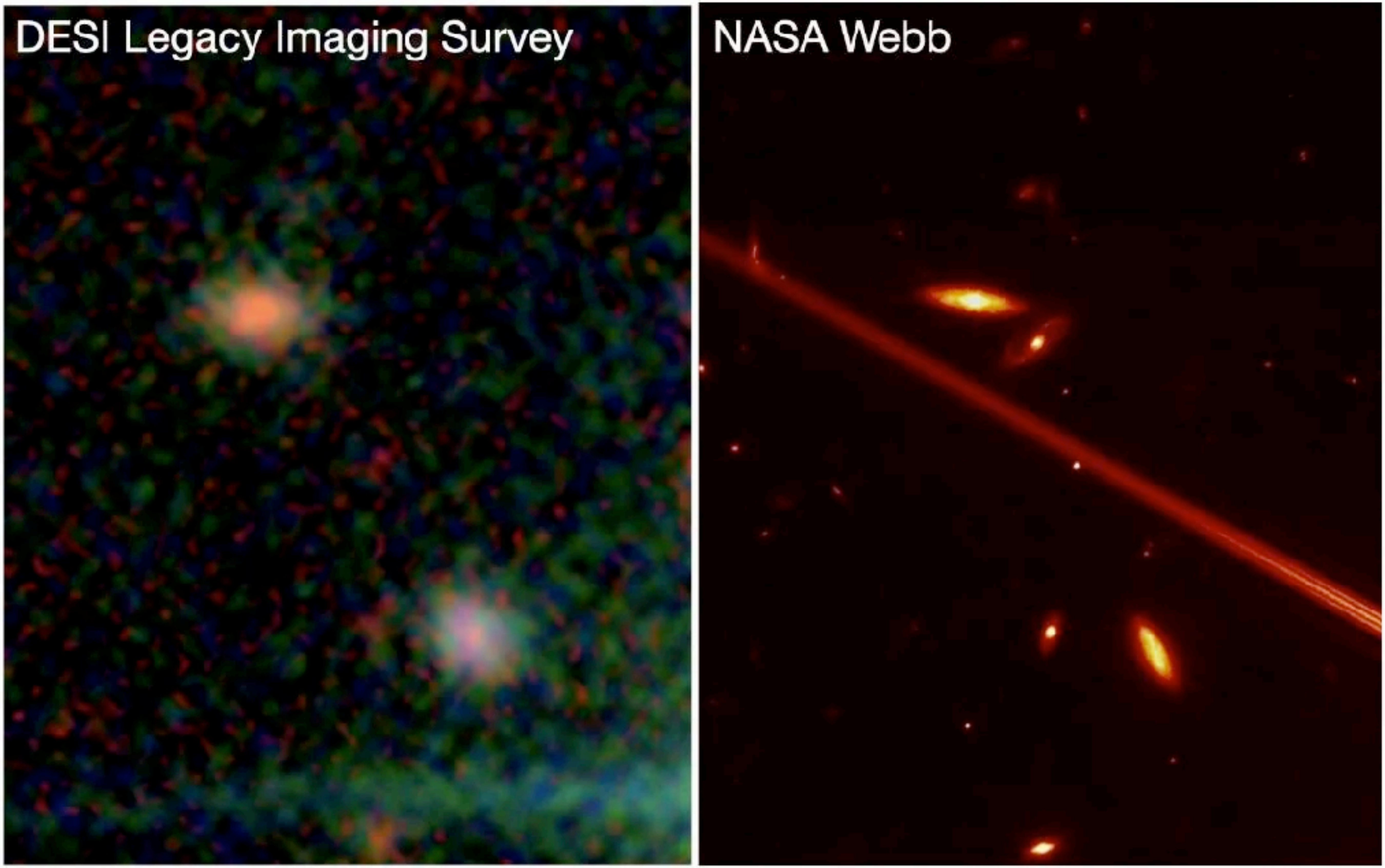
DESI Legacy Imaging Survey
NASA Webb

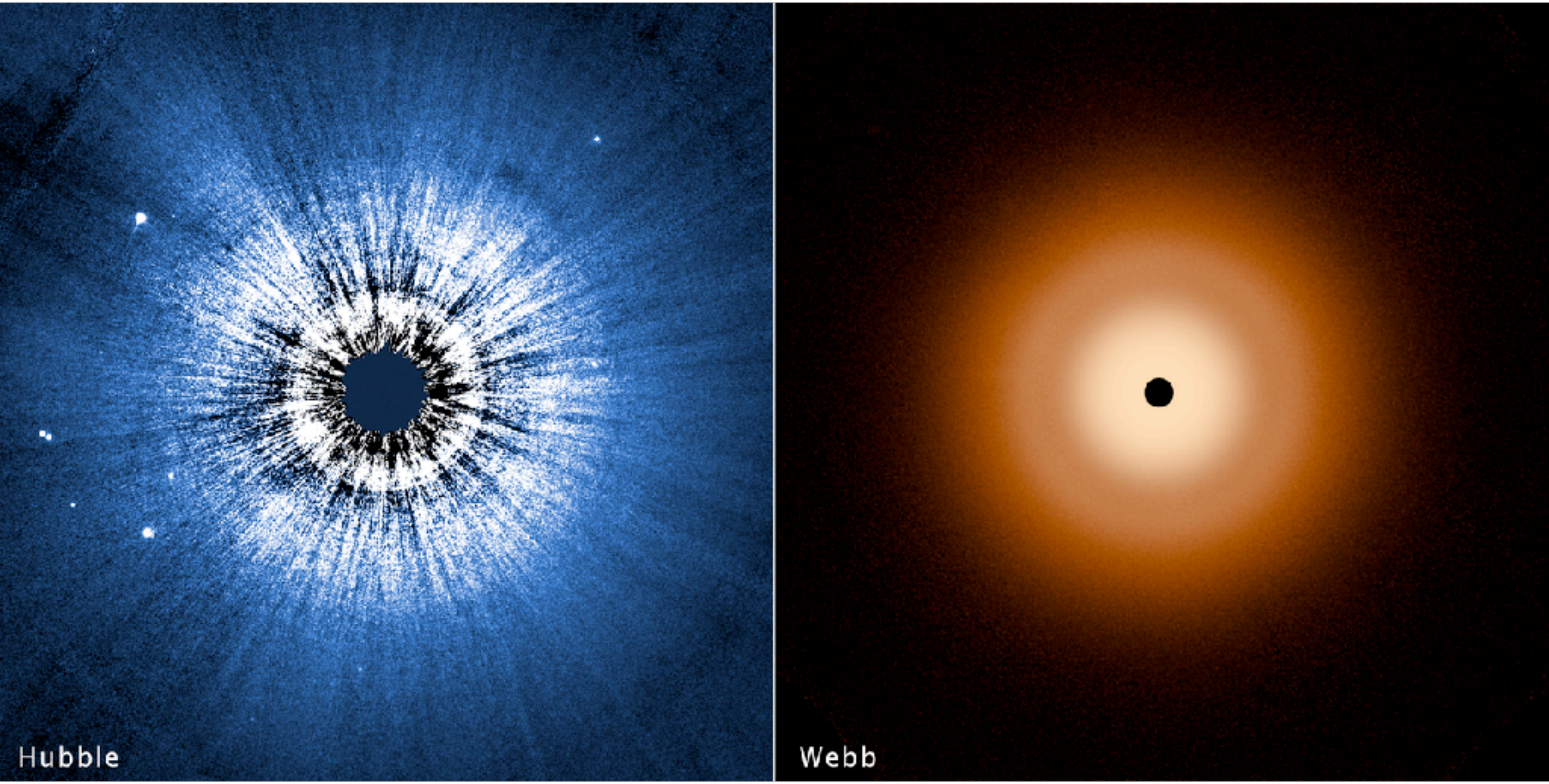

[left]

A Hubble Space Telescope false-color view of a 100-billion-mile-wide disk of dust around the summer star Vega. Hubble detects reflected light from dust that is the size of smoke particles largely in a halo on the periphery of the disk. The disk is very smooth, with no evidence of embedded large planets. The black spot at the center blocks out the bright glow of the hot young star.

[right]

The James Webb Space Telescope resolves the glow of warm dust in a disk halo, at 23 billion miles out. The outer disk (analogous to the solar system's Kuiper Belt) extends from 7 billion miles to 15 billion miles. The inner disk extends from the inner edge of the outer disk down to close proximity to the star. There is a notable dip in surface brightness of the inner disk from approximately 3.7 to 7.2 billion miles. The black spot at the center is due to lack of data from saturation.

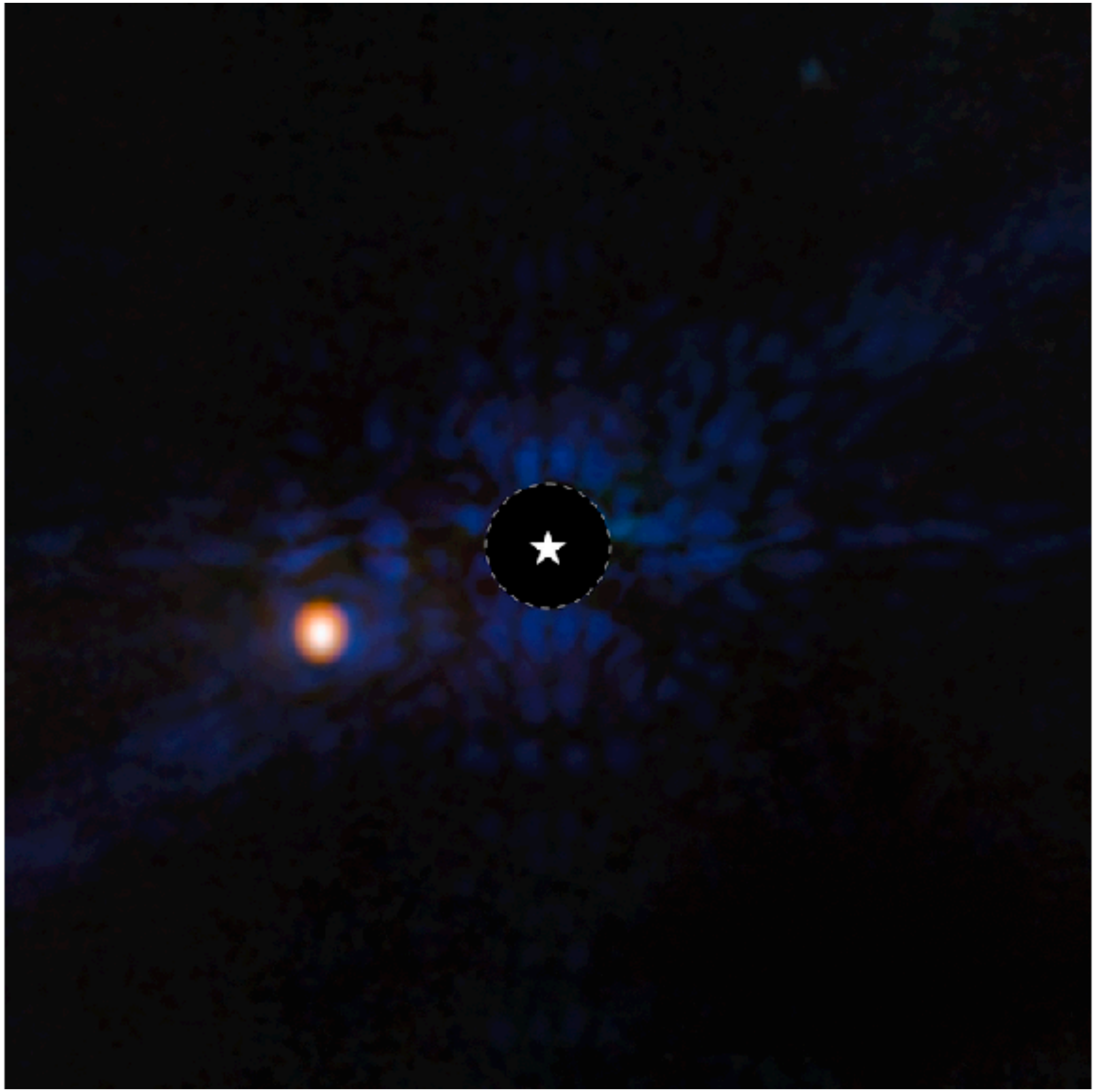

gas-giant exoplanet Epsilon Indi Ab with the MIRI coronagraph

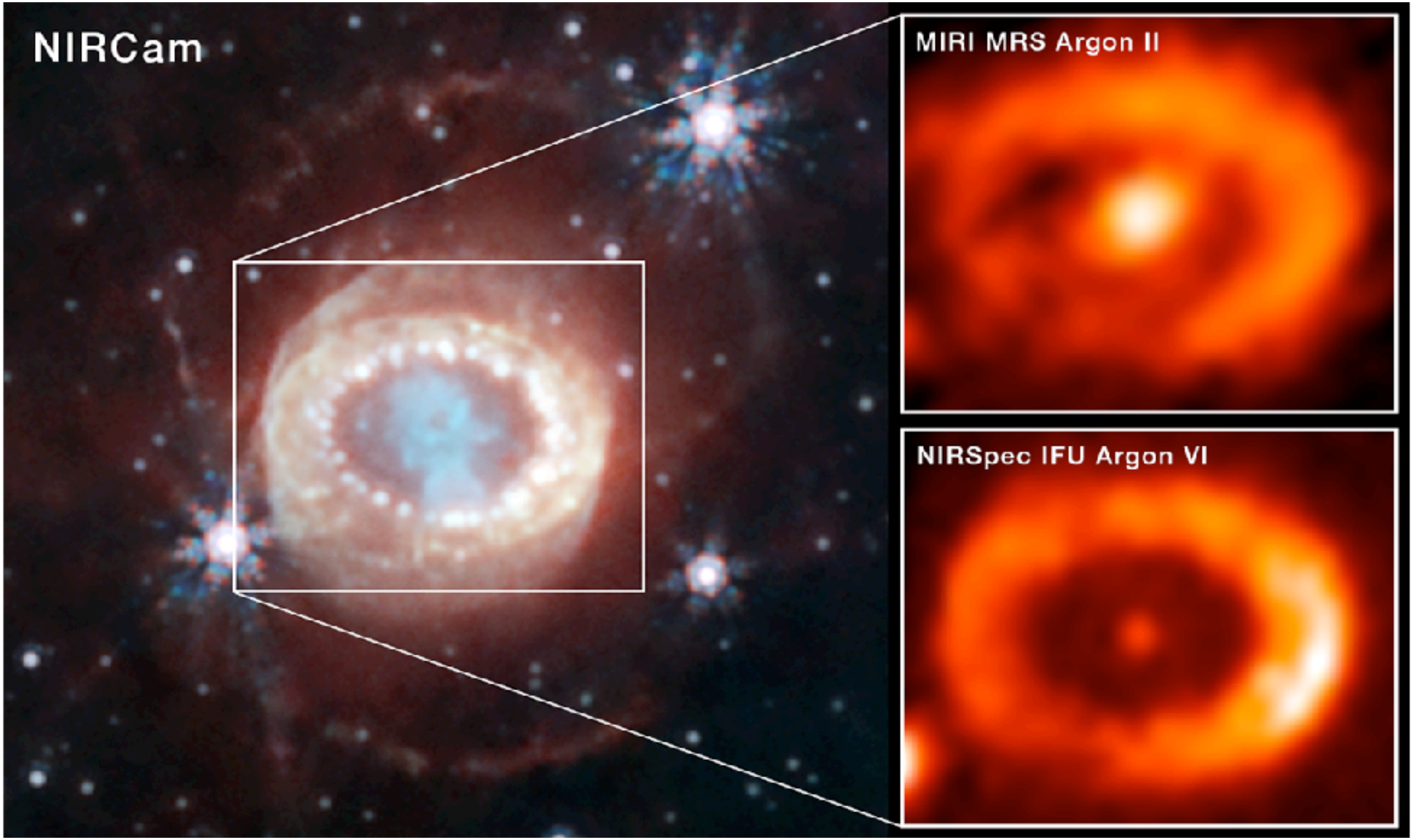
NIRCam
MIRI MRS Argon II
NIRSpec IFU Argon VI

In Hubble's image, the star-filled spiral arms glow brightly in blue, and the galaxies' cores in orange. Both galaxies are covered in dark brown dust lanes, which obscures the view of IC 2163's core at left.

In Webb's image, cold dust takes center stage, casting the galaxies' arms in white. Areas where stars are still deeply embedded in the dust appear pink.

HUBBLE AND WEBB SPACE TELESCOPES

SPIRAL GALAXIES | IC 2163 + NGC 2207

Hubble WFPC2 Filters | F439W F555W F814W **Webb MIRI** Filters | F770W F1130W F1500W

The Evolution of Infrared Space Telescopes

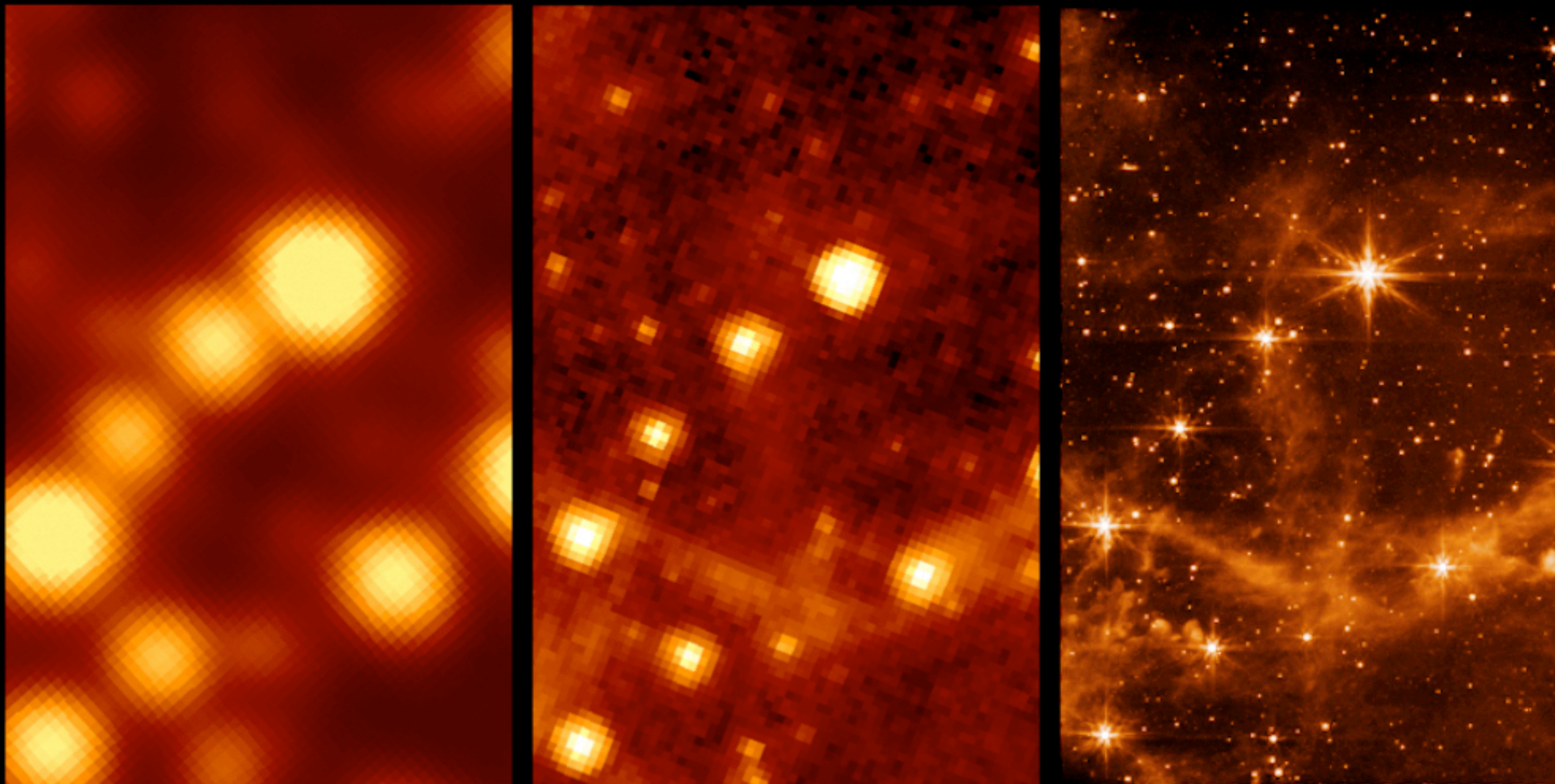

WISE W2 4.6 μm   Spitzer/IRAC 8.6 μm   JWST/MIRI 7.7 μm

Nancy Grace Roman Space Telescope

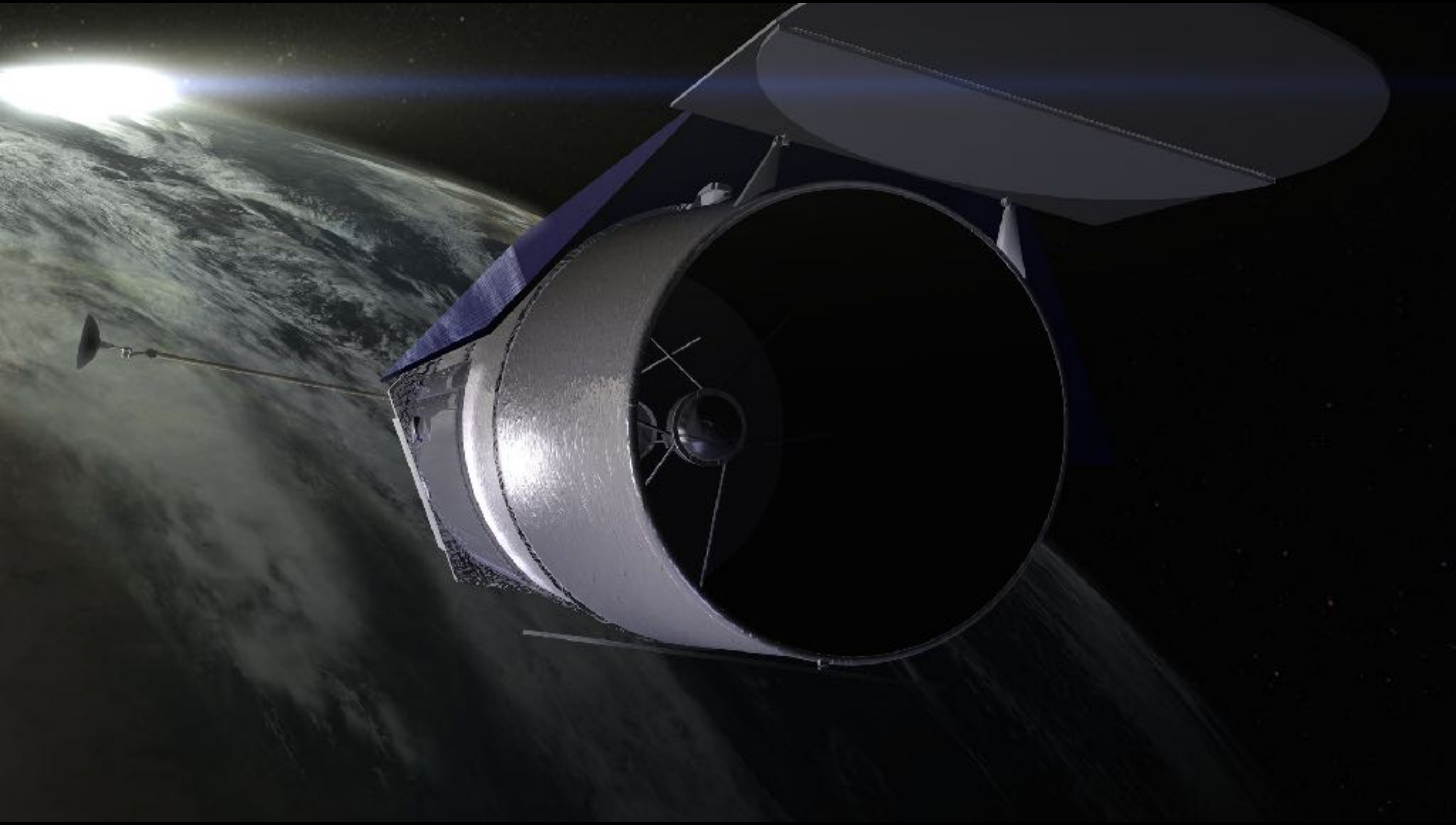

Launch window opens in Late 2026 - but probably 2027

IR Space Telescopes

Telescope	year	diameter [m]	temperature [K]	wavelength [um]	LHe [l]
IRAS	1983	0.51	2	12–100	720
ISO	1995—1998	0.6	3.4	2.4—240	2268
Spitzer	2003—2009	0.85	5.5	3.4—160	337
WIRE	1999—X	0.3	12	9—27	
Akari	2006—2011	0.68	5.5	2.5—160	2300
WISE	2009—2010	0.4	12	3.4—22	
Herschel	2009—2013	3.5	70	60—500	2400
Planck	2009—2013	1.5	56	350—3000	36,000
JWST	2021—2031	6.5	50	1—30	—
OST	2035 ??	9.2	4	30—500	—

Planning for the next big NASA mission

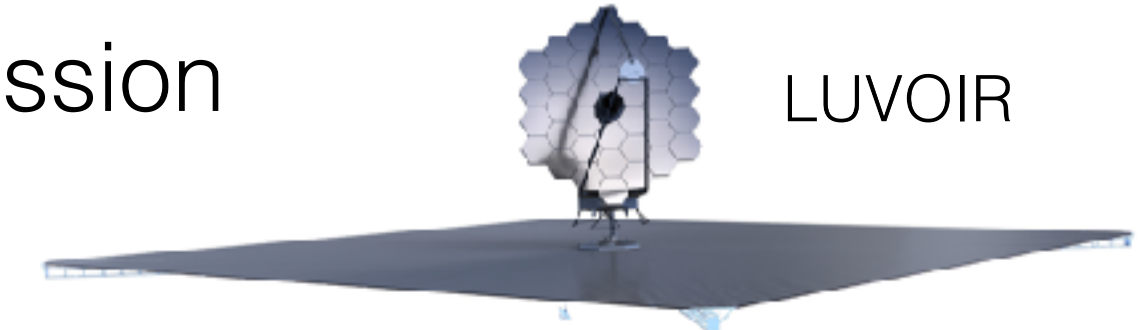

Four large mission concept studies studies were proposed for the last decadal review, but ultimately, the decadal didn't recommend any - they recommended a new hybrid approach.

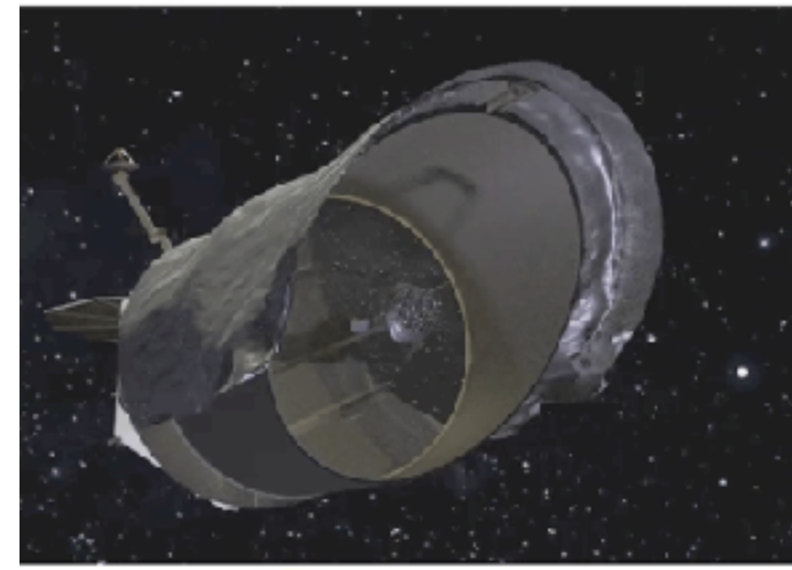

- **Large ultraviolet, optical and infrared (LUVOIR) telescope. Über *Hubble*. 8-15m active surface mirror.**
- Origins Space Telescope (OST) aka FIR Surveyor. Über *Spitzer*. Cold 8-12m mirror.
- X-ray Surveyor. Über *Chandra*.
- **The habitable exoplanet imaging mission (HabEx).**

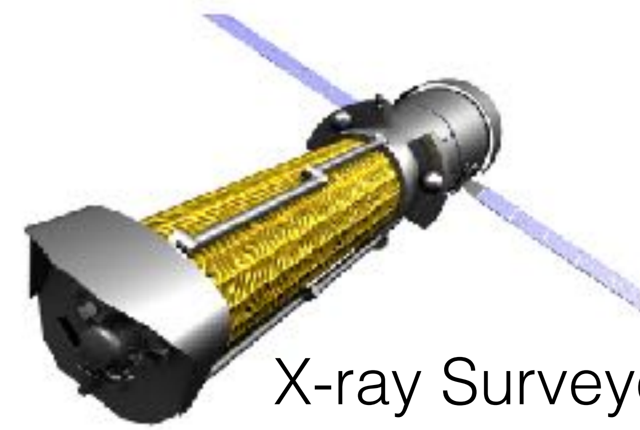

NEW TECHNOLOGIES ENABLE NEW CAPABILITIES TO EXPLORE OUR COSMIC ORIGINS

New Technology	New Capability
Space	Wavelength coverage JWST<—>ALMA
Cold Mirror	Spectroscopic line sensitivity
Large Telescope	Spatial resolution and sensitivity
Large Detector Arrays	Wide field imaging
Integrated Spectrometers	3D mapping

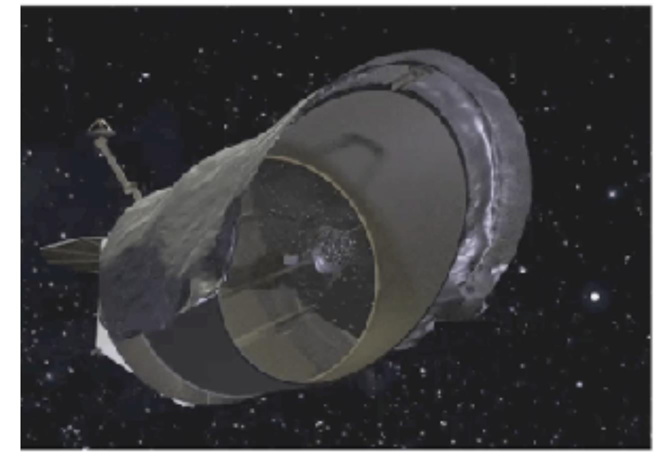

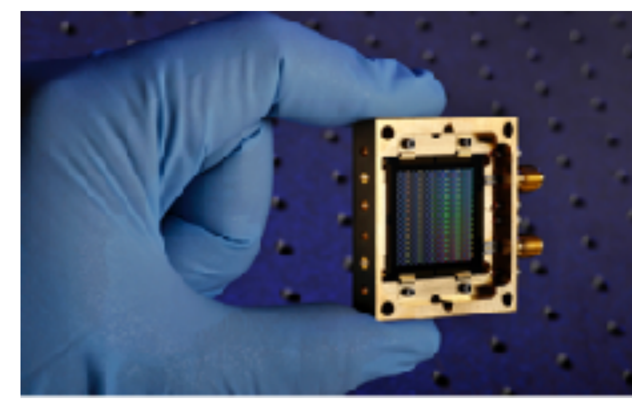

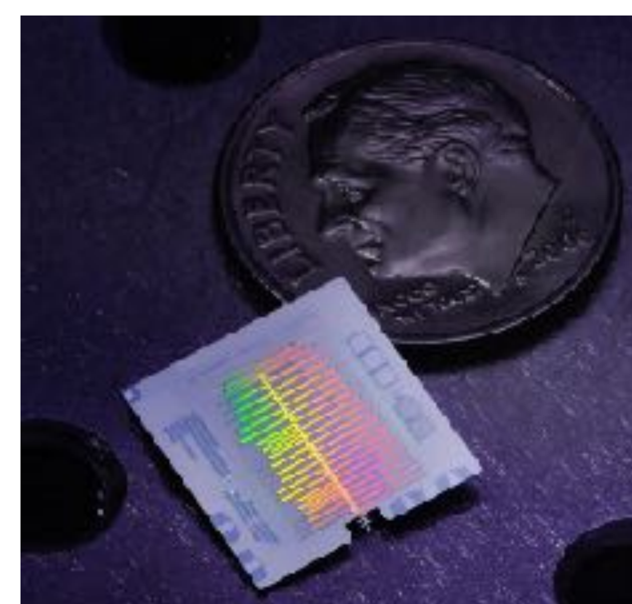

OST Spectral Line Sensitivity

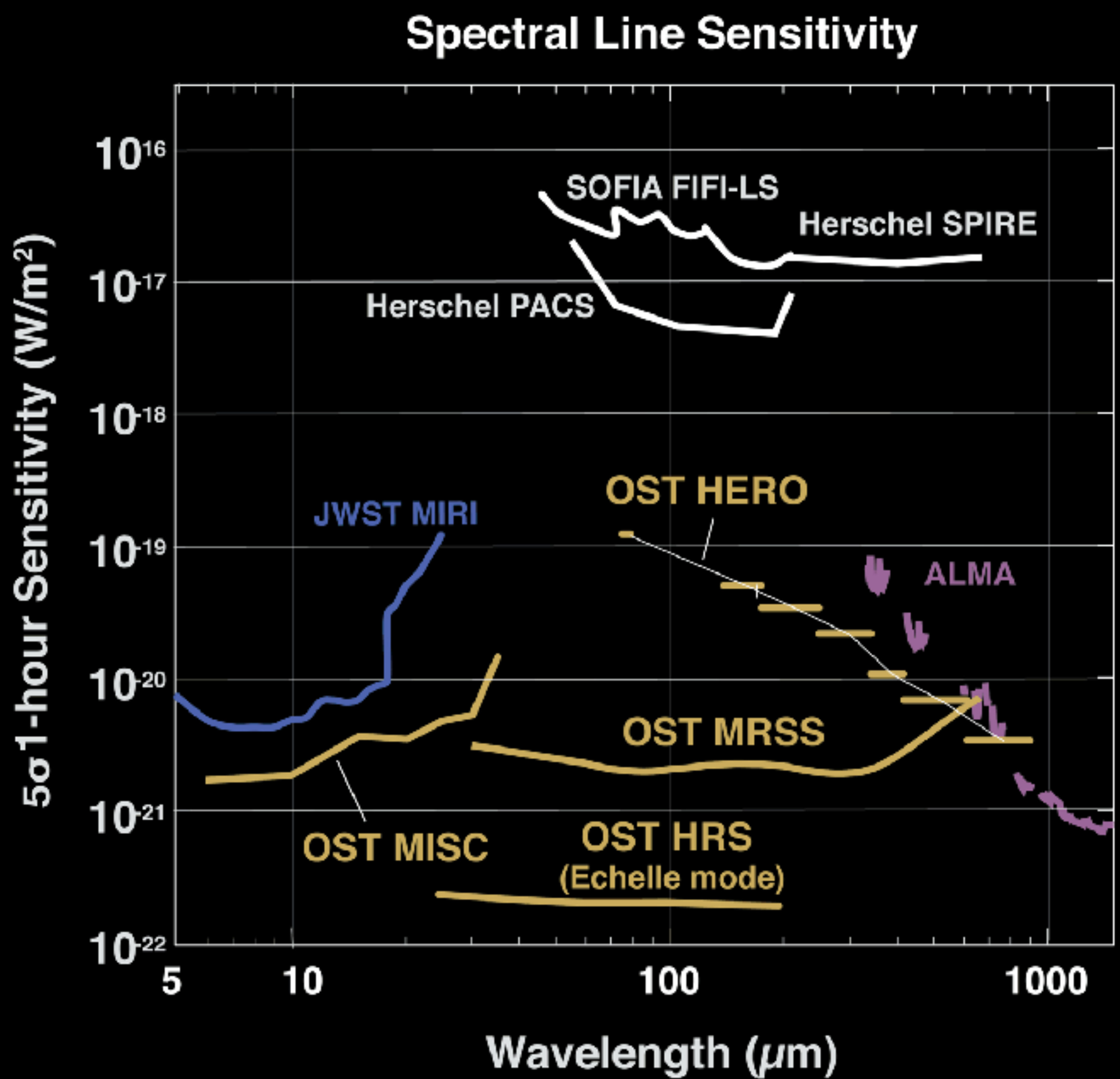

Hubble Space Telescope
1990—2018
2.4 meter
0.1—2.4 µm
260 K

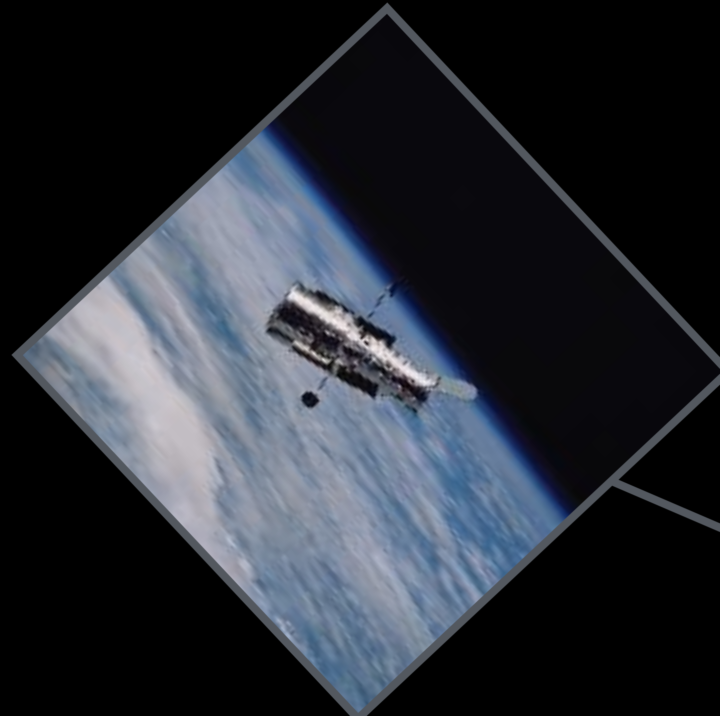

James Webb Space Telescope
2021—2031 (nominal)
6.5 meter
0.6—29 µm
50 K

Origins Space Telescope
2035—2045
~9 meter
5—660 µm
4 K